AKE

Energie und Klima

Vorträge auf der DPG-Frühjahrstagung in Regensburg 2007

2007

Herausgegeben vom Arbeitskreis Energie in der Deutschen Physikalischen Gesellschaft.

Inhaltsverzeichnis

Perspektiven für CO_2-Abtrennung und -Speicherung in Deutschland – eine systemanalytische Betrachtung bis 2050

Peter Viebahn[(1)], Joachim Nitsch [(1)], Manfred Fischedick [(2)]

1 Einführung

In den vergangenen Jahren hat die Diskussion über die CO_2-Abtrennung und Speicherung (engl. Carbon Capture and Storage: CCS) vor dem Hintergrund der Erreichung der angestrebten Klimaschutzziele national wie global stark an Bedeutung gewonnen. Dies gilt um so mehr, als sich im Zuge stark steigender Gas- und Ölpreise und der sich zuspitzenden Debatte um die Energieversorgungssicherheit das energiewirtschaftliche Gewicht in Richtung einer stärkeren Kohlenutzung verschiebt. So basiert rund 60 % der Kraftwerksleistung der aktuell bekannten Kraftwerksplanungen in Deutschland (je nach Quelle werden für das anstehende Kraftwerksersatzprogramm geplante Investitionen mit einer elektrischen Gesamtleistung von 18 bis 25 GW genannt) auf dem Energieträger Kohle.

Die Technologie der CO_2-Abtrennung ist nicht grundsätzlich neu. Sie wird im industriellen Maßstab genutzt und kommt auch bei der Förderung von Erdöl (z.B. im Rahmen des so genannten Enhanced Oil Recovery zur Erhöhung der Ausbeutrate von Erdölfeldern) oder der Aufbereitung von Erdgas (Abtrennung des Begleitgases CO_2) heute schon kommerziell zum Einsatz. Für den Einsatz im Kraftwerksbereich oder für eine zentrale Wasserstoffbereitstellung mit in der Regel deutlich größeren Mengenströmen sind aber noch zahlreiche Fragen offen. Dies gilt auf verschiedenster Ebene auch für den Bereich des Transportes, der Ausgestaltungsmöglichkeiten einer CO_2-Infrastruktur und der Speicherung. In Demonstrationsanlagen (z.B. Vattenfall 30 MW_{th}-Pilotanlage Schwarze Pumpe auf Basis des Oxyfuel Prozesses: geplante Inbetriebnahme 2008) und ersten halbkommerziellen Testanlagen (Planungen der RWE Power AG, bis zum Jahr 2014 ein Kohlekraftwerk mit integrierter Vergasung, CO_2-Abscheidung und Speicherung mit einer Netto-Leistung von 360 MW_{el} zu errichten) sollen maßgebliche Fortschritte bei der Weiterentwicklung der Technologie im Kraftwerksmaßstab erreicht werden.

---

[1] Dr. Peter Viebahn, Dr. Joachim Nitsch, Deutsches Zentrum für Luft- und Raumfahrt, Institut für technische Thermodynamik, Abteilung für Systemanalyse und Technikbewertung, Pfaffenwaldring 38-40, 70569 Stuttgart, Kontakt: peter.viebahn@dlr.de

[2] Dr. Manfred Fischedick, Wuppertal Institut für Klima, Umwelt, Energie, Döppersberg 19, 42103 Wuppertal, Kontakt: manfred.fischedick@wupperinst.org

Die bisher in diesem Themenbereich vorliegenden Untersuchungen beschäftigen sich vorwiegend mit der technischen Machbarkeit des Konzepts der CO_2-Abtrennung und Speicherung. Eine detaillierte Auseinandersetzung mit den ökologischen, ökonomischen und sozialen Auswirkungen über die gesamte Prozesskette (z. B. Energiebilanz, kumulierte Energieaufwendungen, Umweltwirkungen, Rohstoffeinsatz, Risiken und Kosten), wie sie für andere neue Energietechnologien – insbesondere die regenerativen Energien – heute selbstverständlich ist, lag bisher nicht vor. Erst danach kann entschieden werden, wie umweltentlastend diese Technologieoption wirklich ist, welche Vorzüge oder Nachteile sie gegenüber regenerativen Energien besitzt und welchen Beitrag sie zu einer nachhaltigen Wirtschaftsstruktur leisten kann. Die Einbeziehung der CO_2-Abtrennung und Speicherung in die fossile Prozesskette ermöglicht dabei zum ersten Mal einen (aus klimapolitischer Sicht) „Vergleich auf gleicher Augenhöhe“ mit den regenerativen Energieträgern. Auf diesem Vergleich, der auf Basis eines umfangreichen Kriterienrasters durchgeführt wurde, lag der Fokus einer durchgeführten Untersuchung verschiedener Forschungsinstitute, deren Abschlussbericht kürzlich vorgelegt wurde (Wuppertal et al. 2007).

In diesem Beitrag werden folgende Aspekte aus der Studie behandelt:

- Wie stellt sich die Ökobilanz der CCS-Prozessketten dar, und wie ist diesbezüglich die CO_2-arme fossile Stromerzeugung im Vergleich zur regenerativen Stromerzeugung zu werten?
- Welche Rolle kann die CO_2-Abtrennung und Speicherung kostenseitig für den Klimaschutz im Vergleich zu anderen relevanten Optionen und wann leisten?
- Welche Rolle kann die CO_2-Abtrennung und Speicherung als mögliche Brücke in ein regeneratives Energiesystem auf nationaler Ebene spielen?

Neben diesen Aspekten sind in der Untersuchung folgende weitere Bereiche behandelt worden:

- Treibende Kräfte und Haltung relevanter Gruppen zu CCS
- Verfahren zur Abtrennung, Transport und Speicherung
- Energiewirtschaftliche und nicht in der Ökobilanz behandelte ökologische Faktoren
- Anforderungen an eine erfolgreiche internationale Umsetzung von CCS

2 Grundlagen

Die Betrachtung der Rückhaltung und Speicherung von Kohlendioxid bei der Nutzung fossiler Energieträger beschränkte sich im Rahmen der Untersuchung auf den Bereich der Stromerzeugung in Kraftwerken (und die potenzielle zukünftige Wasserstoffbereitstellung, die hier aber nicht betrachtet wird), also auf Anlagen, in denen besonders große Mengen CO_2 zentral (d.h. punktförmig) emittiert werden. Im Hinblick auf eine CO_2-Minderung beim Einsatz fos-

siler Brennstoffe standen bisher die Technologien zur Effizienzsteigerung an erster Stelle des Interesses. Durch den zeitnahen Einsatz dieser Technologien konnte in den letzten Jahrzehnten trotz verstärkter Umweltauflagen (die zum Teil zu einem Brennstoffmehrbedarf geführt haben) eine kontinuierliche Steigerung des Kraftwerkswirkungsgrades erzielt werden. Für Braunkohlekraftwerke liegt das heute realisierbare Wirkungsgradniveau bei 43 %, für Steinkohlekraftwerke bei 46 %, bei Gaskraftwerken lassen sich sogar Wirkungsgrade von 58 % erreichen. Aus thermodynamischen und materialtechnischen Gründen kann dieser Trend nicht beliebig fortgesetzt werden. Eine weitere signifikante CO_2-Minderung bei der fossilen Stromerzeugung erfordert deshalb den Einsatz von heute im wesentlichen bekannten CO_2-Abscheidetechniken oder den Übergang auf innovative, neue Kraftwerkskonzepte (z.B. chemical looping combustion), die eine CO_2-Abscheidung einschließen.

CO_2-Abscheidetechniken dürften eher mittelfristig zur Verfügung stehen (ein großtechnischer Einsatz ist kaum vor dem Jahr 2020 zu erwarten), während die Entwicklung von innovativen, neuen Kraftwerkskonzepten eher langfristig zu sehen ist. Nachteilig wirkt sich für die CO_2-Abscheidung der hohe Eigenbedarf aus, der zu einer signifikanten Wirkungsgradminderung führen (teilweise um 10 %-Punkte und mehr) und das heute erreichte Wirkungsgradniveau wieder deutlich (etwa auf den Stand von vor 20 bis 30 Jahren) absenken wird. Die CO_2-Abtrennung führt dadurch zu einer signifikanten Erhöhung der Stromgestehungskosten und bringt einen erheblichen zusätzlichen Brennstoffverbrauch mit sich, der auch logistisch zu bewerkstelligen ist. Die kostenseitigen Aufwändungen für die CO_2-Abtrennung am Kraftwerk, die die Zusatzkosten der CO_2-Abtrennung und Speicherung dominieren, schwanken derzeit für um 2020 errichtete Kraftwerke zwischen 30 und 60 €/t CO_2. Ziel verschiedener Forschungs-, Demonstrations- und Pilotvorhaben ist es, die Kosten signifikant zu reduzieren, wobei angestrebt wird, die Zusatzosten für die gesamte Prozesskette (d.h. inkl. Transport und Speicherung) auf unter 20 €/t CO_2 zu senken.

Aus heutiger (technologischer) Sicht kommen kurz- bis mittelfristig drei Optionen zur CO_2-Abtrennung in Betracht: Die **Rauchgaswäsche** gilt als vermutlich adäquate Option für die Nachrüstung, insbesondere wenn es gelingt, über neue Waschmittel den Energieaufwand zu verringern. Für den Einsatz der Integrierten Kohlevergasung (**IGCC**-Technik) ist es erforderlich, dass die heute für den Kraftwerksprozess noch unzureichende Verfügbarkeit signifikant verbessert werden kann. Für das **Oxyfuel**-Verfahren kommt es darauf an, durch das im Jahr 2006 gestartete Demonstrationsvorhaben („Schwarze Pumpe“ von Vattenfall) wesentliche Erfahrungen zu sammeln und in die Praxis erfolgreich umzusetzen.

Die Technik der **Abtrennung** von CO_2 **aus den Rauchgasen** (Abtrennung ***nach* der Verbrennung / Post Combustion**) konventioneller Kraftwerke ist heute grundsätzlich verfügbar, es fehlt allerdings noch die Demonstration im kommerziellen Kraftwerksmaßstab. Auf Dauer wird sich diese Technik wahrscheinlich nicht durchsetzen können, wenn es nicht zu einer deutlichen Verringerung des erforderlichen Eigenbedarfs kommt.

Die **CO_2-Abtrennung *vor* der Verbrennung** in Kohle- oder Gaskraftwerken mit integrierter Vergasung **(IGCC und Erdgas-GuD Kraftwerke / Pre Combustion)** ist im Vergleich zur CO_2-Rauchgasabscheidung aus heutiger Sicht das günstigere Verfahren. Prinzipieller Vorteil dieser Technologie ist – neben höheren Wirkungsgraden – die Flexibilität sowohl auf der Brennstoffseite (Input von Kohle, Biomasse, Ersatzbrennstoffe) als auch auf der Produktseite (Output von Strom, Wasserstoff, synthetischen Gase bzw. Kraftstoffen). Hier ist die großtechnische Demonstration der nächste Schritt. Die IGCC-Technik ohne CO_2-Abtrennung ist mittlerweile in einigen Anlagen erprobt (z.B. Buggenum in den Niederlanden und Puertollano in Spanien). Zur Implementierung der CO_2-Abtrennung besteht Verbesserungs- und Entwicklungsbedarf hinsichtlich der Verfügbarkeit von Einzelkomponenten (z.B. Wasserstoffturbine). Mit dem Bau eines IGCC-Kraftwerks mit CO_2-Abtrennung im Kraftwerksmaßstab (450 MW_{Brutto} / 360 MW_{Netto}) bis zum Jahr 2014 will RWE Power den Einstieg in diese Technologie vollziehen.

Das **Oxyfuel-Verfahren** (d.h. die Verbrennung mit Sauerstoff) bietet derzeit die besten Voraussetzungen für die CO_2-Abtrennung hinsichtlich der erreichbaren Gesamtprozesswirkungsgrade und ggf. auch der resultierenden Kosten, da es weitgehend auf Komponenten der klassischen Kraftwerkstechnik basiert. Eine genaue Bewertung ist zurzeit noch nicht möglich, da sich das Verfahren erst am Anfang der Demonstrationsphase befindet. Das Energieunternehmen Vattenfall errichtet derzeit am Standort Schwarze Pumpe im brandenburgischen Spremberg die weltweit erste Pilotanlage für die Braunkohleverbrennung nach dem Oxyfuel-Verfahren. Die Vattenfall-Pilotanlage mit einer Leistung von 30 MW (thermisch) wird zu Forschungs- und Entwicklungszwecken eingesetzt mit dem Ziel, die neue Technologie zur Marktreife zu führen. Sie soll nach einer etwa dreijährigen Bauzeit 2008 in Betrieb gehen. Das CO_2 wird zunächst nicht gespeichert – entsprechende Konzepte (z. B. Transportoptionen) werden aber untersucht.

Tabelle 1 zeigt die Grunddaten der CCS-Kraftwerke, die für die Studie angenommen wurde.

Tabelle 1: Daten zu den CCS-Kraftwerken, die zur Inbetriebnahme in 2020 angenommen wurden

		Steinkohle		**Braunkohle**	**Erdgas**
		Dampfkraftwerk	**IGCC [a]**	**Dampf-KW**	**GuD [b]**
A) Ohne CO_2 Abtrennung					
Leistung	MW_{el}	700	700	700	700
Laufzeit	h	7.000	7.000	7.000	7.000
Nutzungsgrad	%	49	50	46	60
Investitionskosten	€/kW_{el}	950	1.400		400
Laufende Kosten	€/kW_{el},a	48,3	53		34,1
LEC [d], untere Grenze	ct_{EUR}/kWh_{el}	3,51	4,27		3,56
LEC [d], obere Grenze	ct_{EUR}/kWh_{el}	4,89	5,66		4,94
CO_2 Intensität Brennstoff	g CO_2/MJ	92	92	112	56
CO_2 Intensität Strom	g CO_2/kWh_{el}	676	662	849	337

B) Mit CO_2 Abtrennung						
Abscheidemethode		Post-combustion	Oxyfuel	Pre-combustion	Post-combustion	Post-combustion
Lösemittel		Chemisch (MEA) [c]	Konden-sieren	Physika-lisch (Rectisol)	Chemisch (MEA) [c]	Chemisch (MEA) [c]
Leistung	MW_{el}	570	543	590	517	600
Nutzungsgrad	%	40	38	42	34	51
Abnahme Nutzungs-grad	%-points	9	11	8	12	9
Investitionskosten	€/kW_{el}	1.750		2.100		900
Laufende Kosten	€/kW_{el},a	80		85		54
LEC [d], untere Grenze	ct_{EUR}/kWh_{el}	5,52		6,06		5,04
LEC [d], obere Grenze	ct_{EUR}/kWh_{el}	6,13		6,64		6,16
Abscheidegrad	%	88	99,5	88	88	88
CO_2 zu speichern	Mt/a	3,570	4,249	3,400	5,113	1,704

[a] IGCC = Integrated Gasification Combined Cycle (Integrierte Kohlevergasung)

[b] GuD = Gas- und Dampfkraftwerk

[c] MEA = Monoethanolamin

[d] LEC = levelised electricity generation costs (gemittelte Stromerzeugungskosten); Zinssatz: 10%/a, Lebensdauer: 25 a, Annuität: 11%/a

3 Vergleichende Ökobilanzen

Für die ökologische Bewertung von ausgewählten Systemkonfigurationen wird das Verfahren der Ökobilanzierung (Life Cycle Assessment, LCA) nach ISO 14.040ff angewendet. In einem systemübergreifenden Ansatz werden dabei die Stoff- und Energieflüsse, die die Herstellung einer Kilowattstunde Strom bzw. Wasserstoff verursachen, bilanziert und ihre Wirkung auf die Umwelt berechnet.

Für die Stromerzeugung werden auf fossiler Seite die Umweltwirkungen der drei Abscheide-routen Post-Combustion (Braun- und Steinkohle-Dampfkraftwerk sowie Erdgas-GuD), Pre-Combustion (Steinkohle-IGCC-Kraftwerk) und Sauerstoff-Verbrennung (Oxyfuel-Steinkohle-kraftwerk) bilanziert. Als Standort der Kraftwerke wird das Ruhrgebiet gewählt, als Speicher-stätte ein (beliebiges) leeres Gasfeld in Norddeutschland in 300 km Entfernung von den Kraftwerken. Auf regenerativer Seite wird zum Vergleich die Stromerzeugung aus solarther-mischen Anlagen (Standort Algerien) und aus Windkraftanlagen (Standort Nordsee) model-liert. Um den gleichen Referenzstandort wie bei den fossilen Anlagen zu verwenden, wird der Strom mittels Hochspannungs-Gleichstrom-Übertragung (HGÜ) bis zum Ruhrgebiet transpor-tiert. Folgende zentrale Schlussfolgerungen können gezogen werden:

Die in der Diskussion über CCS in der Regel angegebenen hohen CO_2-Minderungsraten durch Abscheidung des CO_2 von 88 % und mehr beziehen sich nur auf die CO_2-Emissionen und zudem nur auf den direkten Kraftwerksbetrieb. Geht man dagegen von einer ganzheitli-

chen Betrachtung aus, fallen fünf Prozent der CO_2-Emissionen – sowohl bei Steinkohle-Dampfkraftwerken als auch bei Erdgas-GuD – bereits in der Vorkette an. Ein verminderter Wirkungsgrad bedingt zudem einen höheren Primärenergieverbrauch und damit eine „größere“ Steinkohle- oder Erdgas-Vorkette. Beides zusammen hat zur Folge, dass die CO_2-Emissionen bei einem Abscheidegrad von 88 % nicht ebenfalls um 88 %, sondern bei einer ganzheitlichen Betrachtung lediglich um 72 - 78 % reduziert werden können. Vor diesem Hintergrund ist die Bezeichnung „CO_2-freies“ Kraftwerk irreführend; treffender ist die Bezeichnung „CO_2-arm“, selbst wenn in der Zukunft der Abscheidegrad am Kraftwerk noch weiter erhöht werden kann.

Ferner ist zu berücksichtigen, dass mit Blick auf den Klimaschutz nicht nur die CO_2-Emissionen, sondern generell die Treibhausgas-Emissionen reduziert werden müssen. So sieht das Kyoto-Protokoll für Deutschland eine Verminderung einer Palette von insgesamt sechs Treibhausgasen (und nicht nur der CO_2-Emissionen) um 21 % bis zum Jahr 2012 vor. Berechnet man die Auswirkungen der CO_2-Abscheidung auf die Treibhausgas-Emissionen, so zeigt sich, dass diese nur unterproportional reduziert werden können. Bei einem CO_2-Abscheidegrad im Kraftwerk von z.B. 88 % können die Treibhausgase insgesamt um 67-78 % reduziert werden (siehe Abbildung 1). Grund hierfür sind ebenfalls der erheblich höhere Primärenergieverbrauch und die mit der Rohstoffförderung und dem -transport einhergehenden und je nach Brennstoff und Brennstoffherkunft relativ hohen Methan-Emissionen. Diese wirken sich bei den getroffenen Annahmen überproportional hoch auf den Treibhauseffekt aus. Verbesserungen in der Vorkette (z.B. durch Erfassung und Nutzung des Grubengases) könnten sich stark Ergebnis verbessernd auswirken.

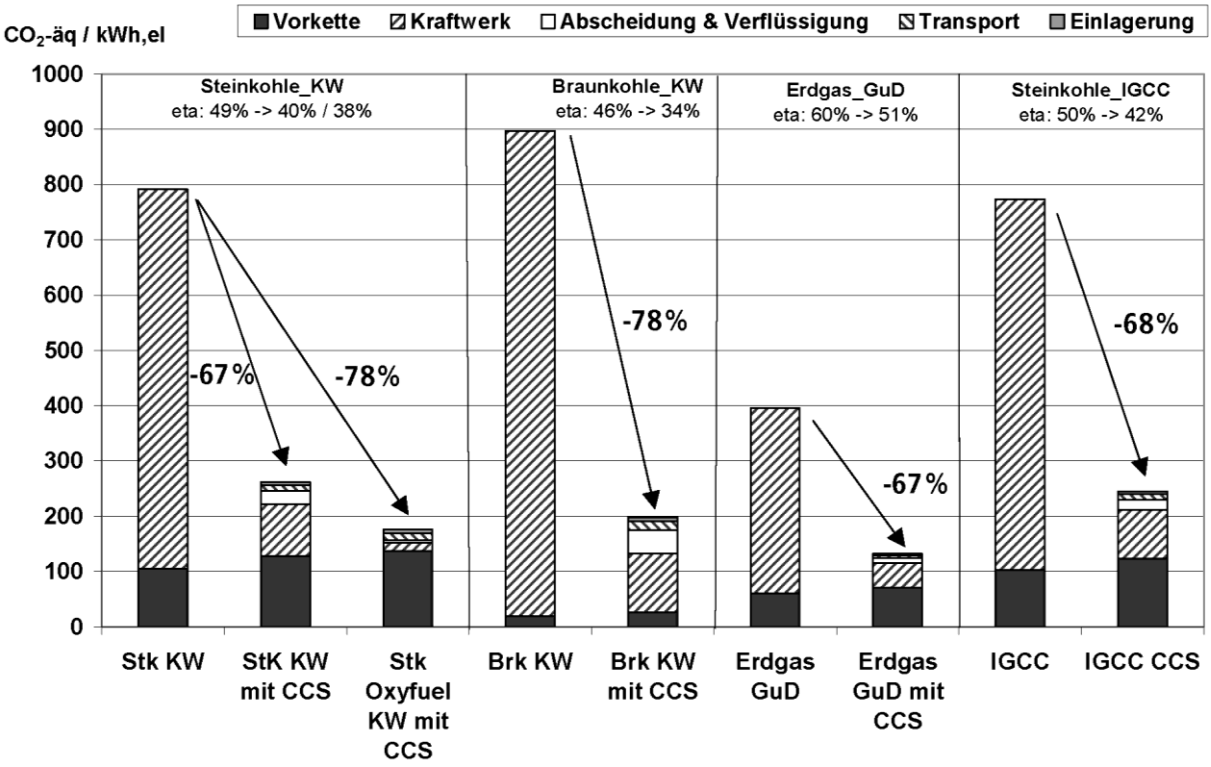

Abbildung 1: Ökobilanz von CCS-Anlagen (hier: Darstellung der Treibhausgase)

Bei der ganzheitlichen Betrachtung relativiert sich damit der erreichbare Minderungseffekt durch CCS-Kraftwerke. Das aus Klimaschutzsicht „beste“ Kraftwerk ohne CCS (Erdgas-GuD) weist mit knapp 400 g CO_2-Äquivalenten pro kWh nur um 51 % höhere Emissionen auf als das „schlechteste“ Kraftwerk mit CCS (Steinkohle-Dampfkraftwerk mit Post-Combustion).

Von allen betrachteten fossilen Kraftwerken schneidet unter den getroffenen Annahmen die Sauerstoff-Verbrennung (Oxyfuel) bei der Treibhausgasbilanz am günstigsten ab. Der Grund liegt in der im Idealfall fast hundertprozentigen Abtrennung des CO_2 mittels der physikalischen Abscheidung. Dadurch sind Netto-Minderungsraten der CO_2-Emissionen von 90 % und der Treibhausgas-Emissionen von 78 % möglich.

Die mit CCS-Technologien erreichbaren Minderungsraten für CO_2 und allgemein Treibhausgase wurden in einem nächsten Schritt mit Alternativtechnologien verglichen. In Abbildung 2 sind am Beispiel der Treibhausgasemissionen im linken Teil zunächst zusammengefasst die fossilen Technologien aus Abbildung 1 dargestellt (ohne und mit CCS; für Kohlekraftwerke ist jeweils die Spannbreite der bisherigen und der zukünftigen Emissionen aufgezeigt). Dem gegenüber gestellt wurden die folgenden Alternativen:

– Einzeltechnologien der Erneuerbaren Energien (hier Wind offshore und Solarthermische Kraftwerke) verzeichnen nur minimale Emissionen (die aus der Herstellung der Anlagen resultieren).

- Aber auch kommerziell erhältliche Anlagen mit Kraft-Wärme-Kopplung erreichen bereits jetzt so niedrige Treibhausgas-Emissionen, wie sie für CCS-Anlagen in 2020 erwartet werden. So verzeichnet ein großes Erdgas GuD Heizkraftwerk etwa die gleichen Treibhausgas-Emissionen wie das beste CCS-Kohlekraftwerk und das CCS-Erdgas-GuD.
- Noch niedrigere Treibhausgas-Emissionen werden in verschiedenen Energie-Szenarien für Deutschland (BMU 2007) und EU-weit (Greenpeace und Erec 2007) erwartet: Selbst ohne CCS liegen die durchschnittlichen Emissionen in 2050 noch unter denjenigen der besten CCS-Kraftwerke und das, obwohl in den jeweiligen Strommixen ein nicht unerheblicher Teil an fossilen Energien enthalten ist. Erreicht wird dies durch einen hohen Anteil an KWK-Anlagen, durch den die eingesetzte Energie optimal genutzt werden kann.

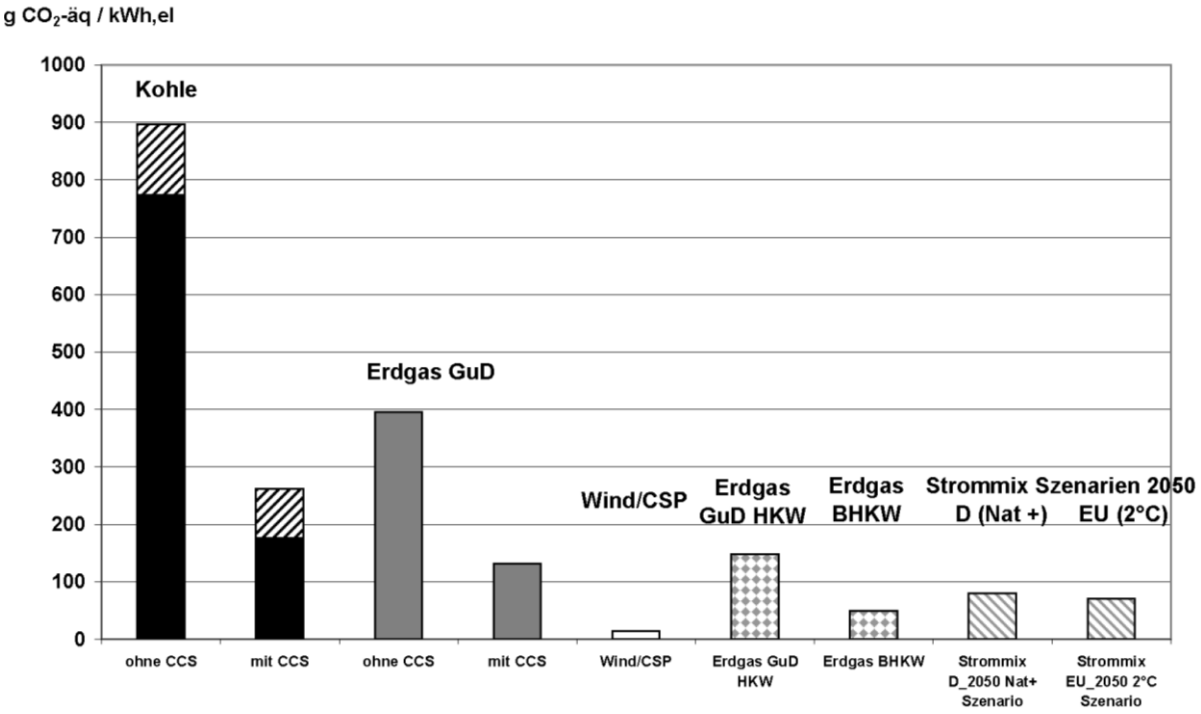

Abbildung 2: Treibhausgas-Emissionen von CCS-Anlagen im Vergleich zu alternativen Technologien und Strommix-Szenarien für 2050

Ingesamt erfordert die CO_2-Abscheidung je nach Verfahren einen zusätzlichen Energieverbrauch von 20 bis 44 %. Dieser höhere Energieverbrauch macht sich in verschiedenen Wirkungskategorien der Ökobilanz direkt proportional bemerkbar. Dies gilt z.B. für die Belastung durch Sommersmog, Eutrophierung, Versauerung von Böden und Gewässern und den Partikelausstoß. Auf der anderen Seite werden einzelne Emissionen wie SO_2, NO_2 oder Staub durch die Reaktion mit dem Lösemittel reduziert, was insgesamt gesehen eine Reduktion bzw. abgemilderten Anstieg einzelner Wirkungskategorien bedingt. Die folgende Abbildung zeigt dies am Beispiel des modellierten Braunkohlekraftwerks (Post-Combustion).

Der um 44 % höhere Energieverbrauch bedingt zunächst einen proportionalen Anstieg bei allen Wirkungskategorien. Durch die genannten anderen Einflüsse ist insgesamt gesehen in der Kategorie Versauerung jedoch eine Reduktion um 3 % zu verzeichnen; die PM10-Äquivalente steigen nur um etwa 24 % an; die Eutrophierung erhöht sich dagegen um 40 % und der Sommersmog um 524 %.

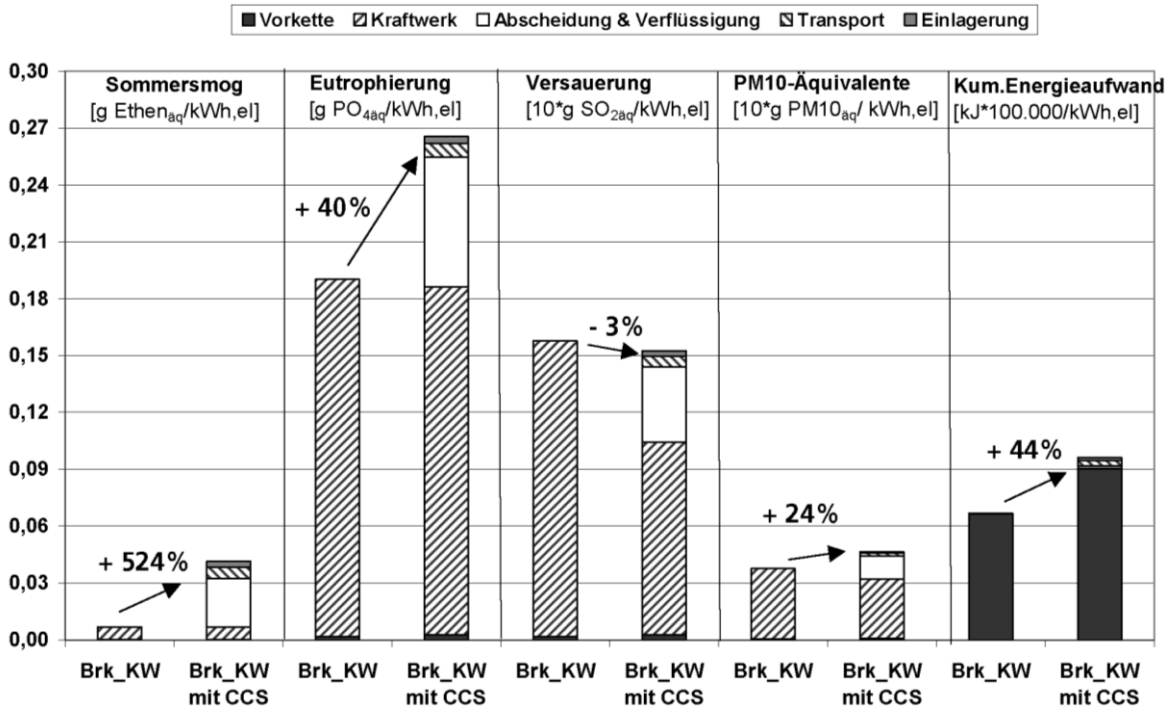

Abbildung 3: Vergleich weiterer Wirkungskategorien für ein Braunkohle-Dampfkraftwerk ohne und mit CCS (Post-Combustion)

In der Vergleichsanalyse weisen die betrachteten regenerativen Energieoptionen dagegen deutlich günstigere Werte auf als die fossilen Kraftwerke mit CO_2-Abtrennung. Solarthermisch erzeugter Strom sowie Strom aus Windkraftanlagen verursachen – inklusive Stromtransport – nur 2 bis 3 % der CO_2-Emissionen, Treibhausgase und kumulierten Energieverbrauch der fossilen Kraftwerke. Aber auch bei den weiteren Wirkungskategorien bleiben die regenerativen Werte noch unter denjenigen der fossilen CCS-Anlagen.

4 Ökonomischer Vergleich von CCS und regenerativen Energietechnologien

Kann die Rückhaltung von CO_2-Emissionen in fossil befeuerten Kraftwerken und ihre Speicherung erfolgreich demonstriert werden, so kann auf der Basis kommerziell einsatzfähiger CCS-Kraftwerke im Jahr 2020 von Stromgestehungskosten frei Kraftwerk zwischen 6,5 und 7 ct/kWh ausgegangen werden (Zinssatz 10 %/a). Längerfristig zu erwartende Brennstoffpreis-

steigerungen lassen einen weiteren Anstieg auf Kosten zwischen 7 ct/kWh (Kohle) und 8 ct/kWh (Erdgas) bis 2040 wahrscheinlich werden. Bei Kohlekraftwerken dürften die brennstoffseitigen Preiseffekte durch weitere technische Fortschritte weitgehend kompensiert werden können. Für das Jahr 2020 sind entsprechend der angestellten Berechnungen CO_2-Vermeidungskosten zwischen 35 und 50 €/t CO_2 ermittelt worden, wenn als Referenzkraftwerk dasselbe Kraftwerk ohne CCS angenommen wird. Dabei liegen Kohlekraftwerke eher beim unteren, Erdgaskraftwerke eher beim oberen Wert. Dies ist weniger als die heute angegebene Kostenbandbreite und unterstellt bereits signifikante Lernerfolge (die höher als die aktuell von Rubin et al. (2007) veröffentlichten Lernraten angenommen wurden), liegt aber dennoch deutlich oberhalb der von der Energiewirtschaft anvisierten Kosten von rund 20 €/t CO_2 für die gesamte Prozesskette.

Regenerative Energien, die heute – geht man von einem repräsentativen Mix aus – noch mittlere Stromgestehungskosten von ca. 13 bis 14 ct/kWh (ebenfalls Zinssatz 10 %/a) aufweisen, können bis 2020 ebenfalls dieses Kostenniveau erreichen, wenn ihre weitere Markteinführung mit ähnlicher Geschwindigkeit wie bisher erfolgt. Seit etwa 1990 folgte ihre Kostenreduktion Lernkurven, deren Lernraten zwischen 15 und 20 % lagen. Eine anhaltende globale Steigerung der Marktpenetration und Lerneffekte lassen für den weiteren Zeitverlauf bei den regenerativen Energien noch signifikante Kostendegressionen erwarten, so dass um 2050 das Kostenniveau der Stromerzeugung aus regenerativen Energien in dem betrachteten charakteristischen Mix bei 6 ct/kWh liegen könnte. Einzelne Technologien könnten Stromkosten von ca. 4 ct/kWh erreichen, wenn die Lernkurve über eine kontinuierliche Ausweitung globaler Märkte weiter genutzt wird (vgl. Abbildung 4).

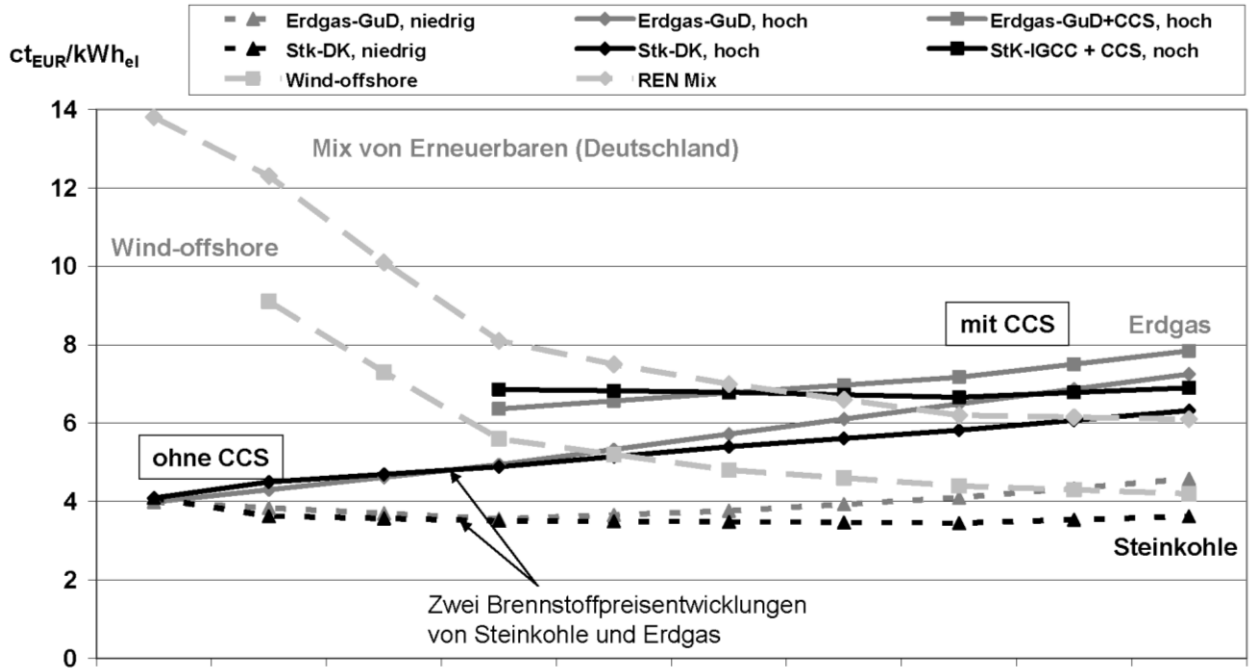

Abbildung 4: Verlauf der Stromgestehungskosten (Neuanlagen) erneuerbarer Energien sowie konventioneller Gas- und Steinkohlekraftwerke ohne und mit CCS (Brennstoffpreise nach Energiepreispfad „DLR 2005“ und für konventionelle KW ohne CCS zum Vergleich nach Preispfad „EWI 2005“)

Bleibt die Ausbaudynamik von regenerativen Energien im Stromsektor hoch, wie es in verschiedenen Szenarien, die einen Umstieg auf eine klimaverträgliche Energieversorgung auf der Basis einer kombinierten Forcierung des Ausbaus erneuerbarer Energien und der Energieeffizienz (z.B. Szenario Naturschutzplus, siehe BMU 2007) beschreiben, so dürften einzelne Technologien (z.B. Wind offshore) zum Zeitpunkt der potenziellen Inbetriebnahme von ersten CCS-Kraftwerken bereits günstigere Stromgestehungskonditionen erwarten lassen und diesen Vorteil im Zeitverlauf weiter vergrößern können. Wesentliche Kostensenkungseffekte kommen dabei durch die globalen Markteffekte, so dass selbst bei einem weniger dynamischen Wachstum der regenerativen Energien in Deutschland noch eine Kostengleichheit von CCS und einzelnen regenerativen Energien zu erwarten ist. Nur bei sehr geringen Brennstoffpreissteigerungen oder über die abgeschätzten Effekte hinaus gehende Kostensenkung in der CCS-Prozesskette stellt sich die Situation für CCS-Anlagen günstiger dar. Hierdurch wird der generelle Effekt zwar nicht aufgehoben, die relative Konkurrenzfähigkeit der regenerativen Energien auf der Zeitachse aber nach hinten verschoben.

Aus ökonomischer Sicht besteht daher den getroffenen Annahmen zufolge kein zwingender Anreiz, CCS-Technologien dem weiteren Ausbau erneuerbarer Energien zur Stromerzeugung vorzuziehen. Sie stellen aber auch keine prohibitiv teure Technologie dar und könnten bei erfolgreicher Kommerzialisierung und geeigneten Rahmenbedingungen (günstige und langzeitstabile Speicheroptionen, gute infrastrukturelle Voraussetzungen, kostengünstige Kohle) in einigen Regionen Teil einer zukünftigen Stromerzeugung werden.

5 Die Rolle von CCS im deutschen Energieversorgungssystem

Im Rahmen dieses Projektes sind für die Analyse der energiewirtschaftlichen Rolle von CCS im Vergleich zu regenerativen Energien drei unterschiedliche Szenarien für die zukünftige Energieversorgung Deutschland entwickelt worden. In allen Szenarien werden die energiebedingten CO_2-Emissionen bis 2050 auf 240 Mio. t/a reduziert, was gegenüber 1990 einer Minderung von rund 75 % entspricht. Die **Szenarien** gehen dabei von folgenden Prämissen aus:

- CCS als Hauptelement einer Klimaschutzstrategie mit „maximalem“ Einsatz von CCS-Technologien im Rahmen einer sonst (Energieverbrauch, Ausbau von regenerativen Energien) weitgehend trendgemäßen Entwicklung, also einer relativ geringen Mobilisierung von Effizienzpotenzialen und eingeschränkter Umsetzung der Ausbaupotenziale bei regenerativen Energien (Kurzbezeichnung = **CCSMAX**);

- Konzentration auf das flächendeckende Ausschöpfen der Energieeffizienzpotenziale und auf den engagierten Ausbau von Technologien zur Nutzung regenerativer Energien, wie er in den Szenarien „NaturschutzPlus“ für das BMU (nach BMU 2004 und BMU 2005) beschrieben wurde (Kurzbezeichnung = **NATP**). Auf den Einsatz von CCS kann in diesem Szenario verzichtet werden;
- CCS als Brücke zum weiteren Ausbau regenerativer Energien bei zeitgleich gegenüber der Referenzentwicklung verstärkter, aber gegenüber NATP deutlich geringerer Effizienzsteigerung und deutlich reduziertem Ausbau regenerativer Energien. Beide Maßnahmen reichen daher zusammen nicht aus, das Klimaschutzziel ohne weitere Maßnahmen, hier also den Einsatz von CCS, zu erreichen (Kurzbezeichnung = **BRIDGE**).

Aus der Szenarioanalyse lassen sich verschiedene maßgebliche Erkenntnisse ableiten. Emissionsmindernde Maßnahmen allein im Strombereich reichen danach grundsätzlich nicht aus, um das Klimaschutzziel zu erreichen. Es sind auch ähnlich umfangreiche Maßnahmen in den Sektoren Wärme- und Kraftstoffversorgung erforderlich. Neben dem Ausbau der regenerativen Energien muss die Ausschöpfung der Effizienzpotenziale dazu einen ganz erheblichen Beitrag leisten. Bei umfangreicherer Nutzung fossiler Ressourcen kommt dafür als Alternative grundsätzlich auch die Wasserstoffbereitstellung mittels Steinkohlevergasung unter Abtrennung und Rückhaltung des CO_2 infrage.

Als Hauptstrategieelement einer Klimaschutzstrategie, entsprechend **Szenario CCSMAX**, stößt CCS an strukturelle und potenzialseitige Grenzen. Der mit 2020 angenommene früheste kommerzielle Einsatzzeitpunkt der CCS-Technologien kommt für die gerade angelaufene erste Welle des Kraftwerksersatzprogramms zu spät. Er erzwingt im Zeitraum bis 2050 extrem hohe Zuwachsraten für CCS-Anlagen und für den Aufbau einer Wasserstoffinfrastruktur. Die Nachfrage nach Steinkohle steigt mit 5.900 PJ/a in CCSMAX auf das dreifache des heutigen Beitrags (Abbildung 5, schwarze Balken). Wasserstoff wäre im Jahr 2050 mit 47 % Anteil an der Endenergie dominierender Energieträger. Die abzuscheidende und zu speichernde CO_2-Menge beläuft sich in 2050 auf jährlich rund 600 Mio. t CO_2/a. Damit sind die möglichen Speicherdauern für CO_2 unter deutschen Verhältnissen auf ein bis zwei Jahrzehnte begrenzt. Da Kostenvorteile der mittels CCS bereit gestellten Endenergien Strom und Wasserstoff gegenüber denen aus regenerativen Energien hergestellten nicht (beim Strom) bzw. nur in geringem Ausmaß (beim Wasserstoff) zu erkennen sind, ist aus wirtschaftlicher Sicht kein entscheidender Anreiz für eine so herausragende Bevorzugung von CCS zu erkennen. Die für einen derartig starken Ausbau von CCS bereits heute erforderlichen hohen Zuwendungen für diese Technologieoption in Form von F+E und Demonstrationsanlagen würde vermutlich eine weitgehende Abwendung von der Förderung von Effizienzstrategien und Ausbaustrategien regenerativer Energien verlangen. Eine angesichts der noch vielen offenen Fragen sehr hohe Anforderung stellt auch dar, dass aufgrund der notwendigen Vorlaufzeiten bereits vergleichsweise kurzfristig eine sehr hohe Sicherheit hinsichtlich der ökologischen Verträglichkeit und Langzeitstabilität der potenziellen CO_2-Speicher erreicht werden müsste.

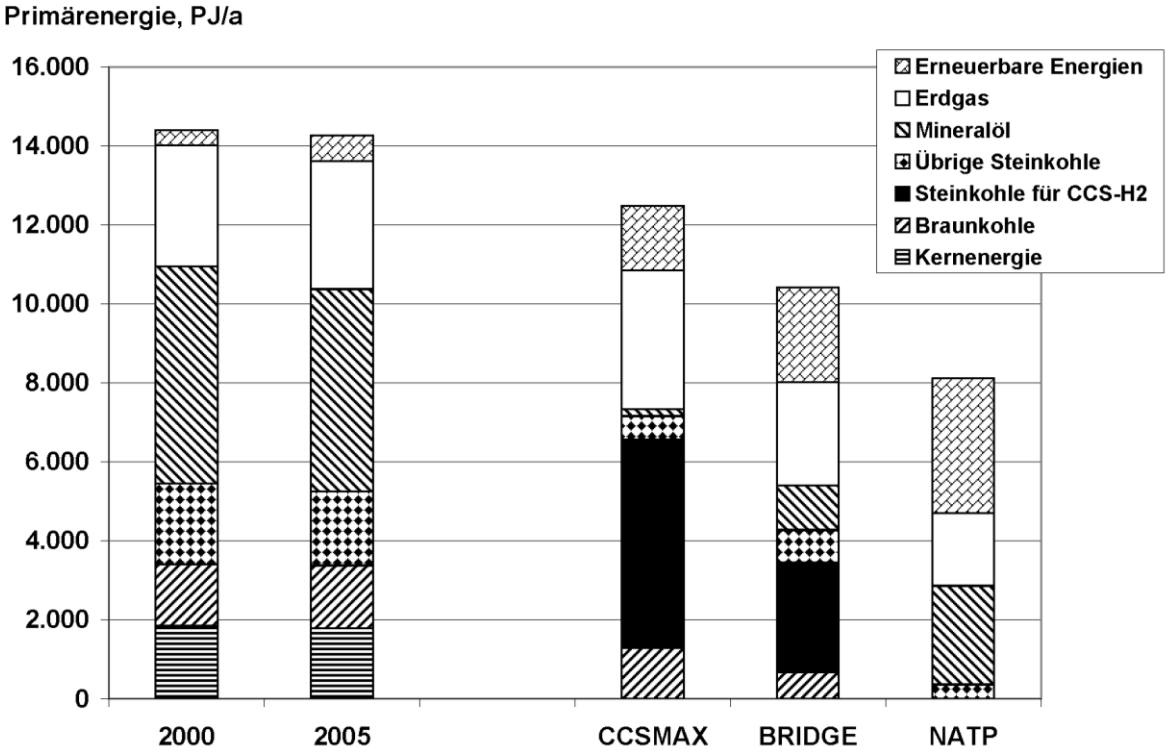

Abbildung 5: Heutige Primärenergiestruktur und Struktur in den Szenarien für das Jahr 2050

Eine Klimaschutzstrategie entsprechend Szenario **NATP**, die ohne CCS-Technlogien auskommt, ist heute noch kein „Selbstläufer". Neben der Beibehaltung des derzeitigen dynamischen Ausbaus regenerativer Energien im Strombereich und ihrer signifikanten Ausweitung im Wärmesektor sind noch beträchtliche zusätzliche energiepolitische Unterstützungsmaßnahmen für deutlich wirksamere Effizienzmaßnahmen in der Nutzung und der Umwandlung von Energie erforderlich, um mit dieser Strategie zeitgerecht das Klimaschutzziel 2050 erreichen zu können. Die bereits relativ kurzfristig wirksamen Maßnahmen Ausbau erneuerbarer Energien und Effizienzsteigerung erlauben es jedoch – falls die notwendigen Unterstützungsmaßnahmen rasch greifen – den Umstrukturierungsprozess harmonischer ablaufen zu lassen, als das im obigen Fall möglich wäre. An den Umbau der Infrastrukturen für die Endenergieträger werden zwar ebenfalls hohe Anforderungen gestellt, die aber stufenweise umgesetzt werden können. Eine insbesondere auf Erhöhung der Energieproduktivität setzende Strategie ist zudem volkswirtschaftlich sinnvoll, da ein großer Teil der zu ergreifenden Effizienzmaßnahmen unabhängig von erzeugungsseitigen Maßnahmen die ökonomisch günstigste Option für den Klimaschutz darstellt. Bei einer Einbeziehung externer Kosten würde sich die gesamtwirtschaftliche Bilanz noch günstiger darstellen. Insofern stellt das Szenario eine „Idealstrategie" dar, die aber kurzfristig sehr wirksame energiepolitische Weichenstellungen verlangt, vor allem eine deutliche Effektivierung und Ausweitung der Energieeffizienzpolitik.

Längerfristig sind in diesem Szenario erhebliche strukturelle Veränderungen notwendig. Dies gilt sowohl für die zunehmende Netz- und Systemintegration regenerativer Energien auf der Stromseite und die Einbeziehung von Stromimportstrukturen (z.B. Strom aus solarthermischen Kraftwerken in Nordafrika) als auch für einen deutlichen Ausbau von Nahwärmenetzen.

Es erscheint aus heutiger Sicht nicht zweckmäßig, beide der o. g. Strategien „mit voller Kraft" bis 2020 durchzuhalten (Ausbau regenerativer Energien und Effizienz wie NATP bis 2020; CCS-Entwicklung wie in CCSMAX), um dann eine der beiden Optionen weitgehend zu ignorieren. Dies stellt keine sinnvolle Vorgehensweise dar, so dass im dritten Szenario diskutiert worden ist, inwieweit beide Strategien miteinander kompatibel in einem Zukunftspfad vereinbar sind.

Bei einer Entwicklung entsprechend **Szenario BRIDGE** sind die zeitlichen Anforderungen an die Einführung von CCS-Technologien und an eine Wasserstoffinfrastruktur geringer als in CCSMAX, da bis 2030 die erforderlichen Beiträge dieser Option noch relativ gering sein können. Auch der bis 2050 zu erreichende Ausbauzustand stößt für den Fall, dass sich CCS-Technologien als eine energiewirtschaftlich sinnvolle und ökologisch tragfähige Option herausstellen, nicht an grundsätzliche Grenzen hinsichtlich erforderlicher Anlagenleistung, Infrastrukturveränderungen und Speicherkapazität. In 2050 wären in diesem Fall rund 330 Mio. t CO_2/a abzuscheiden und zu speichern. Grundsätzlich müssen aber auch hier bis 2020 errichtete fossile Kraftwerke für CCS nachrüstbar sein, wenn der Stromsektor substantielle Beiträge zur CO_2-Minderung beitragen soll. Bei den derzeit laufenden Kraftwerksplanungen ist dies prinzipiell bereits zu berücksichtigen und nach Möglichkeit die Anlagen als so genannte „capture ready" Anlagen auszulegen.

Eine energiewirtschaftliche Entwicklung entsprechend Szenario BRIDGE verlangt in jedem Fall eine Steigerung der energiepolitischen Anstrengungen in allen genannten Feldern, wenn längerfristig engagierte Klimaschutzziele ernsthaft erreicht werden sollen. Die Einbeziehung der „CCS-Technologie" als zusätzliche Klimaschutzoption darf also nicht dazu dienen, in der weiteren Intensivierung der Strategieelemente „Energieeffizienz" und „regenerative Energien" nachzulassen. Vielmehr ist erforderlich, diese bis 2020 mindestens soweit zu mobilisieren, dass sie danach weiter „durchstarten" können, falls sich die CCS-Technologien als energiewirtschaftlich nicht oder nicht in dem gewünschten Umfang als sinnvoll realisierbar herausstellen sollten. Gleichzeitig bietet diese Zeitspanne die Möglichkeit, die Entwicklungs- und Kostenpotenziale von CCS-Technologien gründlich und ohne massiven Zeitdruck auszuloten. Auf der anderen Seite könnte die sukzessive Einführung von CCS (Verfügbarkeit geeigneter langzeitstabiler Speicher vorausgesetzt) als begleitendes Element helfen, die dauerhaft erforderlichen Impulse für weitere Effizienzsteigerungen und einen erweiterten Ausbau der regenerativen Energien leichter durchzuhalten, als dies mit den deutlich höheren Anforderungen im Szenario NATP möglicherweise der Fall wäre. Mögliche Widerstände und trotz massiver Unterstützung und energiepolitischer Flankierung unüberwindliche Hemmnisse

könnten so kompensiert werden. Angesichts der realen Interessenlagen und der unterschiedlichen Einschätzungen von Technologieoptionen im Energiebereich, insbesondere im globalen Kontext, kann daher eine Entwicklung gemäß Szenario BRIDGE als „pragmatische“ Strategie bezeichnet werden.

Der Kostenvergleich von erneuerbaren Energien und CCS-Technologien zur Strom- und Wasserstoffbereitstellung zeigt keine wirtschaftlichen Vorteile für die CCS-Option zum Zeitpunkt ihrer möglichen Einführung um 2020. Letztere verlangt dann die Berücksichtigung von CO_2-Preisen zwischen 40 und 50 €/t CO_2, wenn sie für private Investoren gegenüber der konventionellen fossilen Stromerzeugung attraktiv sein soll. Auch nach 2020 haben die erneuerbare Energien Technologien vermutlich weiter ausschöpfbare Kostendegressionspotenziale. Die Kosten der Stromerzeugung aus Kohle mittels CCS dürften bei entsprechender technischer Weiterentwicklung real dagegen in etwa konstant bleiben. Bezieht man die externen Kosten mit ein, ergeben sich weitere Vorteile für den auf erneuerbare Energien und Energieeffizienz bauenden Entwicklungspfad. Die relative Wirtschaftlichkeit von CCS und erneuerbaren Energien ist aus heutiger Sicht mit vielfältigen Unsicherheiten verbunden. Die o.g. Einschätzungen für die erneuerbaren Energien gehen von einer weltweit dynamischen Marktentwicklung aus, so dass über Massenfertigung und Lernkurveneffekte ganz erhebliche Kostendegressionseffekte ausgeschöpft werden können.

Hemmend für eine umfassende CCS-Strategie könnte sich auch auswirken, dass in Folge einer hauptsächlich auf CCS setzenden Strategie ein früherer – mit hohen infrastrukturellen Herausforderungen verbundener - Einstieg in eine breite Nutzung von (CO_2-armen) Wasserstoff erforderlich ist, während dies bei einer Strategie im Sinne des Szenarios NATP erst gegen Mitte des Jahrhunderts im nennenswerten Umfang notwendig ist.

Aus den genannten Gesichtspunkten folgt, dass eine konsequente Strategie im Sinne des Szenarios NATP mittel- bis langfristig auch die volkswirtschaftlich günstigere Strategie darstellen dürfte und damit energiepolitisch angestrebt werden sollte. Gleichzeitig empfiehlt es sich, die Option CCS weiterhin einer gründlichen Prüfung und insbesondere einer realistischen praktischen Demonstration zu unterziehen, um nach etwa einer Dekade über präzisere Kenntnisse zu den Potenzialen und Grenzen dieser Technologie zu verfügen. Stellt sich dann heraus, dass weltweit die Umstrukturierung der Energieversorgung hinsichtlich Effizienz und EE-Ausbau „nur“ gemäß der im Szenario BRIDGE dargelegten Intensität verläuft, stünde mit CCS eine zusätzliche Klimaschutzoption zur Verfügung.

6 Zusammenfassung

Im folgenden sind zusammenfassend die wichtigsten Thesen der jeweiligen Bewertung wiedergegeben.

Ökologische Bewertung mittels Ökobilanz

- CCS-Kraftwerke können Treibhausgas-Emissionen nur teilweise reduzieren und daher nur eine Chance für die „*CO_2-arme*“ Nutzung fossiler Kraftwerke sein.
- Strom aus Erneuerbaren Energien weist erheblich weniger CO_2- und Treibhausgas-Emissionen als CCS-Kraftwerke auf.
- Mit erdgasbasierten Heizkraftwerken steht schon jetzt eine Kraftwerkstechnologie kommerziell zur Verfügung, die nahezu die gleichen CO_2- und Treibhausgas-Emissionen hat, wie sie für die CCS-Kraftwerke angestrebt wird.
- Der erhöhte Brennstoff-Mehraufwand (und damit verbunden der Anstieg anderer Umweltwirkungskategorien) ist nicht nachhaltig im Sinne einer auf Nachhaltigkeitskriterien basierten Energieversorgung.

Ökonomischer Vergleich mit Erneuerbaren Energien

- CCS ermöglicht einen Kostenvergleich fossiler Energiebereitstellung mit erneuerbaren Energie bei gleicher CO_2-Intensität der Stromerzeugung.
- Die Stromerzeugung mit CCS-Kraftwerken liegt im Bereich zukünftiger Kosten der Stromerzeugung aus erneuerbaren Energien, wenn die Brennstoffpreise langfristig *nur moderat* steigen.
- Sowohl für CCS als auch für Erneuerbare sind deutliche bis sehr deutliche Lerneffekte zu erwarten, die bei CCS-Kraftwerken jedoch von Brennstoffpreis-Steigerungen überlagert werden.

Szenarienanalyse zur Rolle von CCS im deutschen Energieversorgungssystem

- Für die erste Erneuerungswelle des Kraftwerksparks kann CCS in Deutschland noch keinen Beitrag leisten, daher kommt der Nachrüstung („capture ready“) eine signifikante Bedeutung zu.
- CCS ist im Verhältnis zu anderen Klimaschutzoptionen zu sehen und kann diese ggf. mittel- bis langfristig ergänzen.
- Als Hauptstrategieelement einer Klimaschutzstrategie in Deutschland (CCSMAX) stößt CCS an strukturelle und potentialseitige Grenzen.
- Sowohl das CCSMAX-Szenario als auch das Brückenszenario bedingen den Einstieg in eine Wasserstoffwirtschaft.

7 Literatur

BMU (Bundesministerium für Umwelt, Naturschutz und Reaktorsicherheit) 2007: Leitstudie 2007. Aktualisierung und Neubewertung der „Ausbaustrategie Erneuerbare Energien“ bis zu den Jahren 2020 und 2030 mit Ausblick bis 2050. Berlin.

Greenpeace and EREC 2007: Energy (r)evolution. A sustainable world energy outlook. Amsterdam. http://www.energyblueprint.info/ . 26.01.2007.

Rubin, Edward; Yeh, Sonja; Antes, Matt; Berkenpas, Michael; Davison, John 2007: Use of experience curves to estimate the future cost of power plants with CO_2 capture. Int. J Greenhouse Gas Control. 2(2007)188-197.

Viebahn, Peter; Nitsch, Joachim; Fischedick, Manfred; Esken, Andrea; Schüwer, Dietmar; Supersberger, Nikolaus; Zuberbühler, Ulrich; Edenhofer, Ottmar 2007: Comparison of carbon capture and storage with renewable energy technologies regarding structural, economic, and ecological aspects. Int. J. Greenhouse Gas Control. 1(2007)121-133.

Wuppertal Institut, DLR, ZSW, PIK 2007: Ökologische Einordnung und strukturell-ökonomischer Vergleich regenerativer Energietechnologien mit anderen Optionen zum Klimaschutz, speziell der Rückhaltung und Entsorgung von Kohlendioxid bei der Nutzung fossiler Primärenergien. Abschlussbericht. http://www.erneuerbare-energien.de/inhalt/38826/ . Berlin.

Human Induced Climate Change: A Perspective on the IPCC Fourth Assessment Report

Bill Hare
Potsdam Institute for Climate Impact Research (PIK); Potsdam

Introduction

The physical science component of the Intergovernmental Panel on Climate Change[1] (IPCC) Fourth Assessment report (AR4)[2] was concluded in Paris in February of 2007. In this short paper I will outline some of its key findings and offer a perspective on its sea level rise projections. First though some context and background on the IPCC and how the assessment reports are written and adopted. The IPCC Fourth Assessment report consists of four components, built around three disciplinary working groups and a synthesis report. IPCC Working Group I[3] on the Physical Science Basis of Climate Change has produced the assessment of the physical science basis for understanding climate change. Working Group II[4] assesses impacts, adaptation and vulnerability to climate change and Working Group III[5] assesses mitigation of climate change. These reports were completed in Brussels in April 2007 and Bangkok in May 2007 and all can be downloaded in pdf format from the respective working group web sites. The IPCC AR4 Synthesis Report is to be adopted in Valencia, in November 2007, which will then complete the fourth assessment of the IPCC.

[1] http://www.ipcc.ch/
[2] IPCC, 2007: Climate Change 2007: The Physical Science Basis. Contribution of Working Group I to the Fourth Assessment Report of the Intergovernmental Panel on Climate Change [Solomon, S., D. Qin, M. Manning, Z. Chen, M. Marquis, K.B. Averyt, M. Tignor and H.L. Miller (eds.)]. Cambridge University Press, Cambridge, United Kingdom and New York, NY, USA, 996 pp.
[3] http://ipcc-wg1.ucar.edu/
[4] http://www.ipcc-wg2.org/
[5] http://www.mnp.nl/ipcc/pages_media/outreachTAR03.html

IPCC Assessment Reports are written by leading scientists in each disciplinary area and subject to at least three rounds of review – expert, government and expert, and final government review. The reports themselves are distilled into summaries for policy makers (SPMs), which are initially drafted by the co-chairs of the working groups and teams of lead authors of the main assessment report and then subject to review by experts and governments. SPMs are approved line by line by IPCC member governments meeting in Plenary session under the Chairmanship of the Working Group Chairs, are always eminent scientists themselves who command the respect of the scientific community and governments alike. Governments propose changes to the SPMs which must be agreed with the scientists representing the working group writing teams and with the approval of the WG Chairs. In this way the SPMs reflect a commonly owned assessment of the state of scientific understanding of climate change and its effects, and of the opportunities for mitigation and adaptation. The main reports and their chapters are not subject to negotiation and are adopted as a whole by the IPCC.

In this very schematic overview of the AR4 WGI assessment I will give a perspective on improvements in understanding of:

- The causal chain from emissions of greenhouse gases and other forcing agents to climate response
- Climate sensitivity to forcing
- Global and regional projections of climate change in the 21st century
- Coupled climate-carbon cycle interactions
- Sea level rise

In what follows references are made extensively to the IPCC Working Group I report (IPCC, Solomon et al. 2007). It can be found at http://ipcc-wg1.ucar.edu/ and the reader is encouraged to follow the links to the underlying report and its summary for policy makers.

Emissions to climate response

Compared to earlier IPCC assessments[6] there is significantly improved understanding of the relationship between emissions of GHGs and other climate forcing agents (short lived aerosols, air pollutants of various kinds), the effects of these gases and of land use changes and other factors on the response of the climate system[7] at global and regional levels. Figure 1 shows the overall causal chain from emissions to atmospheric concentrations, to radiative forcing of the climate system and on to climate response. On this figure I have highlighted four broad areas of improved understanding which will be covered in this overview.

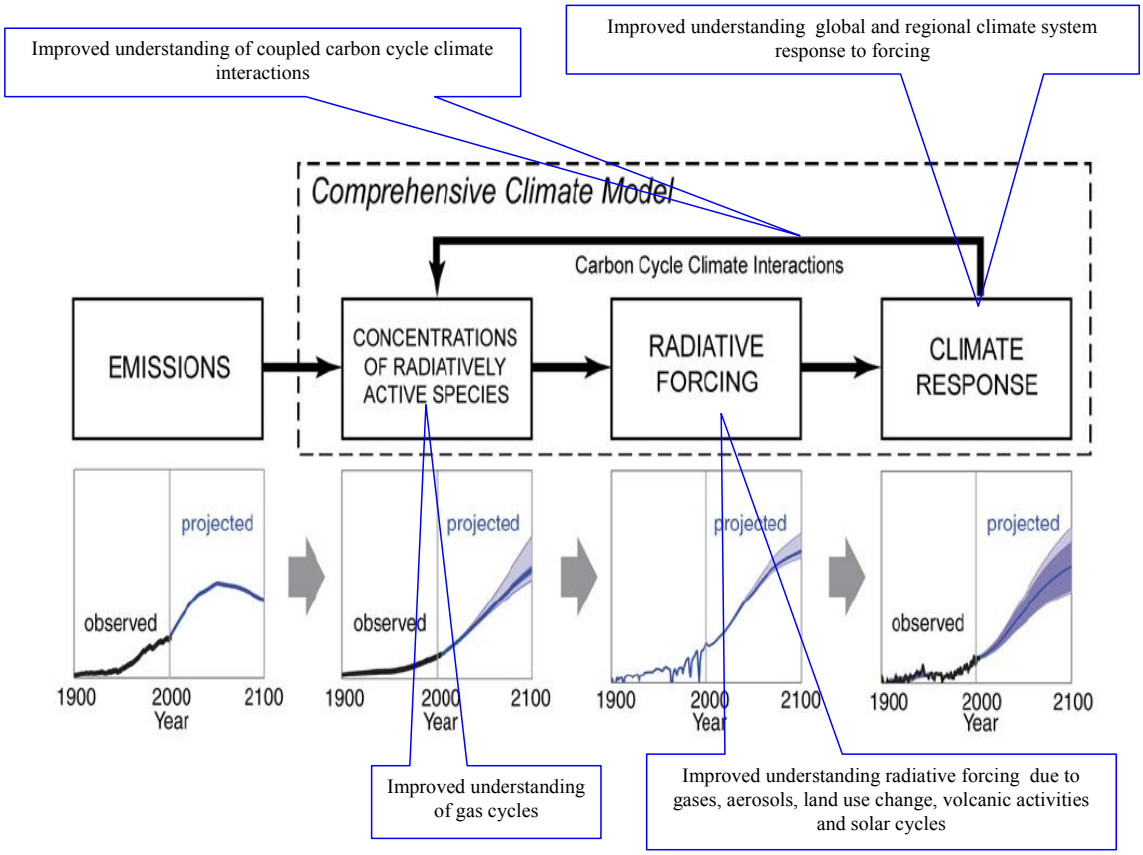

[6] See Agrawala, S. (1998). "Context and Early Origins of the Intergovernmental Panel on Climate Change." Climatic Change **39**(4): 605-620. for background on the IPCC.

[7] The climate system is defined in the IPCC glossary as "the highly complex system consisting of five major components: the atmosphere, the hydrosphere, the cryosphere, the land surface and the biosphere, and the interactions between them. The climate system evolves in time under the influence of its own internal dynamics and because of external forcings such as volcanic eruptions, solar variations and anthropogenic forcings such as the changing composition of the atmosphere and land use change". http://ipcc-wg1.ucar.edu/wg1/Report/AR4WG1_Print_Annexes.pdf

Figure 1 Emission to climate response chain. Based on IPCC AR4 WGI Figure 10.1 with added schematic indication of areas of improved scientific understanding since the Third Assessment Report in 2001.

Increases in greenhouse gas concentrations lead to a change in the earth's energy balance and a forcing of the climate system into a perturbed state (compared to preindustrial) (Arrhenius 1897; Peixoto and Oort 1992). The effects of these gases and other forcing agents are often quantified in terms of their radiative forcing[8] of the lower atmosphere (troposphere) in W/m^2. The simple zero dimensional equation describing the energy balance of the perturbed climate system induced by a radiative forcing is shown in Box 1. The sensitivity of the climate system to radiative forcing is often summarized in terms the climate sensitivity, which is defined as the global mean surface temperature change at equilibrium resulting from a doubling of CO_2 concentrations, usually above the pre-industrial state.

Radiative forcing – Climate response

- Energy balance of the perturbed climate system (relative to the preindustrial state):

$$\Delta Q_G = \lambda_G \Delta T_G + \frac{\delta \Delta H}{\delta t}$$

ΔQ_G Radiative forcing at the top of troposphere

ΔT_G Surface temperature change

λ_G Total global mean feedback parameter

ΔH Total heat content perturbation of the ocean

- Climate sensitivity is as the surface temperature increase *dT2x* at equilibrium for a radiative forcing (*dQ2x*) equivalent to a doubling of CO_2 concentrations (usually above pre-industrial levels 278 ppmv CO_2):

$$dT2x = \frac{dQ2x}{\lambda}$$

[8] Radiative forcing' is the net change in upward and downward irradiance at the tropopause due to the effect of an external climate forcing agent such as a greenhouse gas increase, change in solar irradiance, volcanic eruption or land use change. It is expressed in W/m2 and here at the global mean annual level. A positive warms the surface and a negative forcing tends to cool it. By convention radiative forcing values are for changes relative to a pre-industrial background in 1750 in W/m^2. More details can be found in the IPCC Glossary at http://ipcc-wg1.ucar.edu/wg1/Report/AR4WG1_Print_Annexes.pdf

Box 1 Radiative-forcing climate response relationships.

Quantitative understanding of the past and present radiative forcing of the climate system is quite crucial to understanding past climate changes, attributing these to specific causes and for predicting future changes in climate. Whilst the forcing of well mixed greenhouses gas (CO_2, N_2O, CH_4, fluorinated gases etc) has been reasonably well understood for some time, the radiative forcing of aerosols, land use changes and air pollutants (e.g. tropospheric ozone) are not as well quantified. This is important as the cooling effects of certain species of aerosol can be quite large and outweighs a significant fraction of the positive forcing effects of the well mixed greenhouse gases. As a consequence of advances since the Third Assessment Report (TAR) there is now "very high confidence[9] that the globally averaged net effect of human activities since 1750 has been one of warming, with a radiative forcing of +1.6 [+0.6 to+2.4] Wm^{-2}." (IPCC AR4 WGI SPM). Whilst the quantitative uncertainty remains large, there has been a considerable narrowing of this in the six years since the TAR was completed.

The direct radiative forcing effect of the increase in all of the well mixed GHGs is substantial. CO_2 itself has increased in concentration to around 379 ppmv in 2005 (ca 1.7 Wm^{-2}) and the total CO_2 equivalent concentration of the well mixed GHGs (including CO_2) was estimated to be around 455 ppm CO_2-equivalent (around 2.7 Wm^{-2}). The effects of aerosol and land use changes reduce the net radiative forcing so that the net forcing of all human activities is around 1.6 Wm^{-2} (311 -435 ppm $CO_{2\text{-eq}}$, with a central estimate of about 375 ppm $CO_{2\text{-eq}}$.)

[9] This means a 9 out 10 chance of being correct. See IPCC AR4 Uncertainty Guidance note at http://ipcc-wg1.ucar.edu/wg1/Report/AR4_UncertaintyGuidanceNote.pdf

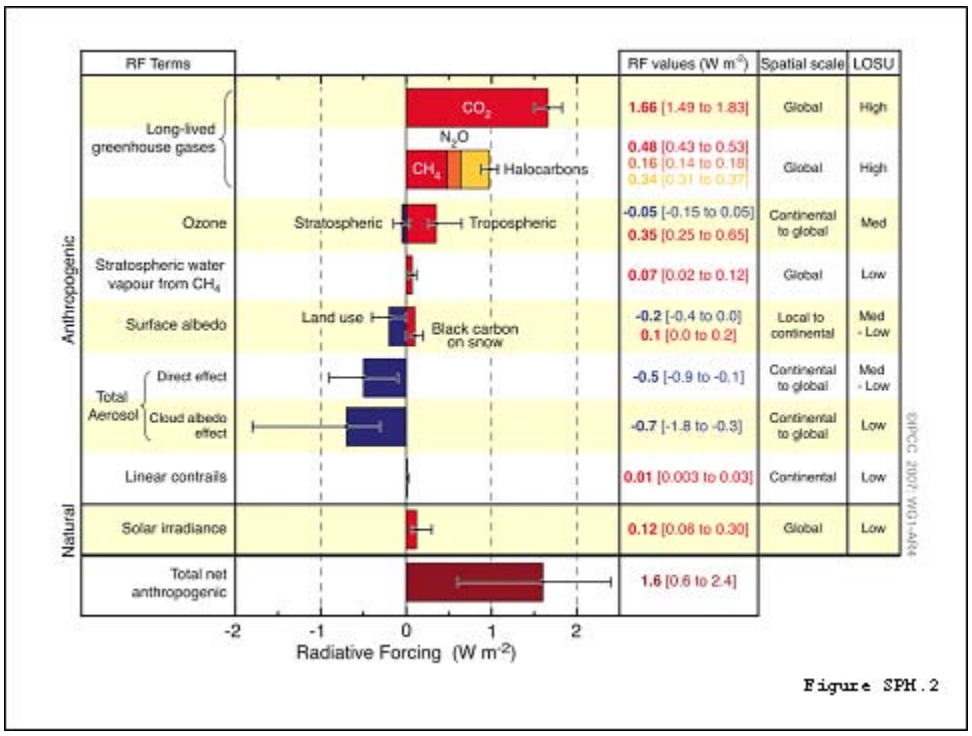

Figure 2 IPCC AR4 Radiative forcing estimates in 2005 (from IPCC AR4 WGI Figure SPM.2).

The AR4 has also found some improvement in understanding of the sensitivity of the climate system to forcing (see Box 1 oben). Since the First Assessment Report in 1990 the IPCC had estimated the climate sensitivity, *dT2x,* to be in the range of 1.5-4.5°C, with a best estimate of 2.5°C[10]. In the AR4 the best estimate has been raised to 3°C and a "likely" range of 2 to 4.5°C, with it being "very unlikely" to be less than 1.5°C. It was not possible to attach a formal likelihood of a *dT2x* above 4.5°C and it was assessed that values higher than 4.5°C cannot be excluded. Understanding the sensitivity of the climate system is clearly very important in assessing the risks from emission of greenhouse gases, and has quite profound effects for policy responses. As can be seen from Figure 3, which shows cumulative density functions for climate sensitivity from four different methods and a range of different studies, there remains a large uncertainty around this quantity. For estimates based on 20th century observations, the main uncertainty in narrowing estimates of *dT2x* relates to the uncertainty in aerosol and volcanic forcing. Cloud feedbacks

[10] Very similar to the range estimated by Charney in the 1970s {Charney, 1979 #55572}

remain the largest source of uncertainty in AOGCM (Atmospheric Ocean General Circulation Model) based estimates of the climate sensitivity.

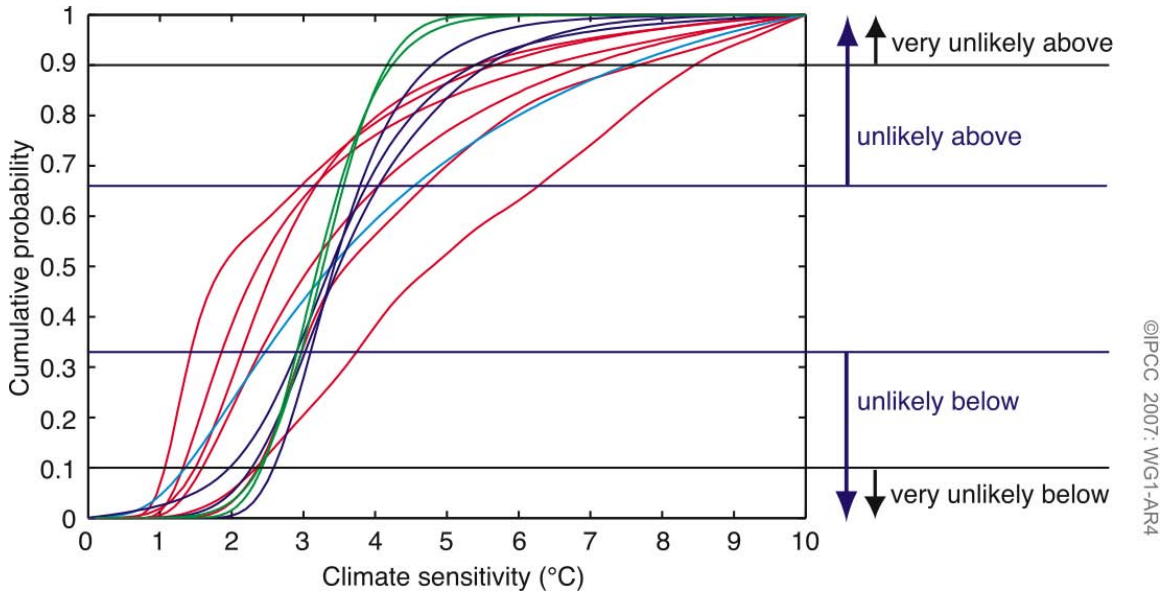

Figure 3 Climate sensitivity estimates -cumulative probability distributions. This figure shows the large range of estimates of climate sensitivity assessed in the AR4. Red lines show estimates based on observed 20th century climate system changes, blue lines show estimates from model climatology, and the cyan coloured lines estimates based in proxy climate records of the past, and the green shows the range from present AOGCMs. After IPCC AR4 WGI Figure TS.2 Technical Summary[11].

Improved climate change projections in AR4

Projections of climate change over the 21st century in response to different emission scenarios are of key interest to policy makers and stakeholders in assessing risks, mitigation and adaptation options. Whilst the question of the equilibrium climate sensitivity is very important, the regional patterns, magnitude and timing of changes to climate are more relevant in the medium term. On decadal timescale the actual warming experience by the climate system is related also to the rates and patterns of ocean heat uptake.

[11] http://ipcc-wg1.ucar.edu/wg1/Report/AR4WG1_Print_TS.pdf and see the footnote 9 for link to AR4 Uncertainty Guidance for likely range definitions.

Comparison of the projections made with climate models for the period since 1990 with observations over the period 1990-2005 has strengthened scientific in confidence in near-term projections for the next few decades. In particular, for the next two decades, the AR4 projects a warming of about 0.2°C per decade for the range of IPCC SRES[12] emission scenarios. The inertia of the climate system, principally due to the enormous heat capacity of the oceans, means that even with radiative forcing held constant at contemporary levels, a further warming of about 0.1°C per decade for several decades would be expected.

Compared to earlier assessment the AR4 had a larger number of climate simulations and projections available from a broader range of models, which provided a quantitative basis for estimating the likelihood of changes in many climate variables of interest. Global mean projections and ranges are shown in Figure 4 and Figure 5. Table 1 below provides a rough comparison of the projections made in the AR4 compared to earlier assessments[13]. Global mean temperature projections in the AR4 are comparable in range to those made using the same IPCC SRES scenarios in the TAR in 2001.

Projected climate changes of interest however are not limited to global means and the AR4 provides insight into effects on a wide range of climate system properties at global and regional scale such as precipitation, sea ice, snow cover and changes in weather extremes,

[12] This refers to the standard set of IPCC non-mitigation (e.g. reference) emissions scenarios in use for the AR4. See http://www.grida.no/climate/ipcc/emission/

[13] This comparison is approximate owing to different approaches taken in each set of projections for emission scenarios and reference period and end periods for projections.

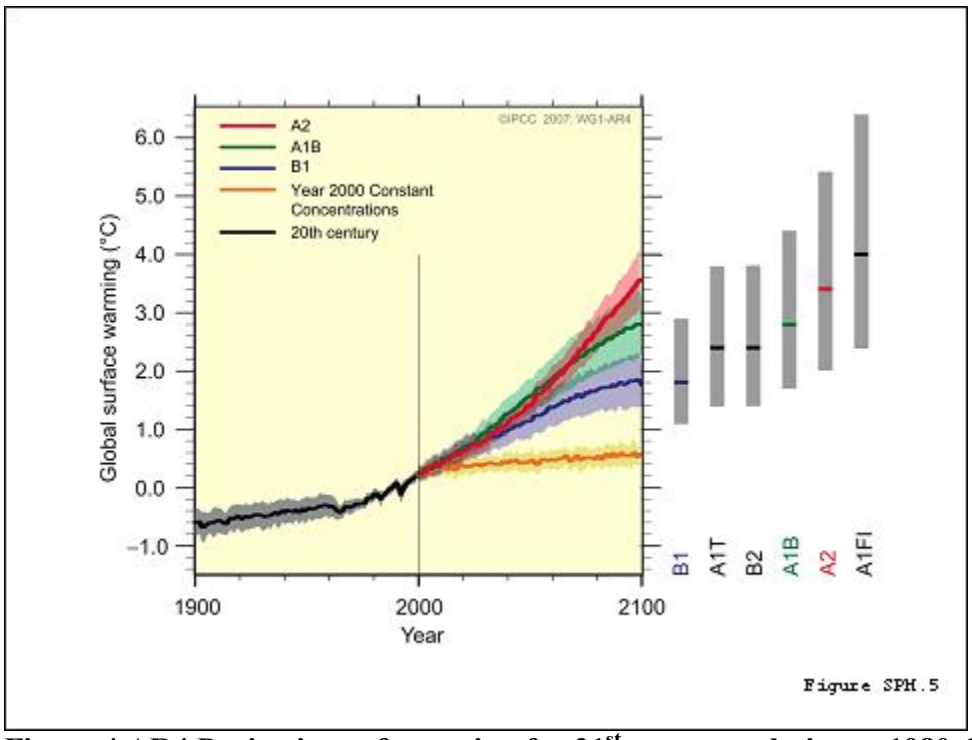

Figure 4 AR4 Projections of warming for 21st century relative to 1980-1999 period for the IPCC SRES scenarios and constant 2000 radiative forcing experiment. The solid lines are the global averages of the models assessed. The grey bars on the right show the best estimate and likely ranges for the IPCC SRES marker scenarios estimated from the AOGCM projections, simpler models and observational constraints. From IPCC AR4 WGI Figure SPM.5-.

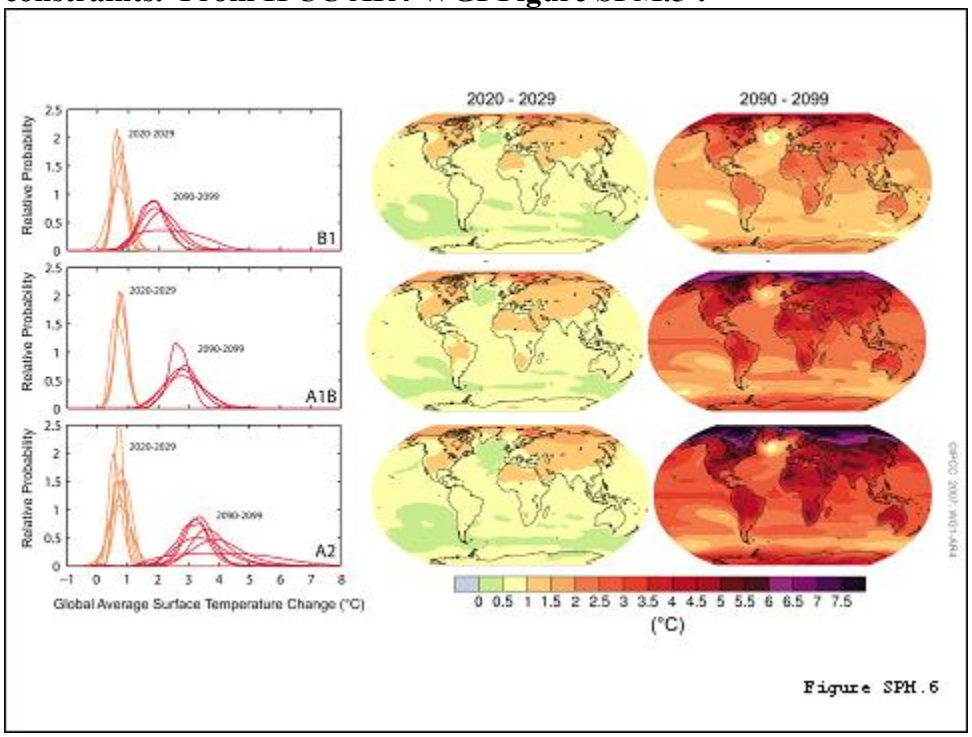

Figure 5 AR4 Projections of warming for 21st century relative to 1980-1999 period for 2020s and 2090s. Model range is shown on the left hand side and the on the right are averages of the models assessed. From IPCC AR4 WGI Figure SPM.6-

Table 1 PCC Assessments 1990-2007

Year	*1990*	*1995*	*2001*	*2007*
Observed global mean change	0.6°C (1880s to 1990)	0.3-0.6°C (1880s to 1990)	0.4-0.8°C (1880s to mid 1990s	0.8°C (0.6-1.0°C) (1880s to 2001–2005)
Human influence due to anthropogenic increase in greenhouse gas concentrations	Unequivocal detection "not likely for a decade or more."	"Balance of evidence suggests a discernable human influence."	"likely" that "most of the observed warming over the last 50 years"	"very likely" "Most of the observed increase in globally averaged temperatures since the mid-20th century"
Projected warming to 2100	2-5°C	1-3.5°C	1.4-5.8°C (SRES range)	1.1-6.4°C (SRES range)
Projected sea level rise to 2100	30-100cm	13-94cm	9-88cm (SRES range)	18-59 cm (SRES range)

Sea Ice Changes

An important component of the climate system and the underpinning of arctic and Antarctic ecosystems is sea ice. The AR4 reported that Arctic sea ice annual average and summer extent has declined since satellite observations began in 1978 at 2.7 [2.1 to 3.3]% per decade and 7.4 [5.0 to 9.8]% per decade respectively to 2005 (WGI SPM). Sea ice extent is projected in the AR4 report to reduce under all of the IPCC SRES scenarios and "in some projections, arctic late-summer sea ice disappears almost entirely by the latter part of the 21st century" (WGI SPM).

Since the AR4 cut off date for peer reviewed literature to be included in the assessment (around mid 2006) further analyses have been published, finding that the rate of ice loss projected by the AOGCMs participating in the AR4 assessment for the period

1953-2006 have substantially underestimated the reduction in late summer ice extent (Stroeve, Holland et al. 2007), and that in general the reliability of these models in this area is low (Eisenman, Untersteiner et al. 2007). Observed September ice extent loss rates from 1979-2006 were 9.12 ± 1.54%/decade with modeled losses less than half this (4.26 ± 0.25%/decade) and for the most recent decade observed loss were 17.91 ± 5.98%/decade, as opposed to modeled losses of 6.65 ± 0.59%/decade. If the models do indeed underestimate the sensitivity of sea ice to warming in the Arctic it seems likely that the transition an ice free Arctic ocean in summer will occur much sooner than projected in the AR4 (Stroeve, Holland et al. 2007). Summer ice extent in the Arctic in summer 2007 was at record low levels (Kerr 2007) continuing the trend found in the AR4 assessment.

Precipitation projections

Significant improvements have occurred in projections of precipitation changes compared to earlier assessments. Warming will intensify the hydrological cycle increasing water vapour content, evaporation and precipitation. Precipitation is projected to increase in the moist tropics and in high latitudes and generally decrease in the subtropics. Figure 6 shows projected changes in precipitation for the 2090s for the SRES A1B emission scenario.

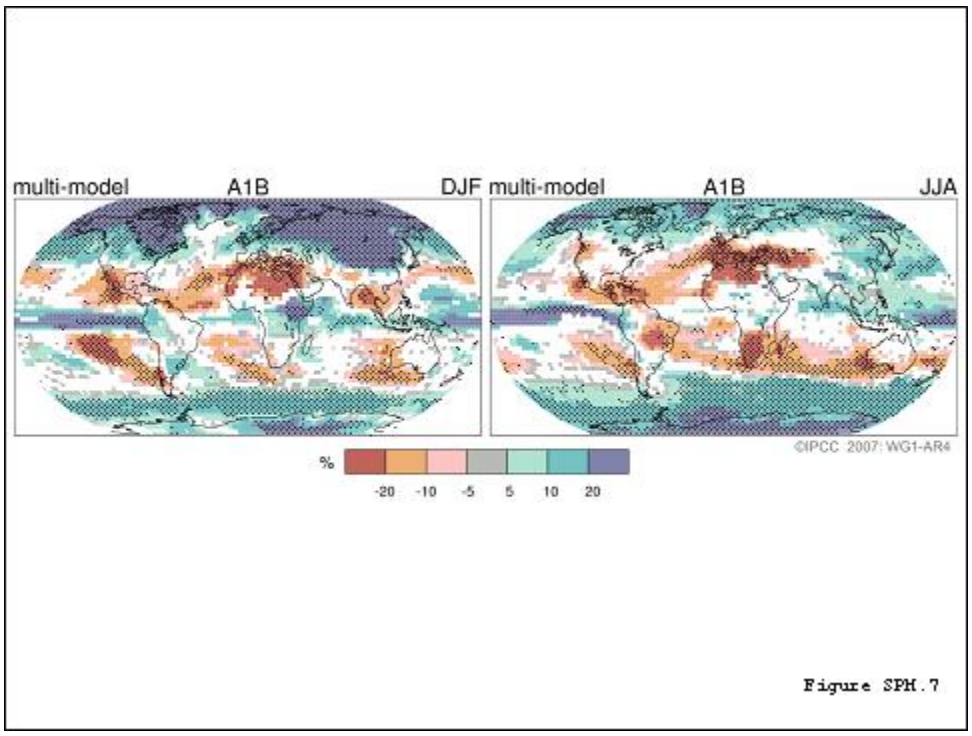

Figure 6 Changes in precipitation 2090–2099 compared to 1980-1999. Multimodel averages are shown for the IPCC SRES A1B Scenario, with the white areas demarking where model agreement is low, with less than 66% of models agreeing in the sign of the change. Stippled areas demark where more than 90% of the models agree in the sign of the change. From IPCC AR4 WGI Figure SPM.7.

Warming is projected to result in reduced snow cover as melting dominates over increased snow fall in most regions.

Projections of extreme weather events

Many extreme weather events are predicted to increase in frequency and/or intensity with warming (see Table 2). In most subtropical and midlatitude regions, although precipitation is projected to decrease, the intensity of precipitation events is also projected to increase. Associated with this is a tendency for increased periods of no rain. Owing to summer warmth and drying in mid-continental regions there is a likelihood of increased drought.

As background, it is to be noted that the mass of water held by the atmosphere is expected to increase with temperature; hence a

global increase in precipitation is projected. Under the Clausius-Clapeyron equation the saturation water vapour pressure increases exponentially with temperature, so that the water holding capacity increases at 7%$^{o}C^{-1}$ (Trenberth, Dai et al. 2003; Trenberth and Shea 2005). Increases in global precipitation are limited however by the energy balance of the atmosphere and AOGCM projections indicate global increases in the range of 1-3%$^{o}C^{-1}$ (Allan and Soden 2007). Increases in extreme precipitation rates can however be expected to follow the amount of water in the atmosphere hence is likely to increase faster than the mean.

Warm temperature extremes (eg heatwaves) are also projected to increase (see Figure 7),

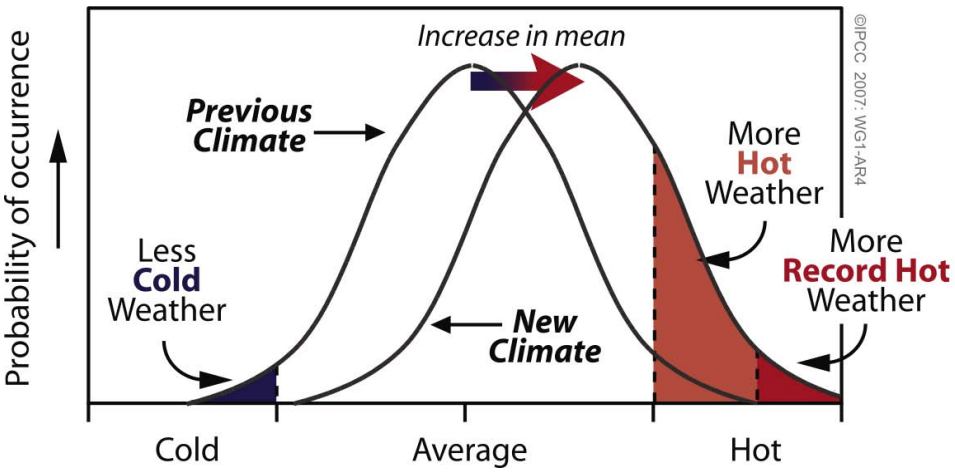

Figure 7 Schematic diagramme showing effect of an increase in the mean temperature in frequency of extreme temperatures. IPCC AR4 WGI Box TS.5,

Table 2 Observed and projected changes in extreme weather events.

Phenomenona and direction of trend	Likelihood that trend occurred in late 20th century (typically post 1960)	Likelihood of a human contribution to observed trend b	Likelihood of future trends based on projections for 21st century using SRES scenarios
Warmer and fewer cold days and nights over most land areas	*Very likely c*	*Likely d*	*Virtually certain d*
Warmer and more frequent hot days and nights over most land areas	*Very likely e*	*Likely (nights) d*	*Virtually certain d*
Warm spells / heat waves. Frequency increases over most land areas	*Likely*	*More likely than not f*	*Very likely*
Heavy precipitation events. Frequency (or proportion of total rainfall from heavy falls) increases over most areas	*Likely*	*More likely than not f*	*Very likely*
Area affected by droughts increases	*Likely in many regions since 1970s*	*More likely than not*	*Likely*
Intense tropical cyclone activity increases	*Likely in some regions since 1970*	*More likely than not f*	*Likely*
Increased incidence of extreme high sea level (excludes tsunamis) g	*Likely*	*More likely than not f, h*	*Likely i*

Source: IPCC AR4 WGI Table SPM.2. Original footnotes to this table refer to WGI Chapters and are retained here; a See Table 3.7 for further details regarding defi nitions.; b See Table TS.4, Box TS.5 and Table 9.4; c Decreased frequency of cold days and nights (coldest 10%); d Warming of the most extreme days and nights each year; e Increased frequency of hot days and nights (hottest 10%); f Magnitude of anthropogenic contributions not assessed. Attribution for these phenomena based on expert judgement rather than formal attribution studies. g Extreme high sea level depends on average sea level and on regional weather systems. It is defi ned here as the highest 1% of hourly values of observed sea level at a station for a given reference period.; h Changes in observed extreme high sea level closely follow the changes in average sea level. {5.5} It is very likely that anthropogenic activity contributed to a rise in average sea level. {9.5}; i In all scenarios, the projected global average sea level at 2100 is higher than in the reference period. {10.6} The effect of changes in regional weather systems on sea level extremes has not been assessed.

Regional projections

A major improvement since the TAR is the higher confidence in projected patterns of climate change at the regional level. This is important for projecting impacts and designing adaptation responses to projected climate change. Figure 8 illustrates the broad consistency between observations and projections of temperature in six world regions.

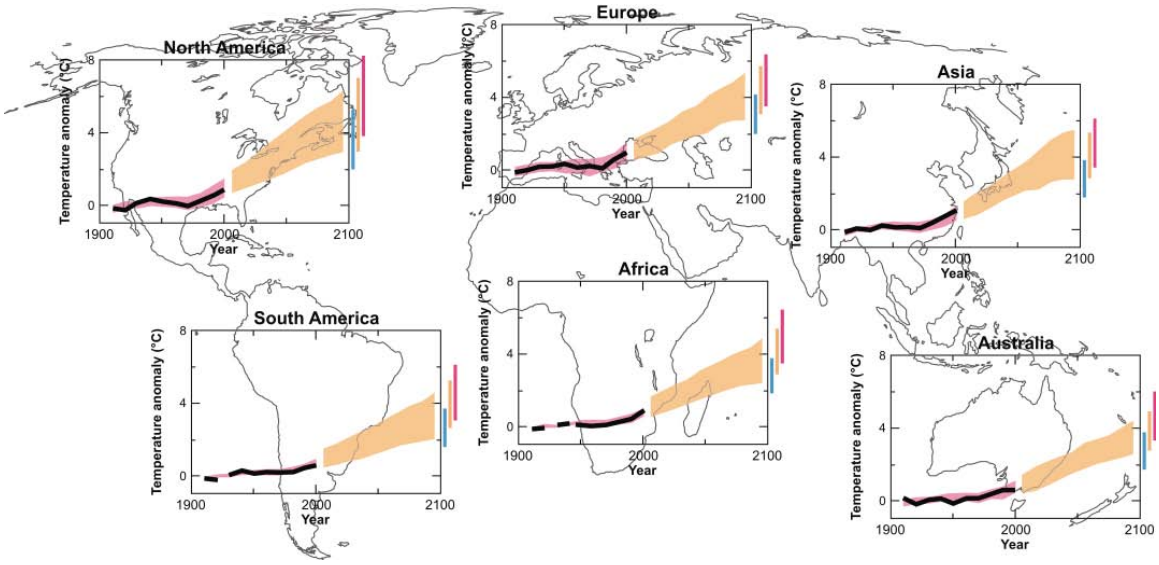

Figure 8 Projected regional changes in temperature compared to observations. Black line is the temperature anomalies fopr for the 1906-2005 period relative to the 1901-1950 period. The envelopes to the right of this are the model projections to 2100 for the A1B scenario. The bars at the end are the ranges for 2091-2100 for the SRES B1 (blue –lowest), A1B (orange – middle) and A2 (red –upper) scenarios. IPCC AR4 WGI Box 11.1,

Carbon cycle climate coupling

The coupling between the carbon cycle[14] and climate is important for determining the response of the climate system to the added greenhouse gases, including fossil CO_2. The AR4 has confirmed the assessment made in the TAR that warming tends to reduce land and ocean uptake of atmospheric carbon dioxide. This increases the fraction of anthropogenic emissions that remains in the atmosphere and can also add CO_2 if warming leads to release of carbon from soils. The magnitude of this feedback remains uncertain.

The overall stronger climate-carbon cycle feedbacks found in the AR4 assessment increases the upper range of temperature increase projected for each emission scenario. For example the global average warming at 2100 for the IPCC SRES A2 scenario is

[14] See IPCC Glossary http://ipcc-wg1.ucar.edu/wg1/Report/AR4WG1_Print_Annexes.pdf

increased more than 1°C. Another way of looking at the implications of a stronger coupling of climate and the carbon cycle is in relation to the emissions required for stabilizing CO_2 at specific levels. A stronger feedback from warming decreases the CO_2 emissions that are allowed to limit increase to a particular CO_2 stabilization level. In the case of a 450 ppm CO_2 stabilization level stronger climate-carbon cycle feedbacks reduce the cumulative allowed emissions over the 21st century from approximately 670 GtC to approximately 490 GtC,

Oceanic acidification

Whilst much of the emphasis in contemporary debates about climate change has been on changes in climate variables such as global mean temperature, extremes in precipitation and heatwaves etc, added CO_2 to the atmosphere has significant direct effects on the climate system. One of these effects is the increasing acidification of the ocean, which was previously overlooked and which is projected to have negative effects on marine shell forming organisms and species and ecosystems dependent on them[15]. The increase in CO_2 from preindustrial times to the present has deceased the ocean pH by about 0.1 Projections using the IPCC SRES emission scenarios show a further reduction in pH of 0.14-0.35 to 2100 (Figure 9).

[15] See IPCC WGII AR4 report at http://www.ipcc-wg2.org/ Technical Summary and Chapter 4.

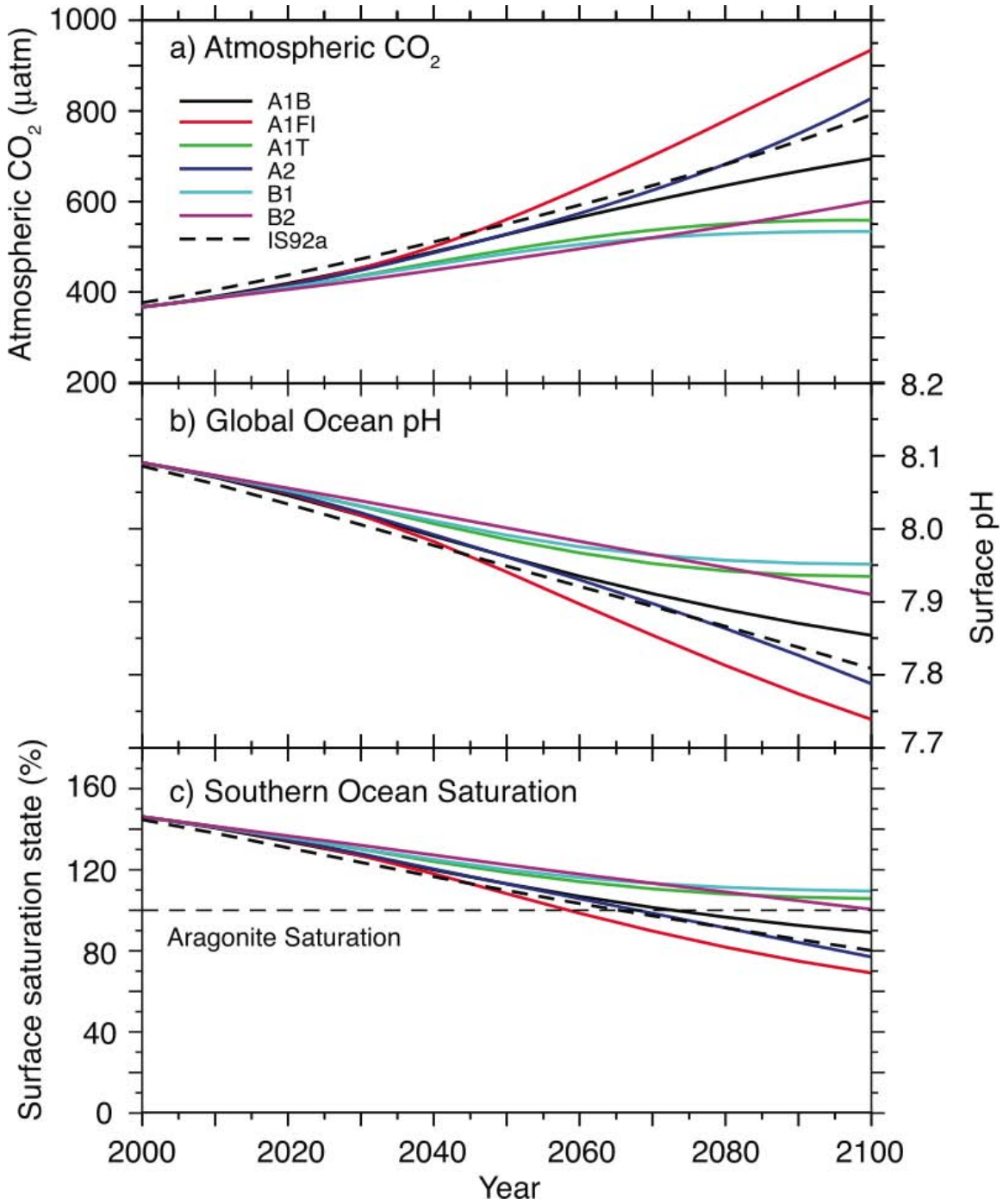

Figure 9 Projected changes in average surface pH for IPCC SRES emissions scenarios and the IS92a scenario. From IPCC AR4 WGI Figure 10.24.

IPCC sea level projections: increasing uncertainty

Over the course of the four main IPCC assessments, from the first in 1990 to the AR4, projection of sea level rise has been a difficult subject, not least because of the question of the response of the ice sheets of Greenland and Antarctica to warming. If melted Greenland and the West Antarctic ice sheets would raise sea level (over many centuries to millennia) by about 6 and 5 metres respectively. Unlike earlier assessments the AR4 does not however have a chapter devoted to this issue. Whereas in the earlier parts of this review I have essentially summarized the findings of the AR4, the sea level rise projection are sufficiently uncertain to warrant a different and more critical approach.

Sea level rise under global warming is essentially due to the response of four main terms: Thermal expansion of the oceans due to warming, the melting of mountain glaciers and small ice caps, and the response of the Greenland and Antarctica ice sheets. Thermal expansion is modeled using AOGCMs or EMICs (Earth System Models of Intermediate Complexity) and in principle is reasonably well constrained, although significant uncertainties remain surrounding heat uptake by the oceans. The response of glaciers and ice caps is also reasonably well bounded, although debate remains on the total volume if ice in these and the rate at which it may be lost (Meier, Dyurgerov et al. 2007). The response of the ice sheets is projected with continental ice sheet models which at present do not describe the fast ice dynamics of ice streams, which are likely to play a major role in the response of ice sheets to warming (Bamber, Alley et al. 2007). Observations of ice sheet changes in recent decades and model base projections appear to be diverging. Table 3 compares observational and model estimates of each of the terms with the total observed sea level rise for the period 1993-2003. The sum of the observational estimates of each term and the observed total SLR are in broad agreement given the overall level of uncertainties: 2.8±0.7 mm/yr vs 3.1± 0.7 mm/yr respectively.

The sum of the modeled estimates of each term and the observed total SLR appear to be quite divergent: 2.0 ± 0.8 mm/yr vs 3.1± 0.7 mm/yr. The main source of this divergence appears to lie in the ice sheet contributions. The Greenland ice sheet observed losses appear to be bigger than the modeled losses, and for Antarctic the observed loss is of the opposite sign to the modeled mass increase. For Antarctica, present continental ice sheet models predict an increase in mass (sea level lowering) with moderate warming due to increased precipitation over the continent, which remains too cold for significant melting. Ice sheet models for Greenland on the other hand predict a negative surface mass balance for this ice sheet at a global average warming above pre-industrial over 1.9°C to 4.6°C.

The ice sheet models used in this assessment at present predominantly estimate surface mass balance changes, with little ice dynamic effects. Observed losses in Greenland have a substantial dynamical component due to accelerated flow of ice streams. In the case of the West Antarctic, which dominates the mass balance of Antarctica, the negative mass balance is essentially due to accelerated ice stream flow (Bamber, Alley et al. 2007).

Table 3 Observed and modelled sources of sea level rise 1993-2003.

Source of sea level rise 1993-2003	Observed mm/yr	Modeled mm/yr
Thermal expansion	**1.60± 0.50**	**1.5± 0.7**
Glaciers and ice caps	**0.77± 0.22**	**0.6± 0.3**
Greenland ice sheet	**0.21± 0.07**	**0.1± 0.1**
Antarctic ice sheet	**0.21±0.35**	**-0.2± 0.4**
Sum of contributions	**2.8±0.7**	**2.0 ± 0.8**
Observed total SLR	**3.1± 0.7**	
Difference (Observed SLR less sum of contributions	**0.3 ± 1.0**	**1.1 ± 1.1**

Sources: The observed column is from IPCC WGI AR4 Table 9.2 and the entries under the modelled column for thermal expansion and glaciers and ice caps are also from this table for all the data that includes all forcings. The entries for the ice sheets are from the estimates reported in Chapter 9 for the 1993-2003 period from models, although not the same model set ups as for the other modelled terms.

The AR4 sea level rise projections are summarized in Table 4 and expressly are described as not including rapid dynamical changes in ice flow. Figure 10 shows each of the terms of the sea level rise projections for the SRES scenarios and added to it is a line added to show the consequence to 2100 if the rate of sea level rise remain unchanged at the 1993-2003 levels. The range of sea level rise projections for the IPCC SRES scenarios is, at its high end, substantially lower than in the earlier assessments (see Table 1) and as can be seen from Figure 10 not greatly outside the rate of rise that is estimated for 1993-2003. If this could be considered a robust finding it would result in a lowered risk assessment for sea level rise impacts compared to earlier assessments. The state of the science does not however permit this conclusion.

Table 4 AR4 Sea level rise projections

	Sea Level Rise (m at 2090-2099 relative to 1980-1999)
Case	Model-based range excluding future rapid dynamical changes in ice flow
B1 scenario	0.18 – 0.38
A1T scenario	0.20 – 0.45
B2 scenario	0.20 – 0.43
A1B scenario	0.21 – 0.48
A2 scenario	0.23 – 0.51
A1FI scenario	0.26 – 0.59

Note that the projection includes the part of the present ice sheet mass imbalance that is due to recent ice flow acceleration and assumes that this will persist unchanged.
Source: From IPCC AR4 WGI Table SPM.3.

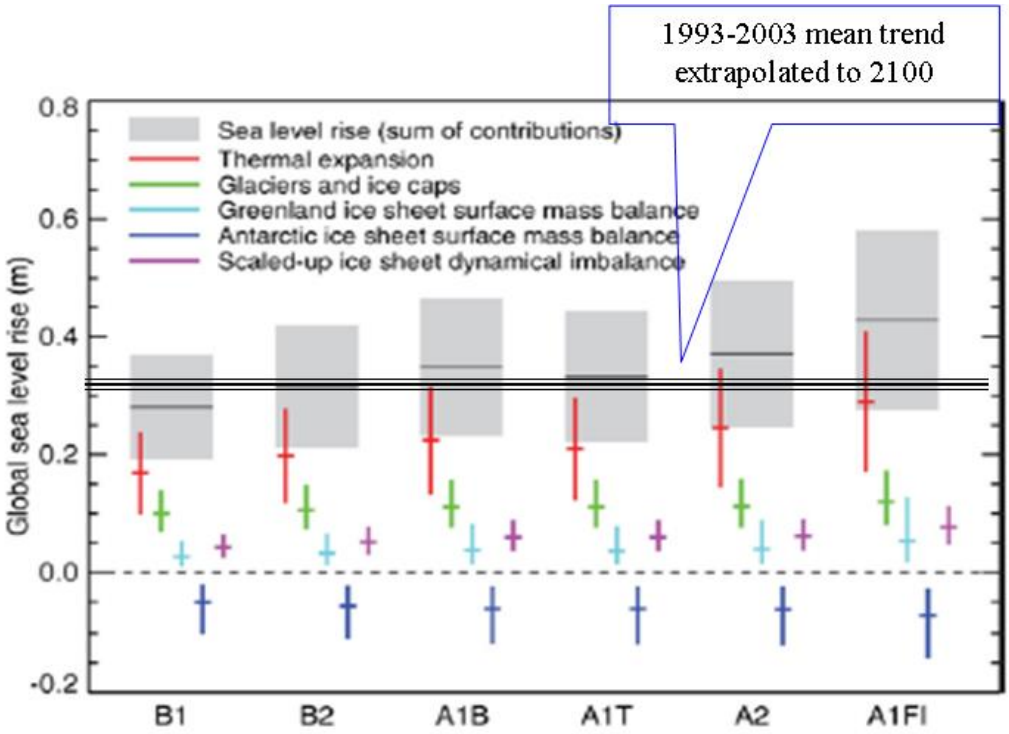

Figure 10 AR4 Sea level rise projections. Projections for total sea level rise for each of the components of sea level rise. Note that the AR4 projection shown in Table 4 does not include the scaled up ice sheet dynamical imbalance shown in this figure. The added line shows the 1993-2003 trend extended for a century unchanged. Adapted from IPCC WGI AR4 Figure 10.33.

A recent attempt to project sea level rise using a semi empirical method based on recent observations of surface temperature and sea level change, using the SRES scenarios, has estimated the likely sea level rise to 2100 to be 0.5-1.4 m (Rahmstorf 2007) A sea level rise in this range and for these emissions scenarios would require only that the observed linear relationship over the last century between SLR rate and temperature persist for the next century (Rahmstorf 2007). The lower end of this range for the same scenarios is very close to the top end of the AR4 range, implying that the uncertainty in sea level rise projections is much larger than would be inferred from the AR4 sea level rise assessment,

The possibility of accelerated ice flow in the 21st century from Greenland and West Antarctic ice sheets (or parts of the East Antarctic ice sheet) cannot be excluded and cannot at present be

reliably quantified. For both ice sheets recent accelerations in ice flow have contributed significantly to recent observed sea level rise but this is not included in the models used in the AR4 assessment. Recent advances in ice sheet modeling (Schoof 2007) tend to support theories advance in the 1960s and 70s that the West Antarctic ice sheets may be unstable to warming (Mercer 1968; Weertman 1974; Mercer 1978). It is to be hoped that by the time of the next IPCC assessment sufficient advances have been made in this are to permit a robust assessment of the risks of sea level rise from the Greenland and Antarctic ice sheets.

Conclusions

The IPCC is a unique international scientific assessment body that has produced consistently high quality state of the art assessments of all aspects of climate change since its inception in 1988. The Fourth Assessment Report is a milestone achievement in this context for the scientific community as whole, involving as it has hundreds of working scientists over several years. The issues raised in this overview and perspective on the AR4 point to necessary developments in the scientific understanding of climate change, particularly here in relation to sea level rise. They also point to ways in which the IPCC can learn so as to guarantee the scientific quality and policy relevance of its next assessment reports,

References

Agrawala, S. (1998). "Context and Early Origins of the Intergovernmental Panel on Climate Change." Climatic Change **39**(4): 605-620.

Allan, R. P. and B. J. Soden (2007). "Large discrepancy between observed and simulated precipitation trends in the ascending and descending branches of the tropical circulation." Geophys. Res. Lett. **34**(18): 1-6.

Arrhenius, S. (1897). "On the Influence of Carbonic Acid in the Air upon the Temperature of the Earth." Publications of the Astronomical Society of the Pacific **9**(54): 14.

Bamber, J. L., R. B. Alley, et al. (2007). "Rapid response of modern day ice sheets to external forcing." Earth and Planetary Science Letters **257**(1-2): 1-13.

Eisenman, I., N. Untersteiner, et al. (2007). "On the reliability of simulated Arctic sea ice in global climate models." Geophys. Res. Lett. **34**(10): 1-4.
IPCC, S. Solomon, et al., Eds. (2007). Climate Change 2007: The Physical Science Basis. Contribution of Working Group I to the Fourth Assessment Report of the Intergovernmental Panel on Climate Change. Cambridge, United Kingdom and New York, NY, USA, Cambridge University Press.
Kerr, R. A. (2007). "CLIMATE CHANGE: Is Battered Arctic Sea Ice Down For the Count?" Science **318**(5847): 33a-34.
Meier, M. F., M. B. Dyurgerov, et al. (2007). "Glaciers Dominate Eustatic Sea-Level Rise in the 21st Century." Science **317**(5841): 1064.
Mercer, J. H. (1968). Antarctic Ice and Sangamon Sea Level. Commission of Snow and Ice: Reports and Discussions, Bern, International Association of Scientific Hydrology.
Mercer, J. H. (1978). "West Antarctic Ice Sheet and Co2 Greenhouse Effect - Threat of Disaster." Nature **271**(5643): 321-325.
Peixoto, J. P. and A. H. Oort (1992). Physics of Climate, Amer Inst of Physics.
Rahmstorf, S. (2007). "A Semi-Empirical Approach to Projecting Future Sea-Level Rise." Science **315**(5810): 368-370.
Schoof, C. (2007). "Ice sheet grounding line dynamics: Steady states, stability, and hysteresis." J. Geophys. Res. **112**(F3): 1-19.
Stroeve, J., M. M. Holland, et al. (2007). "Arctic sea ice decline: Faster than forecast." Geophys. Res. Lett. **34**(9): 1-5.
Trenberth, K. E., A. Dai, et al. (2003). "The changing character of precipitation." Bull. Amer. Meteor. Soc **84**(9): 1205-1217.
Trenberth, K. E. and D. J. Shea (2005). "Relationships between precipitation and surface temperature." Geophys. Res. Lett. **32**(14): 1-4.
Weertman, J. (1974). "Stability of the junction of an ice sheet and an ice shelf." Journal of Glaciology **13**(67): 3-11.

The astronmical theory of palaeoclimates

Michel Crucifix
Institut d'Astronomie et de Géophysique G. Lemaître
Université catholique de Louvain
Louvain-la-Neuve, Belgium

1 Introduction

The climate system is characterised by a spectrum of temporal variations ranging from the minute to several million years (Mitchell, 1976). For example, the cyclonic depressions perturbing regularly our weather manifest a conversion of potential energy into kinetic energy (Peixoto and Oort [1992], p. 378). The cycle takes a few days to complete. In the El-Niño phenomenon, energy and momentum are exchanged between the atmosphere and the upper layer of the ocean. The associated disturbances are propagated via mechanic waves, called Rossby and Kelvin waves, the lifetime of which is several months (Dijkstra [2005], ch. 7). Here, we are interested in an oscillation occurring over several tens of thousand years: the waxing and waning of large ice sheets in the northern hemisphere. We are presently in an *interglacial period* (the "Holocene). The last ice "wax", called the Last Glacial Maximum, occurred between 22 and 19,000 years ago (Yokoyama et al., 2000). About 42 millions cubic kilometres of ice were then distributed over Northern America, Scandinavia and the British Isles, plus an additional 10 millions compared to today over Greenland and Antarctica (Peltier, 2004). This represents all together a sea-level drop of about 130 m compared to today. The previous interglacial occurred roughly between −130 and −110 kyr ago (Kukla, 2000) (kyr = 1000 yr; see also key to symbols).

Sediments accumulated on the ocean floor reveal that glacial-interglacial cycles pace climate since 3 million years (Ruddiman et al., 1986). They are not truly periodic, but they seem organised. From −3 Myr to − 800 kyr, glacial-interglacial cycles occurred according to a smooth periodic cycle of about 40 kyr. Glacial-interglacial cycles then became longer and asymmetric (Hays et al., 1976; Imbrie et al., 1984) with ice volume growing during approximately 80 kyr, followed by a deglaciation spanning roughly 10 kyr. The low ice-volume episode is characterised by relatively steady and high atmospheric concentrations of carbon dioxide (280 ppmv), methane (450 – 600 ppbv) and Antarctic temperatures (EPICA community members, 2004 ; Siegenthaler et al., 2005). Hays et al. [1976] were the firsts to identify periods of 19, 21, 40 and 100 kyr in marine sediments records spanning the last 700 kyr. They noted the coincidence of these periods and those characterising the cycles of certain elements of the Earth orbit, namely eccentricity (100 kyr), obliquity (40 kyr) and precession (19 and 21 kyr) calculated by Berger [1978] on the basis of theoretical works by Vernekar [1972] and Bretagnon [1974] [1]. The dominant thinking has since been that glacial-interglacial

[1] Berger's publication appeared in 1978, but his calculations are already quoted in the Hays et al. Science article.

cycles are caused by changes in Earth orbital elements, as first suggested by Adhémar [1842] and Croll [1875] (the name of Milankovitch [1998] is customary quoted because he was the first one to develop a complete supporting mathematical theory and his book, *the canon of insolation*, is still used as a reference).

Experiments with models of the general circulation of the atmosphere (e.g.: Gallimore and Kutzbach, 1995; Kutzbach and Liu, 1997) clearly demonstrate that realistic changes in orbital parameters influence climate significantly. However, whether the orbital forcing drives climate deterministically on long time scales is still a matter of debate. As early as 20 years ago, Nicolis and Nicolis [1986] attempted to infer the largest Lyapunov exponent characterising the climate evolution of the last million years (they used the 1 Myr deep-sea record of Shackleton and Opdyke [1973] and applied the analysis technique of Wolf et al. [1985]). They concluded that it might not be possible to predict climate much beyond 25-40 kyr because of its intrinsic chaotic nature. More recently, Wunsch [2003] noted that only 15 % of the variance in the marine record of the last 800 kyr lies in the 18-26 and 33-53 kyr bands, thereby implying that at most 15 % of multi-millenial climate variations can be explained as a linear response to the orbital forcing. As a consequence, two alternative paradigms to Milankovitch's view that orbital forcing "drives" glacial-interglacial cycles have been claimed to at least deserve careful consideration: (a) linear interference: the effect of the astronomical forcing just linearly superimposes on a limit cycle (the glacial-interglacial cycle) that would naturally occur as a result of non-linear interactions within the climate system (Wunsch, 2003) and (b) non-linear resonance, or "phase locking": glacial-interglacial cycles manifest a limit cycle of the climate system (they would appear without any external perturbation), but the orbital forcing sets their timing. It is said in that case that the orbital forcing is a pacemaker (the expression is probably from Hays et al. [1976]).

In fact, the most recent literature suggests that climate may have shifted from one regime to the next. Namely, Lisiecki and Raymo [2007] note that amplitude modulations of obliquity are reproduced quasi-linearly in the palaeoclimate record before – 1.4 Myr. This suggests that obliquity linearly drives ice volume at least between – 3 and – 1.4 Myr. They also observe that obliquity amplitude modulations no longer appear in the climate record after –1.4 Myr but, on the other hand, Huybers [2007] note that deglaciations keep almost systematically occurring when obliquity is near a maximum. The latter is highly suggestive of non-linear resonance (Tziperman et al., 2006).

This paper attempts to introduce the reader to the mathematical formalism needed to understand and predict climate variations at the multi-millenial time. It will also address the question of the timing of the next glacial inception. It was already shown that this enterprise requires (a) a solution for the Earth's orbital elements valid over several thousands of years: this is the object of section 2, and (b) a model of climate valid at the corresponding timescales. Several strategies exist and we will attempt to identify their advantages and drawbacks. We conclude on what we would consider to be promising future research directions.

2 Calculating astronomical parameters and insolation

The amount of solar energy received on a surface tangent to the Earth per unit time before its interaction with the atmosphere is called *insolation* (stands for: incoming solar radiation). Insolation averaged over a true solar day is denoted W:

$$
\begin{aligned}
W &= \frac{S}{\pi\rho^2}(H_0 \sin\phi\sin\delta + \sin H_0 \cos\phi\cos\delta) \\
\rho &= \frac{1-e^2}{1+e\cos\nu} \\
\sin\delta &= \sin\varepsilon\sin\lambda \\
H_0 &= \begin{cases} 0, \text{ for } \tan\phi\tan\delta < -1 \\ \pi, \text{ for } \tan\phi\tan\delta > -1 \\ \arccos(\tan\phi\tan\delta) \text{ otherwise} \end{cases}
\end{aligned}
\qquad (1)
$$

(see Key to symbols and Figure 2). The true anomaly (ν) is expressed as a function of time by inverting Kepler's third law (e.g., Brouwer and Clemence [1961], p. 62). Figure 3 (*top left*) shows the mean month-latitude distribution of W assuming ε = 23°20' and e=0. The iso-contours are known as Milankovitch curves because they first appeared in his book (Milankovitch [1998], p. 331). Also shown are the effects of a 1° increase in obliquity and that of an eccentricity of 0.05 with different phases of the longitude of perihelion.

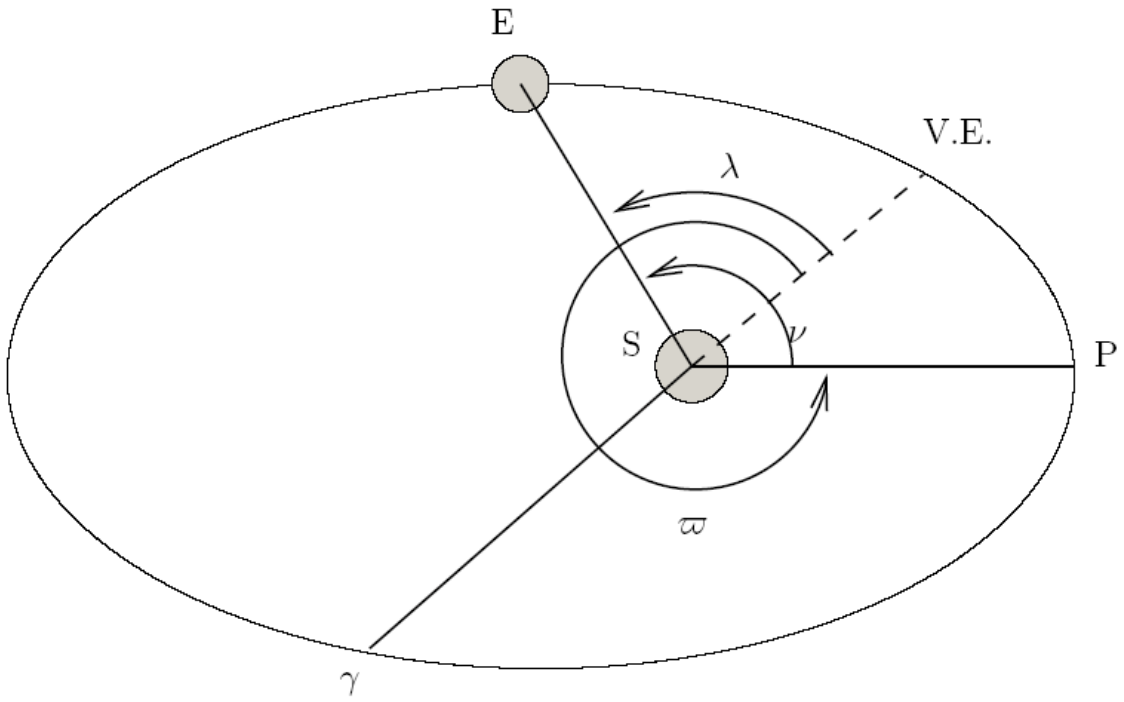

Figure 2: Heliocentric angles relevant for the astronomical theory of climate. *S* stands for Sun, *E* for Earth, *P* for perihelion and V.E. for vernal equinox. See key to other symbols at the end of this article.

Increasing obliquity produces an increase in annual mean insolation poleward of 43°N and 43°S, and a decrease equatorward of these latitudes. Precession has no effect on annual mean insolation but it may greatly modify its seasonal distribution.

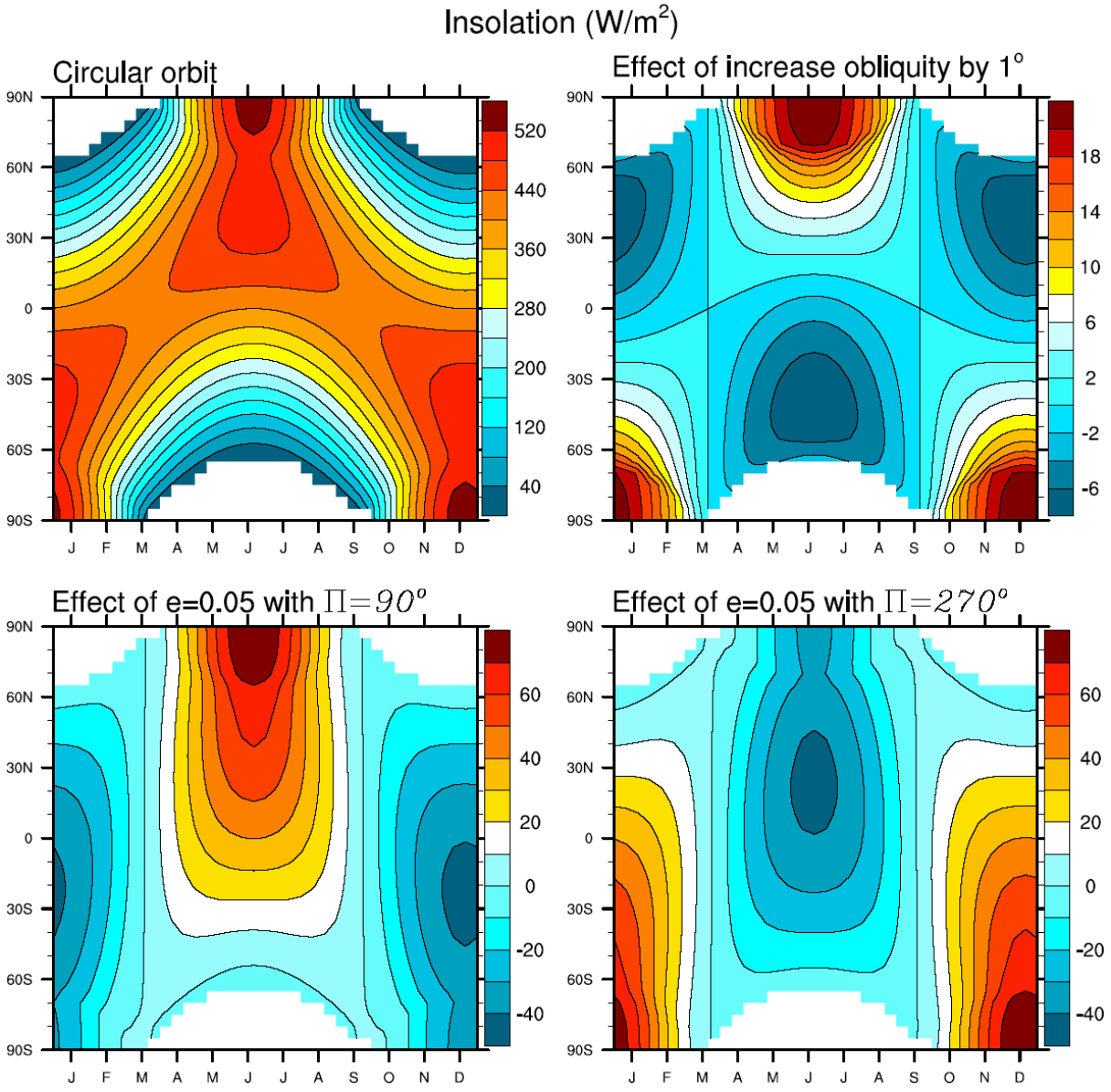

Figure 3: Insolation plotted as a function of latitude (Y-axis) and month (X-axis). The isocontours are called *Milankovitch curves*. The upper-left plot represents the absolute value assuming a circular orbit, while the three other plots give the effect of an increase in obliquity, or that of a non-zero eccentricity with perihelion occurring either in summer (ϖ = 90°) or in winter (ϖ = 270°). Note the different scales and also that an increase in obliquity reduces the annual mean insolation between 43°N and 43°S.

The following step is to determine the long-term variations of a, e, ε and ϖ. The variations of the semi-major axis of the Earth (a) are so small that they do not induce any noticeable change of the mean Earth-Sun distance over the past 250 million years (Laskar et al., 2004), so we can safely assume that a is constant. Eccentricity is obtained from a perturbation of the two-body problem by the other planets first formalised by Lagrange[1781]. The movement of the perihelion with respect to the moving vernal equinox is the combination of two effects: the first one is the general precession in which the torque of the Sun, the Moon and the planets on the Earth's equatorial bulge causes the axis of Earth rotation to wobble like a spinning top with a period of ~ 25,800 years; the second one is the rotation of the elliptical figure of the Earth's orbit relative to the stars, at a period of 100 kyr. The two effects together produce the

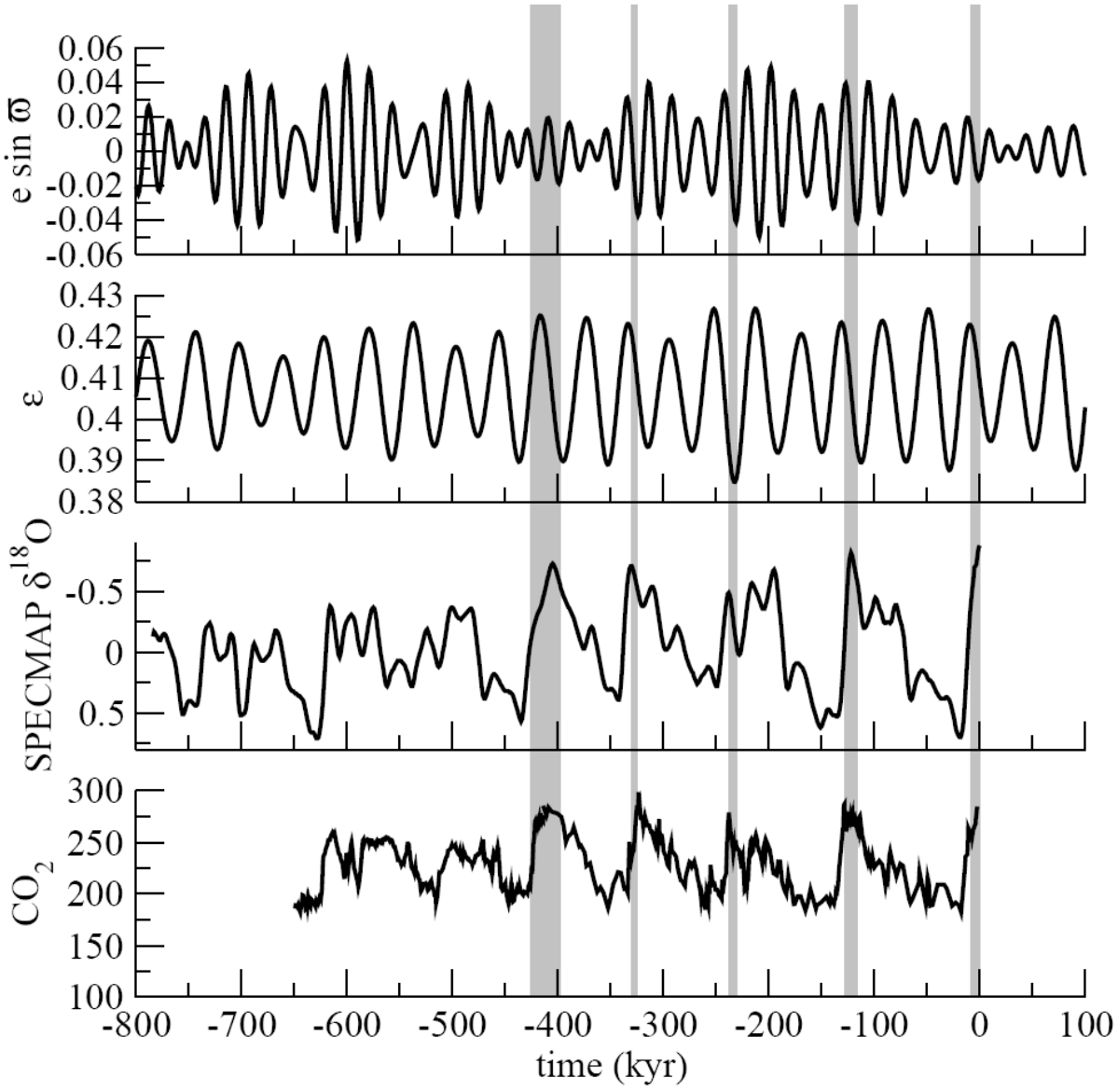

Figure 1: Long term variations of (a) the climatic precession parameter, (b) obliquity, (c) the normalised oxygen isotopic ratio of benthic foraminifera (the Y-axis is configured such that sea-level increases upwards (ice volume increases downwards) and (d) atmospheric CO_2 concentration (in ppmv) reconstructed from ice core records (Petit et al., 1999; Siegenthaler et al., 2005). Time zero corresponds to year 1950 AD. Vertical shadings

indicate interglacials, identified here as periods of CO_2 high stand. Data timescales are taken from the corresponding references.

climatic precession, the mean period of which is 21 kyr. Berger [1978] obtained an analytical solution of the expressions of climatic precession, obliquity and eccentricity available in the following form:

$$\begin{aligned} e\sin\varpi &= \sum_i P_i \sin(\alpha_i t + \eta_i) \\ \varepsilon &= \varepsilon^* + \sum_i A_i \cos(\gamma_i t + \varsigma_i) \\ e &= e^* + \sum_i E_i \cos(\lambda_i t + \phi_i) \end{aligned} \qquad (2)$$

The *climatic precession parameter* ($e\sin\varpi$) provides a measure of the Sun-Earth distance at northern hemisphere's summer solstice. Berger [1978] provides tabulated values of frequency spectrum of orbital parameters (α_i, γ_i and λ_i), along with their amplitudes (P_i, A_i and E_i) and phases (η_i, ζ_i and ϕ_i). Namely, precession is dominated by four periods (23.7, 22.4, 18.9 and 19.1 kyr) and obliquity varies between 22 and 25 with a period of approximately 41 kyr. Eccentricity varies between 0 and 0.05 with periods of 404, 95, 124, 99 and 131 kyr.
Eccentricity is presently small (e=0.017) and the orbit will be very close to a circle in 27 kyr. This situation occurs every 400 kyr. Northern summer solstice occurs today at aphelion. It occurred at perihelion (closest to the Sun) 11 kyr ago (Figure 1).
System (2) provides a solution of suitable precision over roughly ±1 Myr. Numerical integrations have a better accuracy (Laskar et al., 2004 provides a solution roughly valid for ± 20 Myr) but the chaotic nature of the planetary system puts an ultimate limit on the predictability of orbital parameters (Laskar, 1999). It was shown that the choice between two realisations of an ensemble of likely astronomical solutions may however skilfully be guided by identifying interference patterns (beatings) in several-million-year-long geological records (Lourens et al., 2001; Pälike and Shackelton, 2000; Pälike et al., 2004).

3 Climate dynamics at orbital time scales

3.1 General principles

So far we have seen how to compute insolation. Now we need a suitable climate model. The first task is to identify climatic components likely to determine the dynamical characteristics of climate evolution at the orbital time scales. We are thus looking for structures in the climate system having characteristic response time scales of at least several millennia. These are — mainly — the terrestrial biosphere, the oceans, ice sheets (like Greenland or the Northern American ice sheet) and the lithosphere-asthenosphere ensemble (roughly, the upper 300 km of the solid Earth). These slow structures communicate together essentially via the lower 15 km of the atmosphere (this is the troposphere) and, as we shall later see, via changes in sea-level.

- **The atmosphere, to which one can formally associate the continental surface and the "mixed layer" of the ocean (the upper 5 to 50 m),** carries information from one slow component to the next via its dynamical, thermodynamical and chemical properties. It also communicates the effects of changes in Earth orbit to the slow components. The dynamics of the atmosphere are particularly complex and they are usually modelled with 3-dimensional general circulation models. It was established that a reduction in incoming summer insolation (for example, due to the climatic precession effect) increases the net accumulation rate of snow on glaciers (Gallimore and Kutzbach, 1995; Khodri et al., 2001 and Vettoretti and Peltier 2003). Conversely, an increase in summer insolation generally enhances subtropical weather systems, especially African and Indian monsoon (Kutzbach, 1981; Joussaume et al., 1999; Zhao et al., 2005). The atmosphere also responds to an increase in greenhouse gas concentrations by a global warming amplified near the poles (Manabe and Stouffer, 1980; IPCC, 2001; Alexeev et al., 2005). Clouds exert a potentially important but highly uncertain role in amplifying or reducing the effects of changes in ice sheet topography, greenhouse gas concentrations and orbital forcing (Webb et al., 2006; Crucifix, 2006).
- **The terrestrial biosphere** responds to climatic change and, in general, this response amplifies the original climatic change (Claussen et al., 2001; Meir et al., 2006). Namely, expansion of vegetation favoured by an increase in temperature or precipitation results in more absorption of sunlight by the surface (tends to further increase temperature) and increased latent heat release in the atmosphere (may enhance precipitation in semi-arid areas). The biosphere is also a reservoir of organic carbon but how its content responds to climate change is the result of two competing effects difficult to quantify: photosynthesis contributes to store carbon in the soil (photosynthesis rate is sensitive to the concentration of CO_2, temperature and water availability) but heterotrophic respiration (highly sensitive to temperature and humidity) puts in back to the atmosphere. The direct effects of vegetation changes on climate through heat and moisture exchanges are quite rapid, while the biogeochemical impact may take several thousand years to complete (Lenton et al. 2006, Sheffer et al. 2006, Meir et al., 2006).
- **The oceans** also contribute actively to climate dynamics by their physics and biogeochemistry. Poleward heat transport by oceanic currents — partly materialised by surface western boundary currents such as the Gulf Stream and its northerly prolongation, the North Atlantic drift — regulate the formation of sea-ice and promote evaporation at high latitudes (see, for example, Peixoto and Oort [1992] p. 365 for a general introductory text). There is good evidence that the North Atlantic drift extends less to the North during glacial times (Duplessy et al., 1975; Sarnthein et al., 2003; Lynch-Stieglitz et al., 2007), which enhances the cooling effect of the polar ice caps. Besides, the ocean is a gigantesque reservoir of inorganic carbon, either under dissolved form, or stored in the form of calcite ($CaCO_3$) in deep-sea sediments. It is easily seen that the ocean acts as an effective carbon pump by the fact that the deep ocean contains about 6 % more dissolved inorganic carbon per unit volume than the surface (Broecker and Peng, 1987; Levitus and Boyer, 1994). Part of this difference is due to the biological activity (photosynthesis near the surface, and respiration at depth) but it is also determined by the structure of the ocean circulation (Archer et al., 2000). Calcite stored in the sediment has a particularly perverse role (Broecker and Peng, 1987). Dissolution of calcite increases water pH, which shifts the chemical equilibrium of the carbonate oxydo-reduction system in such a way that further

atmospheric CO_2 is absorbed by the oceans. It may be shown that this effect results in a slow positive feedback to oceanic absorption of CO_2 (Broecker and Peng, 1987). Sediment dissolution will ultimately compensate for anthropogenic emissions of carbon dioxide but this may take several tens of thousand years to complete (Archer 2005).

- **Ice sheets** store ice on their large accumulation zones (where the net annual ice mass balance is positive) and loose it on their sides (ablation zones) by melting and iceberg production. Steady state is achieved by a dynamical ice flow from the accumulation zone towards the ablation zones. The characteristic time scale of this flow is of the order of ten thousand years (this is the Nye time scale, see Paterson [1994] p. 279). Ice sheets cool the atmosphere because they have a high albedo and also because their temperature never exceeds 0°C (they constitute a reservoir of latent heat). At last, ice sheets are an important reservoir of freshwater which, when released into the oceans via the rivers or because of iceberg production, may reduce or even disrupt ocean vertical mixing (e.g.: Rahmstorf 2002).
- **The lithosphere** may be viewed as 60 to 100-km thick elastic membrane lying above a viscous-plastic medium (the asthenosphere) (see, e.g.: Peltier, 1974; Lambeck et al., 1996; Peltier et al., 2002). The lithosphere deforms when ice accumulates, and the characteristic time of this deformation is about 5000 years. The resulting depression is about a third of the ice sheet thickness. This phenomenon is called isostasy. As will be shortly shown, isostasy interferes with the dynamics of ice sheets by modifying the altitude of the ablation zones. Isostatic deformation may also promote the formation of proglacial lakes, which are thought to reduce ice melting (Krinner et al. 2004).

In our quest to model the climate system, we are mainly looking for non-linear interactions between the different components. Indeed, non-linearity introduces the possibility of having several equilibriums (stable or unstable) and, hence, the possibility of a limit cycle between glacial and interglacial states. Here are three examples of non-linear mechanisms proposed in the literature thought to have played a role in glacial terminations.

- **Instability due to the nature of the sediment at the ice-sheet / lithosphere interface:** It was suggested that stability of the large ice sheets may be threatened by the fact that a significant portion of their basis lies on marine sediment, which is more "slippery" than continental bedrock (MacAyeal, 1993).
- **Instability caused by the isostatic response:** The depression of the lithosphere under ice effectively lowers the altitude of the ablation zones, which exposes them more to the effects of insolation changes. Furthermore, the slowness of the lithosphere rebound after deglaciation has begun to take place strengthens the altitude gradient of the ice sheet, which in turn increases the flow of ice from the accumulation area to the ablation area (Oerlemans, 1980; Birchfield and Ghil, 1993,Tarasov and Peltier, 1997; Crucifix et al., 2001). This may explain why deglaciation is so rapid once it has begun.
- **Interaction beween sea-level and the oceanic carbon pump.** Formation of sea-ice near the marine platforms of Antarctica causes the formation of a downsloping water current entraining carbon-rich water to the bottom of the ocean. Paillard and Parrenin [2004] then speculated that the efficiency of this pump is greatly reduced when sea level is low because there are less immersed continental platforms. The attractiveness of this mechanism is that it accounts for the observation inferred from the ice core record that a CO_2 increase slightly precedes the decrease in ice volume (Pépin et al. 2001).

At this stage, we know about a series of mechanisms that may potentially explain the dynamics of glacial-interglacial cycles. What is the appropriate strategy to model these interactions more quantitatively in order to gain explicative and predictive skill?

Geophysical fluids (atmosphere, ocean and ice) are difficult to compute, among other things because time and spatial scales are difficult to separate. For example, the general circulation of the ocean is influenced by deep-ocean convective towers occurring in the North Atlantic, the diameter of which is about 200 km (Klinger et al., 1996). Clouds, which effectively influence the radiative balance of the atmosphere, evolve on spatial scales of a few kilometres and their structure is determined by even much smaller scale processes (nucleation, droplet formation, precipitation etc.). Finally, the net mass balance of ice sheets results from an equilibrium between large accumulation areas and narrow ablation zones characterised by a complex topography and large temperature gradients. The ice flow *per se* is influenced by complex and highly non-linear features, such as meltwater channels and fractures.

Attempting to estimate accurately the global carbon, water and energy exchanges within the climate spatial by spatial and time aggregation of all these small processes would be vowed to failure. Any small error, far below what is currently measurable, would certainly grow over time (remember that the complete climate system is generally far from equilibrium). This is the reason why it would be unwise to run a general circulation model over several tens of thousands of years and just "see what it gives". There is no chance of reproducing glacial-interglacial cycles with the right timing. The appropriate modelling strategy must therefore use (a) our knowledge on the physics and sensitivity of each climatic component, and (b) information provided by the palaeoclimate climatic record.

Here, we explore two possibilities: low-order modelling and earth models of intermediate complexity.

3.2 Low-order modelling

One possibility is to construct a model of a few ordinary differential equations that somehow distillates the knowledge on the physics of the components of the climate system estimated to be relevant to describe glacial-interglacial cycles. Such a model must be physically reasonable and respect the elementary principles of energy, entropy and mass conservation. This approach is illustrated here with the Saltzman and Maasch [1990] model (SM90), but we note that other models exist, often simpler but perhaps less rigorously established (e.g.: Paillard, 1998; Tziperman and Gildor, 2003; Paillard and Parrenin [2004]):

$$\dot{\mu} = r_1\tau - r_2\eta - (r_3 - b_3 N)N - r_5 I - (r_4 + b_4 N^2)\mu + F_\mu$$
$$\dot{I} = -s_1\tau - s_2\mu + s_3\eta - s_4 I + F_I$$
$$\dot{N} = -c_0 I - c_2 N + F_N$$
$$\tau = -\alpha I + \beta\mu + F_\tau$$
$$\eta = e_I I + e_\mu\mu + F_\eta$$

with μ: carbon dioxide concentration, I: global volume of continental ice, N: a measure of the global thermohaline circulation of the ocean, τ: global mean temperature η: global mean

extent of sea-ice, and F: external forcing terms. All other factors are parameters. For example, r_1 parameterises the fact that increased global temperature causes a release of CO_2 by the simple effect of reduced solubility of CO_2 in seawater. The term $-r_2\,\eta$ implies that CO_2 tends to be reduced when sea-ice cover is large because it acts as a cap (for example, Stephens and Keeling, 2000, but see also Morales-Maqueda and Rahmstorf, 2002). First-order constraints on these parameterisations and associated parameters may be deduced from more explicit and specialised models of the individual components such as, for example, general circulation models of the atmosphere. On the other hand, it is perfectly acceptable to fine-tune these parameters to force a better agreement between the low-order model and the data in order to improve its predictive skill.

This process is illustrated on Figure 4. The red curve is the normalised ice volume reconstructed from a compilation of oceanic data by Imbrie et al. [1984]. The bold black curve is the realisation of SM90 using initial conditions and parameters given in the original publication. The only forcing term is $F_I=I_{65}$, the normalised summer solstice insolation at 65°N, in reference to Milankovitch's hypothesis that summer insolation determines glacial-

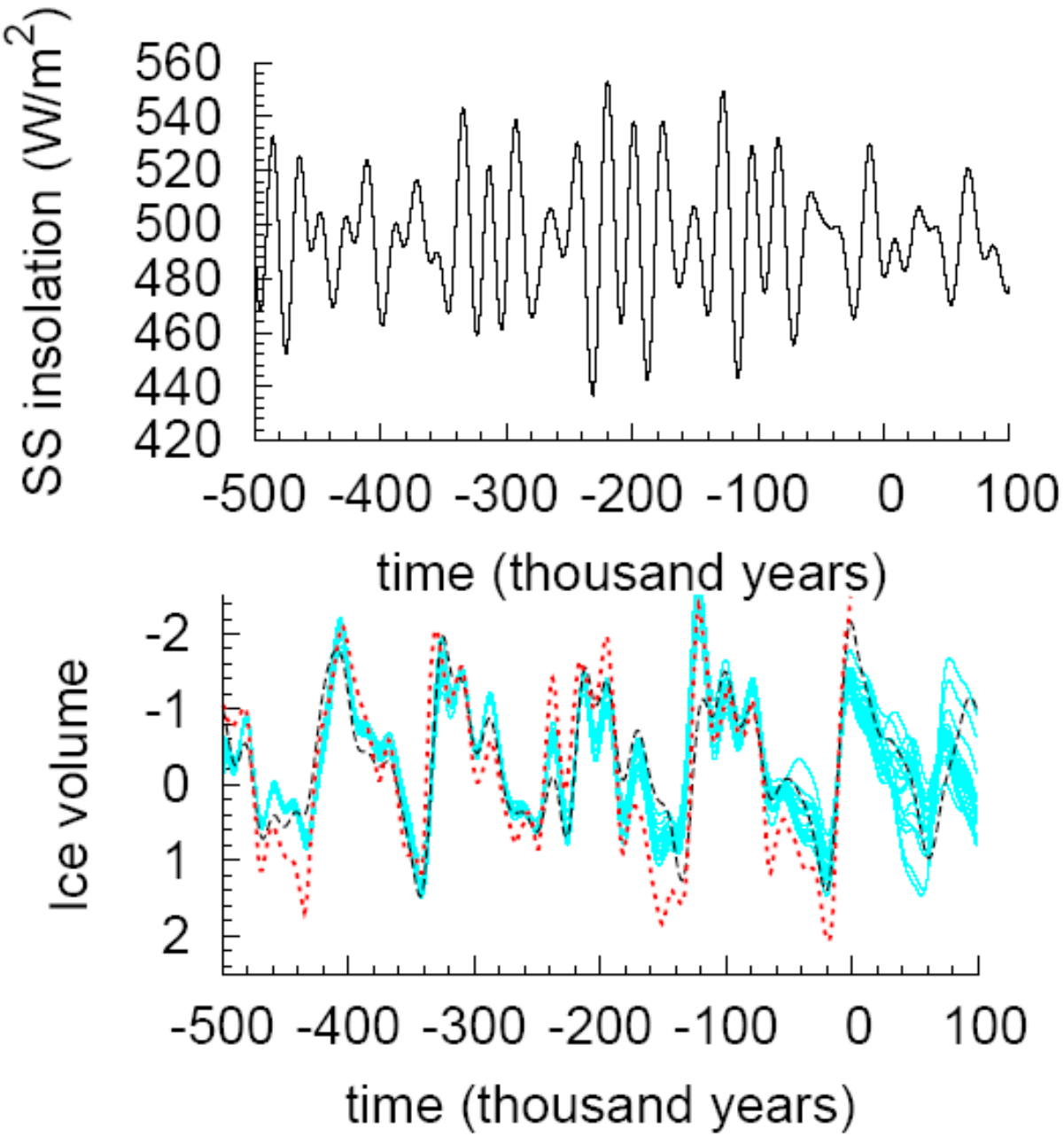

Figure 4: *Upper :* Summer solstice insolation at 65° for the period [-500 kyr ; + 100 kyr], used to force the SM90 model (Saltzman and Maasch [1990]).
Lower: Bold black curve : Time evolution of normalised northern hemisphere ice volume predicted with the SM90 model, compared with the reconstruction of Imbrie et al.,[1984]. Thin cyan curves represent an ensemble of realisations of the SM90 model in which parameters were tuned to improve the match to data. Note the dispersion of the predictions after + 50 kyr.

interglacial cycles via the snow-albedo feedback (Milankovitch, [1998], p. 567). Fine curves were obtained by further tuning the model on data (this study, according to the implementation of the ensemble Kalman filter by Annan et al., 2005), assuming a covariance on data error of 3. It is seen that although all tuned realisations correctly reproduce the timing

of previous glaciations and deglaciations, there is growing uncertainty on the climate evolution of the next 100 kyr. Especially, climate prediction beyond the next glacial maximum (here occurring in ~ 60 kyr) is uncertain. The reader is referred to Hargreaves and Annan [2002] for a more complete assessment of the predictive skill of SM90. Saltzman (2002) is an essential reference to any reader interested in low-order modelling of Pliocene-Pleistocene climates.

3.3 Earth models of intermediate complexity

We have seen that conceptual models may partly be calibrated on observations, or with the help of general circulation climate models. However, some potentially relevant mechanisms may not be directly observed nor simulated with general circulation models. Indeed, these mechanisms may be too slow (e.g.: snow accumulation over ice sheets) or perhaps they only occur under different climate regimes than today's. This is the reason why it was useful to design models having more complex representations of atmosphere, ocean, ice sheet and carbon cycle dynamics than in a low-order model, but yet simple enough to address the long time scales. These models were recently termed *earth models of intermediate complexity* (Claussen et al., 2002). The LLN-2D (Gallée et al. 1992) is one of the first models of this kind. It includes an axi-symmetric atmosphere with quasi-geostrophic approximation, a full computation of radiative transmission, scattering and absorption in the atmosphere, a dynamic representation of the ocean-mixed layer depth and kinetic-energy budgets, and up to three ice sheet dynamical models including isostatic effects. There is no representation of carbon cycle dynamics, such that CO_2 concentration has to be imposed as an external constraint to the model.

The LLN-2D was calibrated on the present-day climate, as well as on the timing and rate of the last glacial inception about 116 000 years ago. These constraints turned to be sufficient to achieve convincing simulations of the last glacial-interglacial cycles (Gallée et al, 1992, Berger et al., 1998). The last glacial maximum is simulated around 18,000 years ago (Figure 5). It was confirmed with this model that variations in CO_2 greatly affect the timing of glacial inception, especially when eccentricity is low. Marine isotopic stage 11 (MIS 11) is a good test case. This is a 30 kyr-long interglacial that started between 430 and 420 kyr ago and ended between 400 kyr and 390 kyr ago (Raynaud et al., 2005). Different simulations were performed with the LLN-2D model to identify the conditions to glacial inception (Figure 5). It was shown that only when both northern-hemisphere June insolation and CO_2 decrease (green and red scenarios on Figure 5, consistent with the ice-core record of Raynaud et al., 2005) does climate enter into glaciation (Loutre 2003). Otherwise, each forcing alone is not able to drive the system into glaciation and the climate remains in an interglacial state for another 20,000 years.

The present orbital configuration bears similarities with that of MIS 11. Indeed, we are today experiencing a low eccentricity and both the precession parameter and obliquity decrease. This is the reason why MIS 11 is said to be *analogous* to the present day (Loutre 2003). Yet, the climate evolution of the present interglacial differs to that of MIS 11: both CO_2 and methane concentrations increased from 260 to 280 ppm over the last 8000 years (Indermühle et al., 1999, Flückiger et al., 2002) instead of decreasing. This is the reason why Berger and Loutre (2002) consider that the next glacial inception is not due before 50,000 years (Figure 5, right-hand-side figures). Archer and Ganopolski (2005) further pushed the timing of glacial

inception to up to 400 kyr from now on the basis of experiments with another model of intermediate complexity (CLIMBER-2) by taking into account modern and future fossil fuel burning emissions of CO_2.

A small digression: Why such a difference in the evolution of greenhouse gases between MIS 11 and the Holocene? Maybe we should not be so surprised because the orbital trends are not quite the same. For example, obliquity is higher today than 400 kyr ago. Nevertheless, there is speculation (Ruddiman, 2005; Ruddiman, in press) that the natural Holocene CO_2 trend was a decline; its increase is essentially due a perturbation caused by CO_2 and CH_4 emissions related to land management and rice plantations. This small but sustained perturbation started

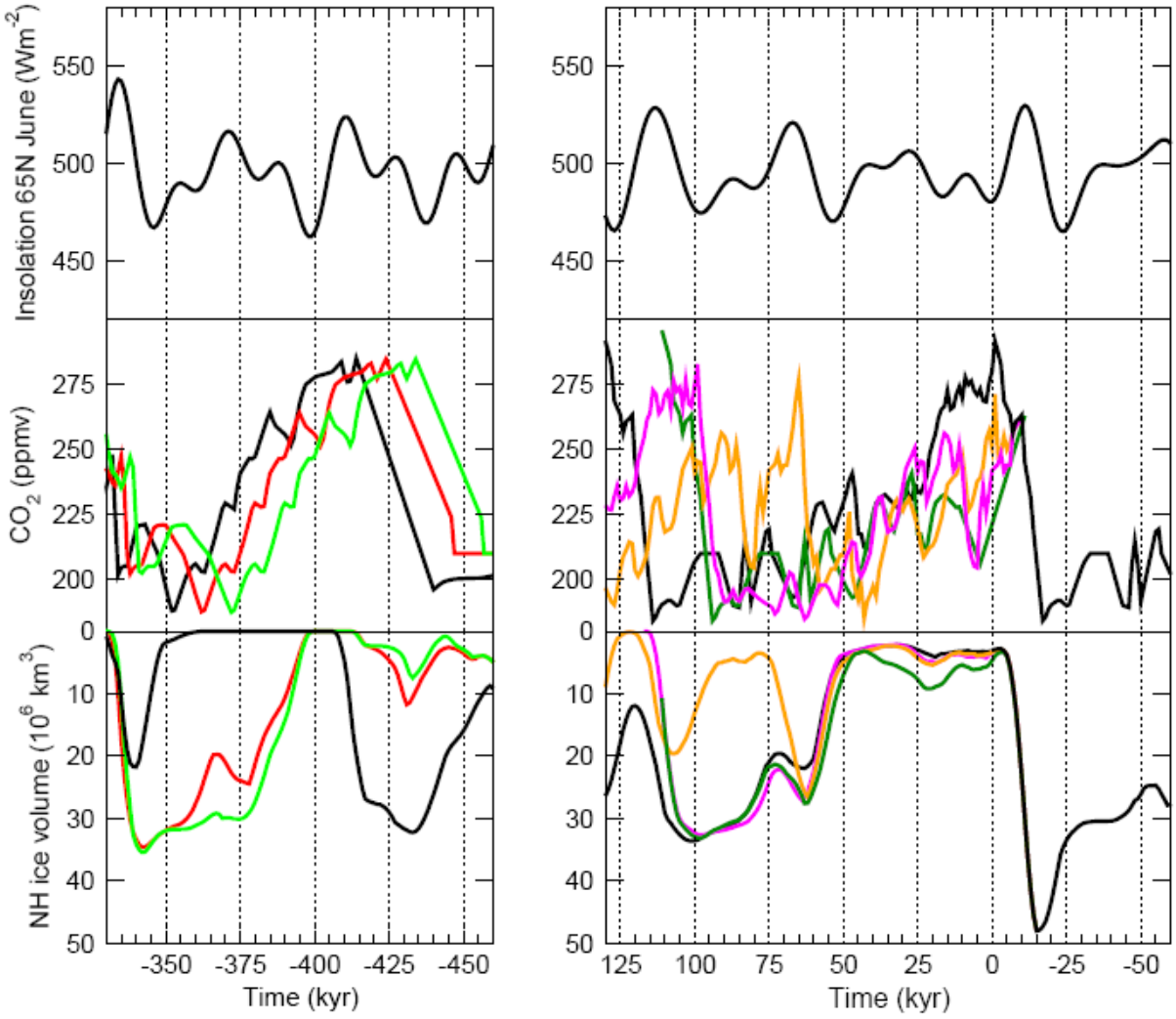

Figure 5: Time evolution of northern hemisphere ice volume simulated by the LLN model (lower) forced by insolation (top) and various scenarios the evolution of CO_2 concentration (middle) for marine isotopic stage 11 (around – 400 kyr, left) and the present interglacial period plus the next 125 kyr (right). Geological plotting conventions are adopted (time and ice-volume axes inverted). The figure illustrates, for these two periods, the sensitivity of simulated ice volume to the exact timing of CO_2 concentration changes.

about 6000 years ago and – according to Ruddiman – it was amplified by natural feedbacks to the point of avoiding glacial inception. All experiments carried out so far, either with the LLN-2D model (Loutre et al., 2007), CLIMBER-2 (Claussen et al., 2005) or even with a general circulation model (Ruddiman et al., 2005) indeed confirm that glacial inception would occur today if CO_2 concentration was below a threshold estimated around 240 ppmv. However, Ruddiman's hypothesis is criticised (see., e.g., Joos et al., [2004]), in part because the human perturbation supposedly needed to avoid glacial inception would have left an imprint on the isotopic signature of atmospheric CO_2, which is not observed. It was however argued (Crucifix and Berger, 2006) that the perturbation does not need to be so big if the climate was close to instability during the Holocene. Whether this was the case or not has not been established. This is the reason why Ruddiman's hypothesis may still be viewed as an insightful and thought-provoking proposal.

4 Conclusion

It is now granted that the orbital forcing somehow influences glacial-interglacial cycles. However, it is not entirely clear whether the orbital forcing is really a necessary driver or just a pacemaker. Current challenges may be summarised as follows. First, we still need to identify and document the mechanisms of climate instability, especially those active during peak glacial and interglacial times. For example, the idea of a link between carbon cycle and sea-level is particularly attractive, but it still needs to be better quantified. To this end, explicit models with appropriate meshes are needed and this implies significant technological challenges (see., e.g., Legrand et al., 2006).

On the other hand, time series analysis has provided significant advances in our qualitative understanding of climate as a non-linear system. It was suggested that a transition from a linear to a non-linear regime occurred about 1.4 Myr ago. The cause of this transition is not known. Addressing this question requires to establish a model of climate able to represent the non-linear interferences between very slow processes (e.g.: tectonics or sedimentogenesis) with glacial-interglacial cycles. This is the domain where low-order modelling is the most useful, assuming that the structure of the equations of these low-order models is consistent with the results of the other models of the hierarchy (general circulation models and earth models of intermediate complexity).

Finally, climate prediction on long time scales requires calibration of climate models on data. The process was first illustrated with the LLN-2D model. This model was calibrated on the present-day climate and on the last glacial inception. The prediction for the future is then a glacial inception in 50 kyr and glacial maximum around 60 kyr. The calibration step may also be formalised by means of a Bayesian method, like Ensemble Kalman filtering. The process was illustrated with SM90 low-order model, using past sea-level data. The prediction for the next glacial maximum is the same as with the LLN-2D model, but it was also shown that the uncertainty of the prediction grows dramatically after that time. The advantages of the low-order model are its negligible computing requirement as well as the easiness of identifying tuneable parameters. From a theoretical point of view, it would be useful to identify those moments of climate history – if they exist – when a small perturbation may modify the course of climate. We think that research in that direction might provide constructive insights into the current debate about the possibly large effects of land management and rice plantations by early civilisations during the Holocene.

Acknowledgments

Thanks are due to Marie-France Loutre for supplying Figure 5. The author is Research Associate with the National Fund for Scientific Research.

Key to symbols

1 Insolation and orbital parameters

ϕ latitude
t time
S total solar irradiance at the mean Earth-Sun distance (usually 1368 W/m^2)
e eccentricity of the Earth orbit
γ direction of vernal point
δ declination
ν The true anomaly, i.e., the angle between the position of the Earth and the direction of the vernal equinox
ϖ longitude of perihelion relative to vernal equinox
ε obliquity, i.e., angle between equator and ecliptic
W Time-mean insolation received in one true solar day
a semi-major axis of Earth's orbit
r Earth-Sun distance
H_0 hour angle at sunset

2 Climate modelling

Note : all variables are taken as a departure from an equilibrium

μ Carbon dioxide concentration
η Global mean extent of sea-ice
N Measure of the global thermohaline circulation of the ocean
I Global volume of continental ice
τ Global mean tempeature
$F_{\mu,I,N}$ External forcing terms.

3 Miscellaneous

ppmv part per million in volume
ppbv part per billion in volume
kyr thousand years
Myr million years

References

Adhémar, J., (1842) Révolutions de la mer: déluges périodiques. Carillan-Goeury et V. Dalmont, Paris.

Alexeev, V., P. L. Langen, and J. R. Bates, (2005) Polar amplification of surface warming on an aquaplanet in "ghost forcing" experiments without sea ice feedbacks. Clim. Dyn., 24, 655-666, doi:10.1007/s00382-005-0018-3.

Annan, J. D., D. J. Lunt, J. C. Hargreaves, and P. J. Valdes, (2005) Parameter progressestimation in an atmospheric GCM using the ensemble Kalman filter. Nonlinear Processes in Geophys, 12, 363-371

Archer, D., (2005) Fate of fossil fuel CO_2 in geologic time. J. Geophys. Res., 110, CO9S05, doi:10.1029/2004JC002625.

Archer, D. and A. Ganopolski, (2005) A movable trigger: fossil fuel co_2 and the onset of the next glacial inception. Geochem. Geophy. Geosy., 6, Q05003, doi:10.1029/2004GC000891.

Archer, D. E., G. Eshel, A. Winguth, W. Broecker, R. Pierrehumbert, M. Tobis, and R. Jacob, (2000) Atmospheric pCO_2 sensitivity to the biological pump in the ocean. Global Biogeochem. Cycles, 14, 1219-1230.

Berger, A., M. F. Loutre, and H. Gallée, (1998) Sensitivity of the LLN climate model to the astronomical and CO_2 forcings over the last 200 ky. Clim. Dyn., 14, 615-629.

Berger, A. and M. F. Loutre (2002). An exceptionally long interglacial ahead? Science, 297:1287–1288.

Berger, A. L., (1978) Long-term variations of daily insolation and quaternary climatic. J. Atmos. Sci., 35, 2362-2367.

Birchfield, G. and M. Ghil, (1993) Climate evolution in the Pliocene and Pleistocene from marine-sediment records and simulations: Internal variability versus orbital forcing. J. Geophys. Res., 98, 10385-10399.

Bretagnon, P., (1974) Termes à longues périodes dans le système solaire. Astron. Astroph., 30, 141-154.

Broecker, W. S. and T.-H. Peng, (1987) The role of $CaCO_3$ compensation in the glacial to interglacial atmospheric CO_2 change. Global Biogeochem. Cycles, 1, 15-29.

Brouwer, D. and G. M. Clemence, (1961) Methods of celestial mechanics. Academic Press.

Claussen, M., V. Brovkin, R. Calov, A. Ganopolski, and C. Kubatzki, (2005) Did humankind prevent a Holocene glaciation ? Clim. Change, 69, 409-417.

Claussen, M., V. Brovkin, and A. Ganapolski, (2001) Biogeophysical versus biogeochemical feedbacks of large-scale land cover change. Geophys. Res. Lett., 28, 1011-1014.

Claussen, M., L. Mysak, A. Weaver, M. Crucifix, T. Fichefet, M. F. Loutre, S. Weber, J. Alcamo, V. Alexeev, A. Berger, R. Calov, A. Ganopolski, H. Goosse, G. Lohmann, F. Lunkeit, I. Mokhov, V. Petoukhov, P. Stone, and Z. Wang, (2002) Earth system models of intermediate complexity: closing the gap in the spectrum of climate system models. Clim. Dyn., 18, 579-586.

Croll, J., (1875) Climate and timein their geological relations: a theory of secular changes of the Earth's climate. Appleton, New York.

Crucifix, M., (2006) Does the Last Glacial Maximum constrain climate sensitivity? Geophysical Research Letters, 33, L18701, doi:10.1029/2006GL027137.

Crucifix, M. and A. Berger, (2006) How long wil out interglacial be. Eos, Trans. Am. Geophys. Union, 87, 352.

Crucifix, M., M. F. Loutre, K. Lambeck, and A. Berger, (2001) Effect of isostatic rebound on modelled ice volume variations over the last 200 kyr. Earth Planet. Sci. Lett., 184, 623-633.

Duplessy, J.C., L. Chenouard, and F. Vila. Weyl's theory of glaciation supported by isotopic study of Norwegian core K 11. *Science*, 188:1208–1209, 1975.

Dijkstra, H. A., (2005) Non-linear physical oceanography. Atmospheric and oceanograhic sciences library, Springer, 2nd edition.

EPICA community members, (2004) Eight glacial cycles from an Antarctic ice core. Nature, 429, 623-628.

Flückiger, J., E. Monnin, B. Stauffer, J. Schwander, T. F. Stocker, J. Chappellaz, D. Raynaud, and J. M. Barnola, (2002) High-resolution Holocene n_2O ice core record and its relationship with CH_4 and co_2. Global Biogeochem. Cycles, 16, 1010, doi:10.1029/2001GB001417.

Gallée, H., J. P. van Ypersele, T. Fichefet, I. Marsiat, C. Tricot, and A. Berger, (1992) Simulation of the last glacial cycle by a coupled, sectorially averaged climate-ice sheet model. Part II : Response to insolation and CO_2 variation. J. Geophys. Res., 97, 15, 713-15, 740.

Gallimore, R. G. and J. E. Kutzbach, (1995) Snow cover and sea ice sensitivity to generic changes in Earth orbital parameters. J. Geophys. Res., 100, 1103-1120.

Hargreaves, J. C. and J. D. Annan, (2002) Assimilation of paleo-data in a simple Earth system model. Clim. Dyn., 19, 371-381.

Hays, J., J. Imbrie, and N. Shackleton, (1976) Variations in the earth's orbit : Pacemaker of ice ages. Science, 194, 1121-1132.

Huybers, P., (2007) Glacial variability over the last two millions years: an extended depth-derived agemodel, continous obliquity pacing, and the Pleistocene progression. Quaternary Sci. Rev., 26, 37-55, doi:10.1016/j.quascirev.2006.07.013.

Imbrie, J. J., J. D. Hays, D. G. Martinson, A. McIntyre, A. C. Mix, J. J. Morley, N. G. Pisias, W. L. Prell, and N. J. Shackleton, (1984) The orbital theory of Pleistocene climate: Support from a revised chronology of the marine $\delta O^{1}8$record. Milankovitch and Climate, Part I, A. Berger, J. Imbrie, J. Hays, J. Kukla, and B. Saltzman, eds., D. Reidel, Norwell, Mass., 269-305.

Indermühle, A., T. F. Stocker, H. Fisher, H. Smith, M. Wahlen, B. Deck, D. Mastroianni, J. Tschumi, T. Blunier, R. Meyer, and B. Stauffer, (1999) Holocene carbon-cycle dynamics based on CO_2 trapped in ice at Taylor Dome, Antarctica. Nature, 398, 121-125.

IPCC (2001). Climate Change 2001: The Scientific Basis. Contribution of Working Group I to the Third Assessment Report of the Intergovernmental Panel on Climate Change. Cambridge University Press, Cambridge, United Kingdom and New York, NY, USA, 2001. 881pp.

Joos, F., S. Gerber, I. C. Prentice, B. L. Otto-Bliesner, and P. J. Valdes, (2004) Transient simulations of Holocene atmospheric carbon dioxide and terrestrial carbon since the Last Glacial Maximum. Global Biogeochem. Cycles, 18, doi:10.1029/2003GB002156.

Joussaume, S., K. E. Taylor, P. Braconnot, J. F. B. Mitchell, J. E. Kutzbach, S. P. Harisson, I. C. Prentice, A. J. Brocolli, A. Abe-Ouchi, P. Bertlein, C. Bonfils, B. Dong, J. Guiot,

K. Herterich, C. D. Hewitt, D. Jolly, J. W. Kim, A. Kislov, A. Kitoh, M. F. Loutre, V. Masson, B. McAvaney, N. McFarlane, N. de Noblet, W. R. Peltier, J. Y. Peterschmitt, D. Pollard, D. Rind, F. Royer, M. E. Schleisinger, J. Syktus, S. Thompson, P. Valdes, G. Vettoretti, R. S. Webb, and U. Wyputta, (1999) Monsoon changes for 6000 years ago: Results of 18 simulations from the Paleoclimate Modeling Intercomparison Project (PMIP). Geophysical Research Letters, 26, 859, 862.

Khodri, M., Y. Leclainche, G. Ramstein, P. Braconnot, O. Marti, and E. Cortijo, (2001) Simulating the amplification of orbital forcing by ocean feedbacks in the last glaciation. Nature, 410, 570-574.

Klinger, B. A., J. Marshall, and U. Send, (1996) Representation of convective plumes by vertical adjustment. J. Geophys. Res., 101, 18175-18182, doi:10.1029/96JC000861.

Krinner, G., J. Mangerud, M. Jacobson, M. Crucifix, C. Ritz, and J. Svendsen, (2004) Enhancement of ice sheet growth by ice dammed lakes. Nature, 427, 429-432.

Kukla, G. J., (2000) The last interglacial. Science, 287, 987-988.

Kutzbach, J. E., (1981) Monsoon climate of the early Holocene: Climate experiment using the Earth's orbital parameters for 9000 years ago. Science, 214, 59-61.

Kutzbach, J. E. and Z. Liu, (1997) Response of the African monsoon to orbital forcing and ocean feedbacks in the middle Holocene. Science, 278, 440-443.

Lagrange, J. L., (1781) Théorie des variations séculaires des éléments des planètes 1. Nouveaux mémoires de l'Académie Royale des Sciences et Belles-Lettres, Berlin, 199-276.

Lambeck, K., P. Johnston, C. Smither, and M. Nakada, (1996) Glacial rebound of the British Isles - III: Constraints on mantle viscosity. Geophys. J. Int., 125, 340-354.

Laskar, J., (1999) The limits of earth orbital calculations for geological time-scale use. Phil. Trans. R. Soc. Lond. A, 357, 1735-1759.

Laskar, J., P. Robutel, F. Joutel, F. Boudin, M. Gastineau, A. C. M. Correia, and B. Levrard, (2004) A long-term numerical solution for the insolation quantities of the Earth. Astrom. Astroph., 428, 261-285.

Legrand, S., E. Deleersnijder, E. Hanert, V. Legat and E. Wolanski (2006), High-resolution solution, unstructured meshes for hydrodynamic models of the Great Barrier Reef, Australia, Estuarine Coastal and Shelf Science, 68 (1-2), 36-46.

Lenton, T. M., M. S. Williamson, N.R. Edwards, R. Marsh, A. R. Price, A. J. Ridgwell, J. G. Shepherd and S. J. Cox, (2006) Millenial timescale carbon cycle and climate change in an efficient Earth model, Climate Dynamics 26, 687-711.

Levitus, S. and T. P. Boyer, (1994) World Ocean Atlas 1994. NOAA Atlas NESDIS 3, Nat. Oceanic and Atmos. Admin, U.S. Dep. of Comm., Washington, D. C.

Lisiecki, L. E. and M. E. Raymo, (2007) Plio-Pleistocene climate evolution: trends and transitions in glacial cycles dynamics. Quaternary Sci. Rev., 26, 56-69, doi:10.1016/j.quascirev.2006.09.005.

Lourens, L. J., R. Wehausen, and H. J. Brumsack, (2001) Geological constraints on tidal dissipation and dynamical ellipticity of the Earth over the past three million years. Nature, 409, 1029-1033.

Loutre, M. F., (2003) Clues from MIS11 to predict the future climate. A modelling point of view. Earth Planet. Sci. Lett., 212, 213-234, doi:10.1016/S0012-821X(03)00235-8.

Loutre, M. F., A. Berger, M. Crucifix, S. Desprat, and M. F. Sánchez-Goñi, (2007) Interglacials as simulated by the LLN-2D NH and MoBidiC climate models, pp. 547-582 in Sirocko, F., M. Claussen, M. F. Sánchez Goñi, and T. Litt, eds., (2007) The climate of past interglacials, volume 7 of Developments in Quaternary Science. Elsevier.

Lynch-Stieglitz, J., J. F. Adkins, W. B. Curry, T. Dokken, I. R. Hall, J. C. Harguera, J. J.-M. Hirschi, E. V. Ivanova, C. Kissel, O. Marchal, T. M. Marchitto, I. N. McCave, J. F. McManus, S. Mulitza, U. Ninnemann, F. Peeters, E.-F. Yu, and R. Zahn, (2007) Atlantic meridional overturning during the Last Glacial Maximum. Science, 316, 66-69.

MacAyeal, D., (1993) Binge/purge oscillations of the Laurentide ice sheet as a cause of the North Atlantic's Heinrich events. Paleoceanogr., 8, 775-784.

Manabe, S. and R. J. Stouffer (1980). Sensitivity of a global climate model to an increase of CO_2 concentration in the atmosphere. J. Geophys. Res., 85:5529–5554.

Meir, P., P. and J. Grace (2006) The influence of terrestrial ecosystems on climate, Trends in Ecology and Evolution 21, 254-260.

Milankovitch, M., (1998) Canon of insolation and the ice-age problem. Narodna biblioteka Srbije, Beograd, english translation of the original 1941 publication.

Mitchell, J. M. M., (1976) An overview of climatic variability and its causal mechanisms. Quat. Res., 6, 481-494.

Morales-Maqueda, M. A. and S. Rahmstorf, (2002) Did antarctic sea-ice expansion cause glacial co_2 decline? Geophys. Res. Lett., 29, 1011, doi:10.1029/2001GL013240.

Nicolis, C. and G. Nicolis, (1986) Reconstruction of the dynamics of the climatic system from time-series data. Proc. Natl. Acad. Sci. USA, 83.

Oerlemans, J., (1980) Model experiments on the 100, 000-yr glacial cycle. Nature, 287, 430-432.

Paillard, D., (1998) The timing of Pleistocene glaciations from a simple multiple-stae climate model. Nature, 391.

Paillard, D. and F. Parrenin, (2004) The Antarctic ice sheet and the triggering of deglaciations. Earth Planet. Sc. Lett., 227, 263-271.

Pälike, H., J. Laskar, and N. J. Shackelton, (2004) Geologic constraints on the chaotic diffusion of the solar system. Geology, 32, 929-932, doi:10.1130/G20750.1.

Pälike, H. and N. J. Shackelton, (2000) Constraints on astronomical parameters from the geological record for the last 25 Myr. Earth Planet. Sc. Lett., 182, 1-14.

Paterson, W. S. B., (1994) The physics of glaciers. Pergamon, New York, 3rd edition.

Peixoto, J. P. and A. H. Oort, (1992) Physics of climate. American Institute of Physics, New York, 520 pp.

Peltier, W., (1974) The impulse resonse of a Maxwell Earth. Rev. Geophys., 12, 649-669.

Peltier, W. R., (2004) Global glacial isostasy and the surface of the ice-age Earth: the ICE-5G (VM2) model and GRACE. Ann. Rev. Earth Planet Sci., 32, 111-149.

Peltier, W. R., I. Shennan, R. Drummond, and B. Horton, (2002) On the postglacial isostatic adjustment of the British Isles and the shallow visocleastic structure of the Erth. Geophys. J. Int., 148, 443-475.

Pépin, L., D. Raynaud, J.-M. Barnola, and M. F. Loutre, (2001) Hemispheric roles of climate forcings during glacial-interglacial transitions. J. Geophys. Res., ïn press".

Petit, J. R., J. Jouzel, D. Raynaud, N. I. Barkov, J.-M. Barnola, I. Basile, M. Bender, J. Chappellaz, M. Davis, G. Delaygue, M. Delmotte, V. M. Kotlyakov, M. Legrand, V. Y. Lipenkov, C. Lorius, L. Pepin, C. Ritz, E. Saltzman, and M. Stievenard, (1999) Climate and atmospheric history of the past 420, 000 years from the Vostok ice core, Antarctica. Nature, 399, 429-436.

Rahmstorf, S., (2002) Ocean circulation and climate during the past 120, 000 years. Nature, 419, 207-214.

Raynaud, D., J.-M. Barnola, R. Souchez, R. Lorrain, J. R. Petit, P. Duval, and V. Y. Lipenkov, (2005) The record for marine isotopic stage 11. Nature, 463, 39-40, doi:10.1038/43639b.

Ruddiman, W. F., (2005) The early anthropogenic hypothesis a year later - an editorial reply. Clim. Change, 69, 427-434.

Ruddiman, W. F. (in press) The early anthropogenic hypothesis a year later: challenges and responses. Rev. Geophys., doi:10.1029/2006RG0002067.

Ruddiman, W. F., M. Raymo, and A. McIntyre, (1986) Mutuyama 41, 000-year cycles: North Atlantic Ocean and northern hemisphere ice sheets. Earth Planet. Sci. Lett., 80, 117-129.

Ruddiman, W. F., S. J. Vavrus, and J. E. Kutzbach, (2005) A test of the overdue-glaciation hypothesis. Quat. Sci. Rev., 24, 1-10, doi:10.1016/j.quascirev.2004.07.010.

Saltzman, B., (2002) Dynamical paleoclimatology, volume 80 of International Geophysics Series. Academic Press.

Saltzman, B. and K. A. Maasch, (1990) A first-order global model of late Cenozoic climate. Trans. R. Soc. Edinburgh Earth Sci, 81, 315-325.

Sarnthein, M., U. Pflaumann, and M. Weinelt, (2003) Past extent of sea ice in the northern North Atlantic inferred from foraminiferal paleotemperature estimates. Paleoceanogr., 18, doi:10.1029/2002PA000771.

Shackleton, N. J. and N. D. Opdyke, (1973) Oxygen isotope and paleomagnetic stratigraphy of equatorial Pacific core V28-238: Oxygen isotope temperatures and ice volumes on a 10^5 year and 10^6 year scale. Quat. Res., 3, 39-55.

Sheffer, M., V. Brovkin and P. M. Cox (2006) Positive feedback between global warming and atmospheric CO2 concentration inferred from past climate change, Geoph. Res. Lett., 33, L10702.

Siegenthaler, U., T. F. Stocker, D. Lüthi, J. Schwander, B. Stauffer, D. Raynaud, J.-M. Barnola, H. Fisher, V. Masson-Delmotte, and J. Jouzel, (2005) Stable carbon cycle-climate relationship during the Late Pleistocene. Science, 310, 1313-1317.

Stephens, B. B. and R. F. Keeling, (2000) The influence of Antarctic sea-ice on glacial-interglacial CO_2 variations. Nature, 404, 171-174.

Tarasov, L. and W. R. Peltier, (1997) Terminating the 100 kyr ice age cycle. J. Geophys. Res., 102, 21665-21693.

Tziperman, E. and H. Gildor, (2003) On the mid-Pleistocene transtion to 100-kyr glacial cycles and the asymmetry between glaciation and deglaciation times. Paleoceanography, 18, 1001, doi:10.1029/2001PA00027.

Tziperman, E., M. E. Raymo, P. Huybers, and C. Wunsch, (2006) Consequences of pacing the Pleistocene 100 kyr ice ages by nonlinearphase locking to Milankovitch forcing. Paleoceanography, 21, PA4206, doi:10.1029/2005PA001241.

Vernekar, A. D., (1972) Long-term global variations of incoming solar radiation. Meteor. Monogr., 34, 21 pp. and talbles.

Vettoretti, G. and W. R. Peltier, (2003) Sensitivity of glacial inception to orbital and greenhouse gas climate forcing. Quat. Sci. Rev., 23, 499-519.

Webb, M. J., C. A. Senior, D. M. H. Sexton, W. J. Ingram, K. D. Williams, M. A. Ringer, B. J. McAvaney, R. Colman, B. J. Soden, R. Gudgel, T. Knutson, S. Emori, T. Ogura, Y. Tsushima, N. G. Andronova, B. Li, I. Musat, S. Bony, and K. E. Taylor, (2006) On the contribution of local feedback mechanisms to the range of climate sensitivity in two GCM ensembles. Clim. Dyn., 27, 17-38, doi:10.1007/s00382-006-0111-2.

Wolf, A., J. B. Swift, H. L. Swinney, and J. A. Vastano, (1985) Determining Lypunov exponents from a time series. Physica D, 16, 285-317, doi:10.1016/0167-2789(85)90011-9.

Wunsch, C., (2003) Determining paleoceanographic circulations, with emphasis on the Last Glacial Maximum. Quat. Sci. Rev., 22, 371-385.

Yokoyama, Y., K. Lambeck, P. de Deckker, P. Johnston, and L. K. Fifield, (2000) Timing of the last glacial maximum from observed sea-level minima. Nature, 406, 713-716.

Zhao, Y., P. Braconnot, O. Marti, S. P. Harrison, C. D. Hewitt, A. Kitoh, Z. Liu, U. Mikolajewicz, B. Otto-Bliesner, and S. L. Weber, (2005) A multi-model analysis of the role of the ocean on the African and Indian monsoon during the mid-Holocene. Clim. Dyn., 25, 777-800, doi:10.1007/s00382-005-0076-7.

Figures:

Figure 1: Long term variations of (a) the climatic precession parameter, (b) obliquity, (c) the normalised oxygen isotopic ratio of benthic foraminifera (the Y-axis is configured such that sea-level increases upwards (ice volume increases downwards) and (d) atmospheric CO_2 concentration (in ppmv) reconstructed from ice core records (Petit et al., 1999; Siegenthaler et al., 2005). Time zero corresponds to year 1950 AD. Vertical shadings indicate interglacials, identified here as periods of CO_2 high stand. Data timescales are taken from the corresponding references.

Figure 2: Heliocentric angles relevant for the astronomical theory of climate. *S* stands for Sun, *E* for Earth, *P* for perihelion and V.E. for vernal equinox. See key to other symbols at the end of this article.

Figure 3: Insolation plotted as a function of latitude (Y-axis) and month (X-axis). The isocontours are called *Milankovitch curves*. The upper-left plot represents the absolute value assuming a circular orbit, while the three other plots give the effect of an increase in obliquity, or that of a non-zero eccentricity with perihelion occurring either in summer ($\varpi = 90°$) or in winter ($\varpi = 270°$). Note the different scales and also that an increase in obliquity reduces the annual mean insolation between 43°N and 43°S.

Figure 4: *Upper :* Summer solstice insolation at 65° for the period [-500 kyr ; + 100 kyr], used to force the SM90 model (Saltzman and Maasch [1990]). *Lower:* Bold black curve : Time evolution of normalised northern hemisphere ice volume predicted with the SM90 model, compared with the reconstruction of Imbrie et al.,[1984]. Thin cyan curves represent an ensemble of realisations of the SM90 model in which parameters were tuned to improve the match to data. Note the dispersion of the predictions after + 50 kyr.

Figure 5: Time evolution of northern hemisphere ice volume simulated by the LLN model (lower) forced by insolation (top) and various scenarios the evolution of CO_2 concentration (middle) for marine isotopic stage 11 (around – 400 kyr, left) and the present interglacial period plus the next 125 kyr (right). Geological plotting conventions are adopted (time and ice-volume axes inverted). The figure illustrates, for these two periods, the sensitivity of simulated ice volume to the exact timing of CO_2 concentration changes.

Effects of the 11-Year Solar Cycle on the Atmosphere from the Surface to the Lower Thermosphere

Marco A. Giorgetta[(1)], Hauke Schmidt[(1)] and Guy P. Brasseur[(2)]

[(1)] Max Planck Institute for Meteorology, Hamburg, Germany

[(2)] National Center for Atmospheric Research, Boulder, USA

Abstract

The solar irradiation on Earth is the driving force for the circulations in atmosphere and oceans on Earth. Weather and climate are sensitive to variations of the solar irradiation, occurring for different reasons. This presentation focuses on changes in the atmospheric circulation and composition caused by variations in the solar irradiation at the top of the atmosphere, as resulting from the variations in the solar emission associated with the 11-year sun spot cycle. A numerical model is used to study the differences in temperature and ozone in the middle atmosphere between maximum and minimum insolation conditions of the 11-year cycle. The model successfully reproduces the major increases in temperature and ozone in the stratosphere for solar maximum conditions, showing that the major processes for this problem are included in the model. The analysis of the processes in the simulations leads to a better understanding of the occurrence of a secondary maximum in temperature and ozone in the lower tropical stratosphere.

Introduction

Solar energy absorbed by the Earth system is the main source for the circulations in atmosphere and oceans, the distribution of ice and the existence of life. The insolation at the top of the atmosphere and the local availability of solar energy on the planet varies for a number of reasons: variations in the solar emission, variations in the sun Earth distance, variations in inclination and direction of the Earth rotation axis with respect to the orbital plane, the rotation rate of the planet, the scattering and absorption in the atmosphere and at the Earth surface. Such variations happen over many time scales. This work focuses on the effects of changes in the solar emission, in association with the 11-year sun spot cycle, on the circulation and composition of the atmosphere, specifically of the stratosphere and mesosphere. Sunspots, visible as dark spots on the bright solar disk, were discovered after the invention of telescopes and the time series going back to the early 17th century clearly shows a variation in sun spot number with an 11-year period along with other longer-term changes (Figure 1). The well-known Maunder minimum is a period in the 17th century when sunspots were apparently absent from the sun surface. The occurrence of the Little Ice Age, which approximately paralleled this period, hence motivated the hypothesis that sunspot numbers and climate on Earth correlate.

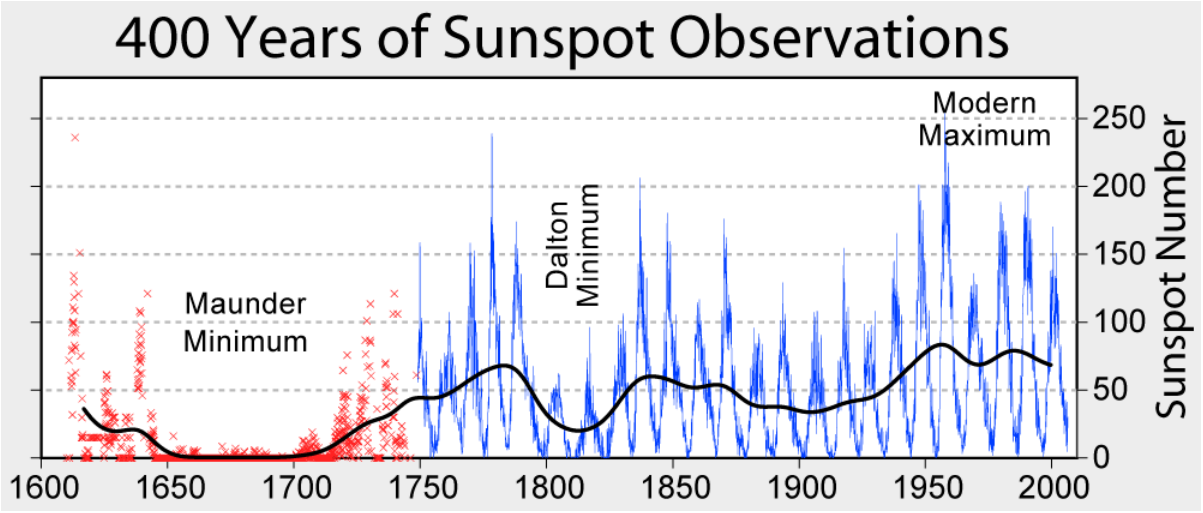

Figure 1. Sunspot number observed from the year 1610 to the present. Source: http://en.wikipedia.org/wiki/Image:Sunspot_Numbers.png

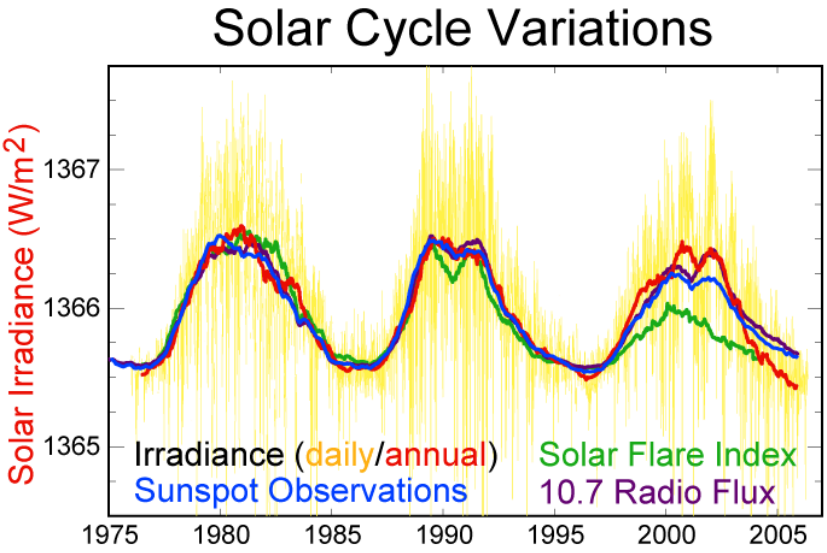

Figure 2. Total solar irradiance (daily: yellow, annual: red) and for comparison indices for sunspot number (blue), solar flares (green), and 10.7 radio flux (purple) scaled to the amplitude of the annual solar irradiation. Source: http://en.wikipedia.org/wiki/Image:Solar-cycle-data.png

Direct measurements of the solar irradiation at the top of the atmosphere became available with satellite-based radiometers (Froelich, 2006: Figure 1; Rottman, 2006: Figure 2). The time series, as produced from the different instruments employed over time, shows an average of total solar irradiation of 1366 W/m^2 (Froelich, 2006: Figure 9), the so-called solar constant, and an oscillation over 11 years with a peak to peak amplitude of ~1.3 W/m^2 or 0.1% of the solar constant. This 11-year cycle in top-of-the-atmosphere solar irradiation correlates

positively with the 11-year solar sun spot time series and some other indices of solar variability (Figure 2). The correlation between dark sunspots and the solar emission, and hence irradiation on Earth, is positive because the decrease in solar emission in sunspots is overcompensated by more intense emission from other features on the sun surface. Whether and how such small fractional changes of the total solar irradiation can explain climate variations on Earth on timescales of decades is an issue of current research. An important feature of the 11-year variation in solar irradiation is, however, its spectral dependence, which in combination with atmospheric chemistry may lead to larger effects than expected otherwise.

Spectrally resolved observations of the solar irradiation show that the 11-year changes are small in the near infrared and visible range, about 0.1%, but much larger in shorter wavelengths in the UV and extreme UV (Rottman, 2006:Figure 6), where however only little energy is transported to Earth. The irradiation at the Lyman alpha wavelength (121 nm) is for example more than 60% larger in solar maximum conditions than in minimum conditions. Such large fractional changes in spectral irradiance become important at wavelengths where the radiation photolyses atmospheric molecules, and hence drives atmospheric chemistry. The well known ozone layer results from such photochemical processes, which are sensitive to changes in UV irradiation. In general, the shorter the wavelength, the lower the spectral power and the higher the altitude in the atmosphere, where the wavelength can be important for heating or photolysis. Chemical changes of the atmosphere then change the radiative properties of the atmosphere also for longer wavelengths, leading possibly to larger modifications in the temperature distribution and in the circulation, which can feed back to the chemistry of the atmosphere. Thus, atmospheric chemistry can potentially amplify the effect of the 11-year solar cycle on the atmosphere due to the much-intensified spectral solar signal in the photolytically important UV and extreme UV radiation.

An excellent collection of papers resulting from the 2005 ISSI workshop on “Solar Variability and Planetary Climates” in Berne, Switzerland, has been published in *Space Science Reviews,* 125**,** 2006. This special volume presents the current state of knowledge on the effects of variations in solar emission on the climate variability on Earth, including also results of this study (Schmidt and Brasseur, 2006).

The HAMMONIA model

To test the feasibility of such amplifying mechanisms, numerical models have been developed. This study makes use of the HAMburg MOdel of the Neutral and Ionized Atmosphere (HAMMONIA). The HAMMONIA model is a general circulation model (GCM) developed specifically to study the effects of the spectrally resolved variations in the solar irradiation and of particle fluxes on the atmosphere from the surface up to the lower thermosphere (Schmidt et al., 2006). The HAMMONIA GCM is based on the ECHAM5 GCM, which is a GCM for studies of the tropospheric climate and its middle atmosphere extension MAECHAM5. Hence HAMMONIA includes all processes of ECHAM5 and MAECHAM5 and additional atmospheric processes, which are considered at the time to be important for the investigation of 11-year solar cycle effects. In particularly noteworthy is the atmospheric chemistry coupled by transport and radiation to the general circulation and the

high spectral resolution in the UV and extreme UV, down to 5nm, for the computation of photolysis and heating rates.

The HAMMONIA model resolves horizontally structures up to total wave number 31 in spherical harmonics. The associated Gaussian grid, on which non-linear terms of the dynamics equations and physical processes are computed, has a resolution of 3.75°x*~3.75° in longitude and latitude. In the vertical, the model resolves the atmosphere in 119 layers from the surface to 1.7e-7hPa, which corresponds to ~250km for solar minimum conditions and to ~350km for solar maximum conditions. (This altitude difference develops mainly in the lower thermosphere, where temperatures differ up to 500K between solar minimum and maximum conditions.)

The use of a high vertical resolution allows simulating the quasi-biennial oscillation (QBO) in the equatorial stratosphere (Giorgetta et al., 2006). The QBO is the main mode of variability in this region of the atmosphere and has effects on the circulation in higher latitudes, as discussed also for the 11-year solar cycle. Interferences of the influences of the QBO and the solar cycle have been discussed (Labitzke, 1987). The HAMMONIA model allows such interferences since the QBO is simulated internally.

Experiments

The experiments consist of two simulations over 35 years each, which differ by the spectrally resolved solar irradiation given as upper boundary condition at the top of the atmosphere. The first simulation, MIN, is driven by a solar spectrum as observed in September 1986, which is typical for solar minimum conditions. The second simulation, MAX, is driven by a solar spectrum as observed in November 1989, typical for solar maximum conditions. Thermospheric NO production is increased by 33% for solar maximum. Sea surface temperature and sea ice is specified from an observed climatology of 1979-1996. The spin-up periods of the integrations are discarded. This experimental design has the following main characteristics:

- The boundary conditions are free of interannual variations. Interannual variations in the simulated circulation, in temperature or in chemistry must therefore result from the modeled system itself.
- Using constant solar irradiance conditions, for solar minimum and solar maximum, the solar effects can be investigated as differences between the maximum and minimum simulations in the annual or seasonal means of the 35 years of simulation. (A much longer and more expensive simulation would be necessary to draw statistically robust conclusions if a spectral solar cycle is prescribed as upper boundary condition instead of constant spectra.)

Results

Ozone

The ozone layer in the stratosphere and lower mesosphere has a photochemical origin and

creates the necessary heating for a positive upward temperature gradient, thus defining the stratosphere. An increase in ozone concentration in this layer is expected for higher solar irradiation because of the increase in UV radiation and hence more photolysis. A comparison of the zonal and annual mean ozone distribution in both experiments shows indeed an increase of ca. 3% in ozone mixing ratio in the upper stratosphere between 10 and 1 hPa in MAX compared to MIN (Figure 3). This positive change is statistically significant at the 95% level (gray shading). Some larger relative changes are found at higher levels, where however the absolute volume mass-mixing ratio is much smaller than within the ozone layer in the upper stratosphere. Soukharev and Hood (2006) have analyzed ozone changes observed by different in satellite-based instruments: SBUV, SAGE and HALOE. They found statistically significant changes of similar amplitude in the upper tropical stratosphere, but there is some disagreement between the different observations as well as between the observations and the model simulations. Possible reasons for the disagreement between the different instrumental observations are the different lengths of the records, and possible contaminations by the effects of major volcanic eruptions of Pinatubo in 1991 and El Chichon in 1982. Effects of major volcanic eruptions and El Nino influences are entering the observations, but they are present in the model simulations, where climatological lower boundary conditions are used for sea surface temperature.

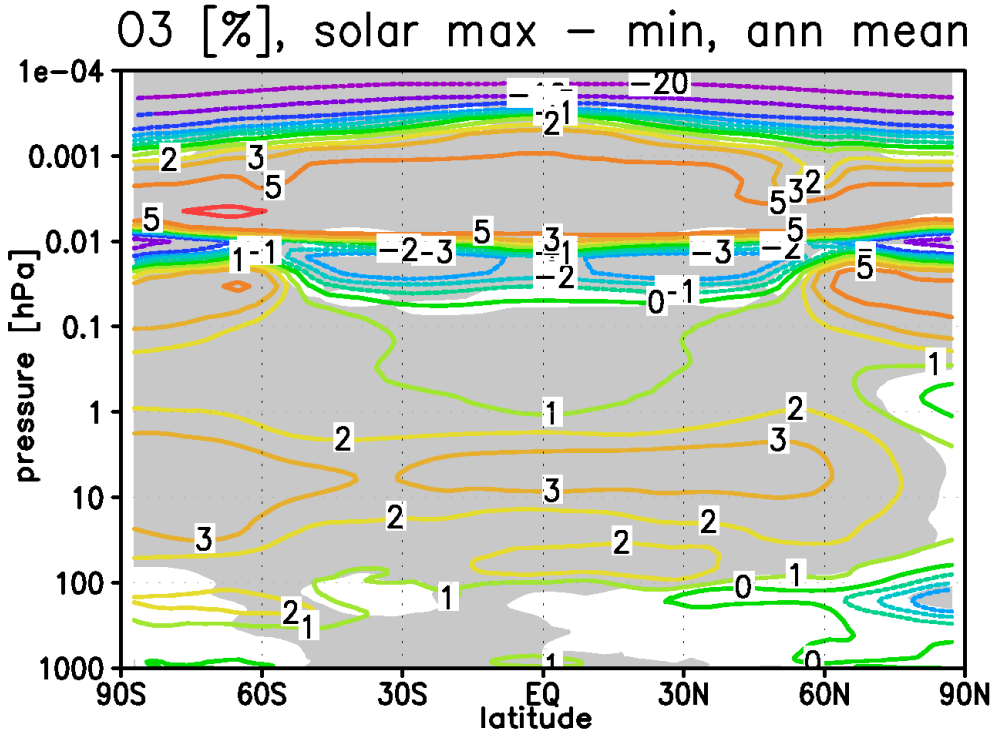

Figure 3. Percent change in annual and zonal mean ozone volume mixing ratio in the MAX simulation with respect to the ozone distribution in the MIN simulation. Grey shading indicates that the difference is statistically significant at the 95% confidence level following a t-test.

In the lower mesosphere, relative changes are nearly 0, but positive changes of up to 5% occur in the mesopause region, between about 0.01 and 0.001 hPa, or 80 to 95 km. These features correspond well to observations from the HALOE instrument on the UARS satellite (personal communication G. Beig, Puna, India). Negative changes are simulated in a transition layer below 0.01 hPa, and larger negative relative changes occur above the mesopause region, where however the ozone mixing ration is very small.

Temperature

The zonal and annual mean temperature is increased in MAX compared to MIN by up to 1 K at the stratopause. Higher temperature changes are found in the mesopause region, and much higher signals occur in the lower thermosphere above the displayed region. Temperature changes are statistically significant in most places except for the equatorial stratosphere, where the high temperature fluctuations caused by the QBO in zonal wind mask the solar signal, and in the higher Southern latitudes, where again the high natural variability renders the differences insignificant. The high Northern latitudes show a significant warming at the stratopause, vertically aligned with a significant cooling in the lower stratosphere. This signature is characteristic for a change in the interaction of planetary scale waves with the zonal mean flow, and further interactions with gravity waves. A further consequence of these dynamical effects is the secondary warming of about 0.3 K in the annual mean found above the tropical tropopause. The temperature signals in the high Northern latitudes and above the tropical tropopause are related to dynamical processes in the wintertime circulation, but they are visible and statistically significant even in the annual mean.

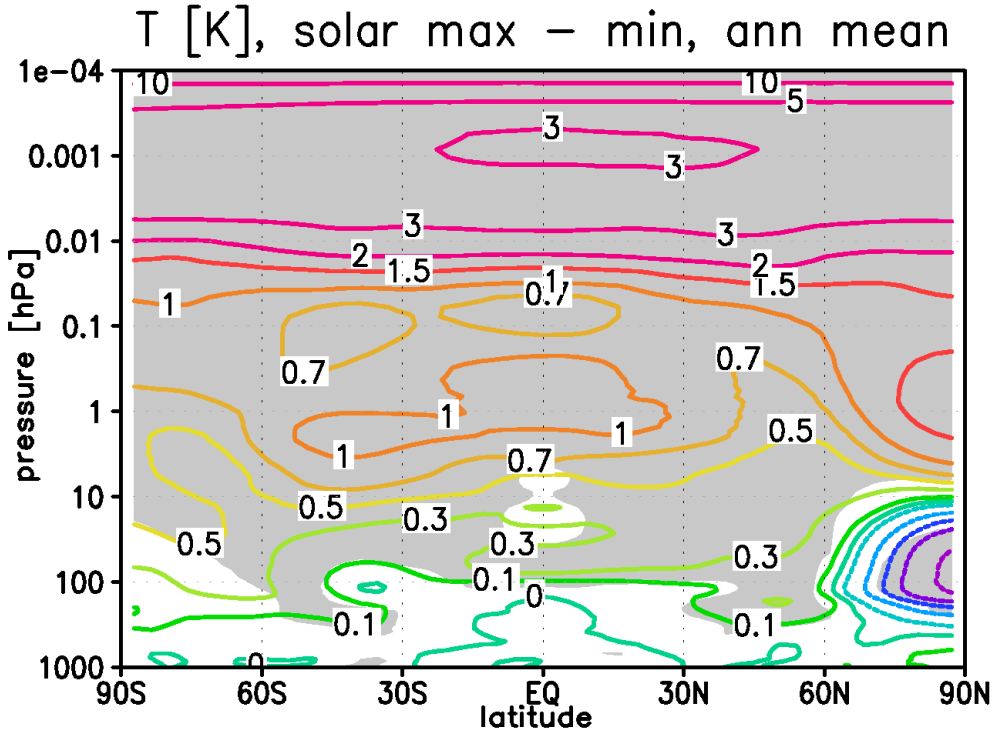

Figure 4. Difference in annual and zonal mean temperature in K between the MAX and the

MIN simulation. Grey shading indicates that the difference is statistically significant at the 95% confidence level following a t-test.

The overall positive solar signal in stratospheric temperature is confirmed by observational studies, based on instruments (Scaife, 2000: SSU/MSU) or the ERA-40 reanalysis of the ECMWF (Crooks and Gray, 2005). These studies find increases of >2K and 1.75K, respectively, in the upper tropical stratosphere, where the model shows a signal larger than 1K. The secondary maximum above the tropical tropopause is also found in the ERA-40 data.

The secondary maximum in the solar temperature signal, found in the annual mean, is primarily a signal existing in the winter months of the Northern hemisphere. From November to March, the temperature increase amounts to 0.6 to 0.9K and is statistically significant. Its occurrence in the Northern winter is indicative of a mechanism involving extratropical planetary waves and their interaction with the winter mean circulation, which is an important process in the Northern hemisphere. (In the Southern hemisphere, extratropical planetary waves are weaker and, for most of the time, cannot propagate into the stratosphere.) Kodera and Kuroda, 2002, proposed a hypothesis for the solar influence on this wave mean-flow interaction in the stratosphere and lower mesosphere and the resulting temperature effects above the tropical tropopause. Important steps are: (a) The temperature gradient between the tropical upper stratosphere and the high northern latitudes is increased in early winter in MAX vs. MIN because of the increased solar heating in the tropics; (b) the polar vortex can develop stronger; (c) planetary waves excited in the winter troposphere are less able to propagate into the stronger vortex, so that planetary wave breaking is less intense; (d) because of the reduced wave breaking, the Brewer Dobson circulation is weaker, i.e. the tropical upwelling and the high latitude sinking of air is reduced; (e) the reduced tropical upwelling becomes results in a reduced adiabatic cooling, hence a net warming in the lower tropical stratosphere, above the tropopause, where timescales for radiative cooling or heating are long. This hypothesis can be confirmed by the analysis of the simulated processes in the HAMMONIA simulations. The reduction of the tropical upwelling also produces the secondary maximum in ozone above the tropical tropopause due to a reduced upward advection of air with low ozone (Figure 3). This secondary ozone maximum has only a minor effect on the temperature.

Summary

Variations on the sun surface, visible as dark sunspots, are known since the 17th century. The 11-year sun spot cycle is the most prominent feature together with a period of minimum sunspot counts in the second half of the 17th century, the so-called Maunder minimum. The occurrence of the little Ice Age in the 17th century, apparently at the same time as the Maunder minimum, started early discussions on a possible connection between sun spot number and solar emission, and the climate on Earth. This study makes use of a specifically adapted numerical model, the HAMMONIA whole atmosphere model, for studies of solar cycle effects on the Earth atmosphere. Model simulations for solar minimum and maximum conditions are compared with respect to ozone and temperature structures in the stratosphere and mesosphere. It is found that the model can reproduce the main features of the observed solar cycle signals confirming that the model includes the relevant processes. Further the

simulations allowed confirming a hypothesis for the explanation of a secondary temperature signal above the tropical tropopause, which is observed only during Northern winter.

References

Crooks, S. A., and L. J. Gray, Characterization of the 11-year solar signal using a multiple regression analysis of the ERA-40 dataset, J. Climate, 18, 996-1015, 2005.

Froehlich, C., Solar irradiance variability since 1978, Space Sc. Rev., 125, 53-65, 2006.

Giorgetta M. A., E. Manzini, E. Roeckner, M. Esch, and L. Bengtsson, Climatology and forcing of the quasi-biennial oscillation in the MAECHAM5 model, J. Climate, 19, 3882-3901, 2006.

Kodera K., and Y. Kuroda, Dynamical response to the solar cycle, J. Geophys. Res., 107, 4749, doi:10.1029/2002JD002224, 2002.

Labitzke, K., Sunspots, the QBO, and the stratospheric temperature in the North polar region, Geophys. Res. Lett., 14, 535-537, 1987.

Rottman, G., Measurements of total and spectral solar irradiance, Space Sc. Rev., 125, 39-51, 2006.

Scaife, A., J. Austin., N. Butchart, S. Pawson, M. Keil, J. Nash, and I. N. James, Seasonal and interannual variability of the stratosphere diagnosed from UKMO TOVS analyses, Quart. J. Roy. Meteor. Soc., 126, 2585-2604, 2000.

Schmidt, H. and G. P. Brasseur: The response of the middle atmosphere to solar forcing in the Hamburg Model of the Neutral and Ionized Atmosphere. Space Sc. Rev., 125, 345-356, 2006.

Schmidt, H., G. P. Brasseur, M. Charron, E. Manzini, M. A. Giorgetta, T. Diehl, V. I. Fomichev, D. Kinnison, D. Marsh, and S. Walters, The HAMMONIA chemistry climate model: Sensitivity of the mesopause region to the 11-year solar cycle and CO_2 doubling, J. Climate, 19, 3903-3931, 2006.

Soukharev, B.E., and L.L. Hood, The solar cycle variation of stratospheric ozone: Multiple regression analysis of long-term satellite data sets and comparisons with models, J. Geophys. Res., 111, D20314, doi:10.1029/2006JD007107, 2006.

Climate Change and the Role of Photovoltaics in the Energy Mix

Eicke R. Weber

Fraunhofer-Institute for Solar Energy Systems ISE,
and
Faculty of Mathematics and Physics,
Faculty of Applied Sciences,
Albert Ludwig University, Freiburg, Germany

The evidence for anthropogenic, i.e. man-made influence on the global climate, is rapidly becoming overwhelming, as has been summarized convincingly in the recent report of the Intergovernmental Panel on Climate Change (IPCC) (1). The report describes in detail our current understanding and predictions for the global climate, based on an impressive accumulation of the currently available data and climate models. One of the most important conclusions is that we need to keep the atmospheric concentration of CO_2 below 500 ppm in order to limit the unavoidable increase of global average temperatures below 2°C, otherwise the earth might experience major and irreversible changes of climatic conditions.

Based on the predictions of the IPCC report governments started to initiate policies aimed at reducing the emission of climate gases such as of CO_2, as was discussed at the recent G-8 summit in Heiligendamm, Germany. Simultaneously, a public debate started about the impact of the gradual global warming on the living conditions in the different regions of the earth. A recent article in a highly respected German newspaper stated that Germany has not much to fear, it might even profit from global warming (2). However, this kind of discussion might be missing a very important consequence of the unprecendeted change of atmospheric composition by human emission of climate gases, most notably of CO_2.

The detailed analysis of ice core samples such as the famous study by Petit et al. (3) from

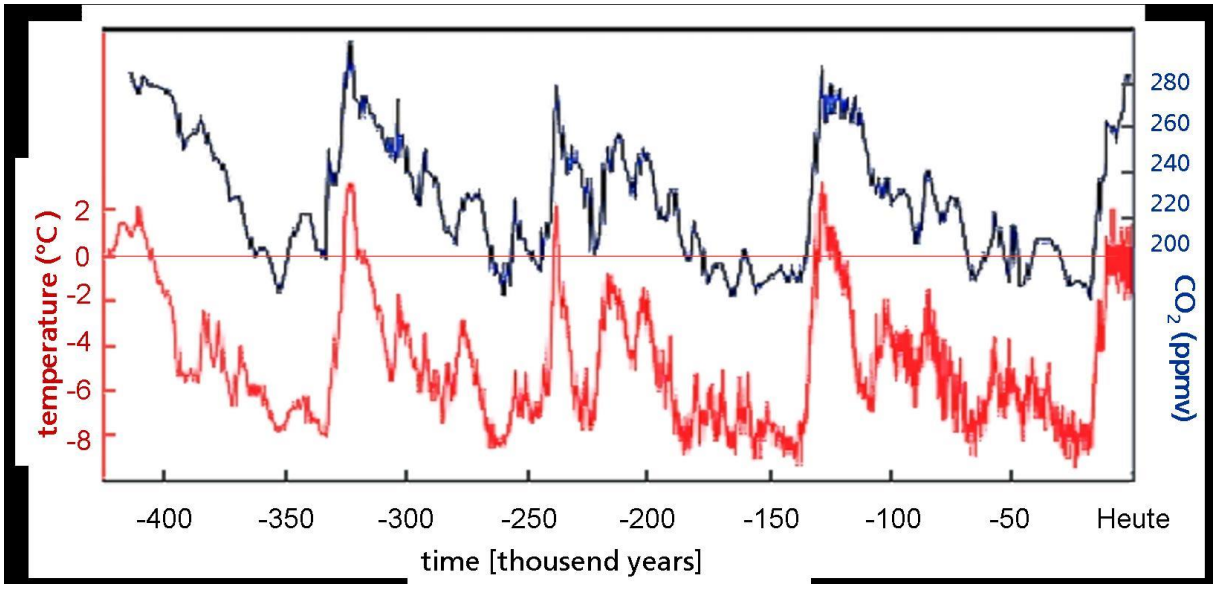

Fig. 1: The detailed analysis of ice core samples demonstrates that global climate has been very unstable in the last more than 400 kyrs. Shown here is a result of the famous study by Petit et al. (3) from Vostock ice core samples, which shows a close

correlation between temperature and atmospheric CO_2 concentration in the last 400kyrs.

Vostock ice core samples demonstrates that global climate has been very unstable in the last more than 400 kyrs, see Fig. 1 (3). In these studies, the analysis of bubbles in the ice allows to determine the oxygen isotope ratio that yields the respective temperature when a specific layer of ice was deposited, and simultaneously the CO_2 content of the atmosphere at that time. In this analysis a striking correlation between the average temperature and the CO_2 content of the atmosphere is revealed: periods of high temperatures correspond to periods of high CO_2 content, and vice versa. This observation alone does not allow to conclude whether times of increased CO_2 content resulted in periods of high temperatures, or whether increases in average temperature resulted in higher CO_2 content, but the correlation has been obviously strong within the last more than 400kyrs. It is worth to note for the later discussion that variations of the CO_2 content between 200ppm and 290ppm corresponded to temperature changes between – 8°C and +2 °C, see Fig. 1. The major and often abrupt changes in temperature, including the last ice age about 30kyrs ago, are quite well understood. These so-called Milankovitch-cycles are caused by periodic changes of planetary parameters such as the tilt of the Earth's spin axis to the orbital plane, the eccentricity of the orbit, and the season of Earth's closest approach to the sun, see e.g. Muller et al. (4).

The unstable earth climate in the last 400+ kyrs changed about 12kyrs ago to a sudden and quite unique stabilization of the global temperature, as evident from the landmark study of Ganopolski et al (5), see Fig. 2. This period of stable climate in the earth history is known as the Holocene. Before the Holocene, the temperature record shows many events of catastrophic global climate impact such as major volcanic eruptions and meteor impacts (events labelled with numbers in Fig. 2), but global climate models cannot explain this sudden stabilization of the earth temperature in the Holocene. One might just state that obviously in this period no major disruption of the earth climate occurred (6).

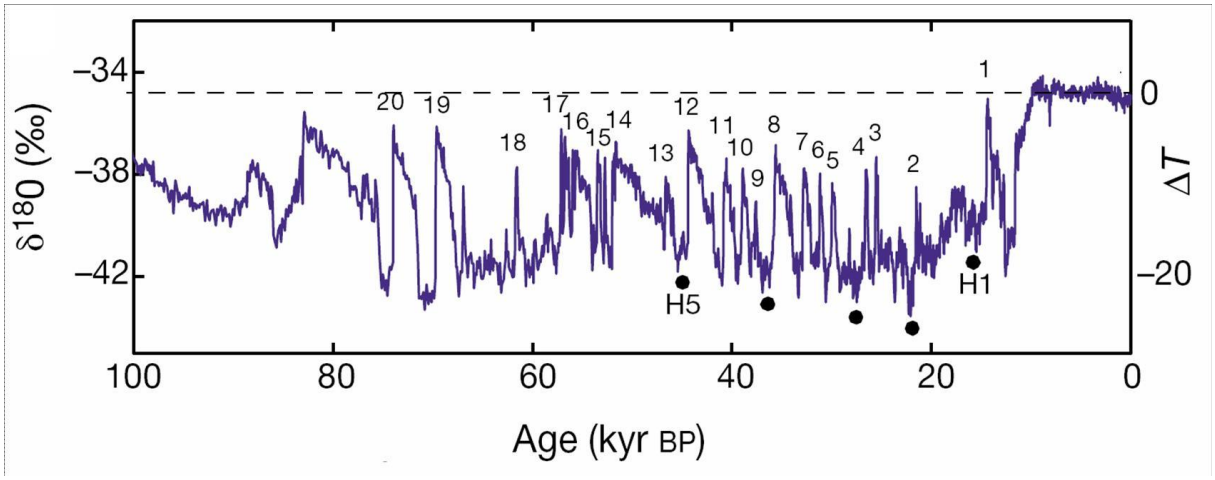

Fig. 2: Temperature record of the last 100kyrs, established by Ganopolsky and Rahmstorf (5). The unstable earth climate changed abruptly about 12kyrs ago to a quite unique stabilization of the global temperature. This period in the earth history is known as the Holocene. Before the Holocene, the temperature record shows many events of catastrophic global climate impact such as major volcanic eruptions and meteor impacts (events labelled with numbers).

It is worth noting that just in the Holocene a dramatic change of the human population occurred: whereas the human genome has been stable in the last ca. 1 Myrs, the human population had to struggle for survival during most of this time and increased in number only very slowly. However, in the Holocene this changed drastically, humans changed from a society of hunters and fruit collectors to farmers. First systematic agriculture occurs, followed by organized settlements and villages. Finally, in the last 7 kyrs, organization in cities and states can be observed, accompanied by the rapid advances in Materials Engineering that ultimately led to the technological and generally well-organized world we live in today. It has been argued that besides the stable climate the stabilization of the oceanic water level in the Holocene was crucial fort his development (7), but as this occured simultaneously it is difficult to argue which factor was ultimately responsible for the explosive development of humankind in the Holocene. However, there can be no doubt that the stable climate was a necessary condition for this process, as otherwise the development of organized societies might have occured much earlier within the last 1 Myrs.

Within the last 120 years the content of the earth atmosphere of CO_2 and other climate gases has drastically increased, see Fig. 3 (7). Today, the earth atmosphere contains more than 380ppm of CO_2. For comparison, in the last more than 400kyrs this value varied between 200 and 290 ppm, accompanied by the drastic changes of average temperatures represented in Fig. 1. Moreover, current climate models predict that due to the ever increasing human energy demand it will be almost unavoidable for global CO_2 levels to exceed 500ppm, and even more if not drastic measures in increasing energy efficiency (EE) and production of CO_2 -free, at best renewable energy (RE) are taken (1).

Our current global debate on climate change is generally focussed on the issue of global warming, i.e. a gradual increase in temperature and oceanic water levels, and it is hoped that the drastic measures currently discussed to increase EE and RE will limit and even decrease the global CO_2 emissions so that the global temperature increase might be limited to only 2°C. Numerous studies are being conducted how this temperature change might affect the economies of different world regions, which might even result in the conclusion that countries in the North like Germany do not have to be afraid of the effects of global warming (2).

However, this type of consideration leaves out a major, maybe most threatening issue: the anthropogenic change of the composition of our atmosphere, most notably the CO_2 content, might result in an end of the Holocene, the period of climate stability, and thus result in an irreversible change of the earth climate system from the stability we enjoyed in the last 10,000 years to the instable climate that was so typical for the earth in most of the last more than 400kyrs. With this, we might destroy the very basis of our highly developed, complex industrialized societies as the new kind of earth climate after the end of the Holocene might be characterized by storms of hitherto unknown strengths, rapid changes of temperatures humans will have difficulties to cope with, catastrophic, rapid melting of ice near the poles and on Greenland, changes of rain patterns such as the monsun that can be disastrous for billions of people, even a sudden ice age in Northern Europe cannot be excluded if the gulf stream stops due to a decrease of salinity caused by the amount of melting ice.

What can be done to avoid this frightening scenario? Obviously, a sustained, global effort is needed to limit and then even decrease global emissions of climate gases as soon as possible.The first task clearly is to increase energy efficiency and decrease waste of energy on all levels. Secondly, conventional energy production from fossil fuels should be changed to reduce CO_2 emissions as much as possible. Efforts to control and sequester CO_2 from such

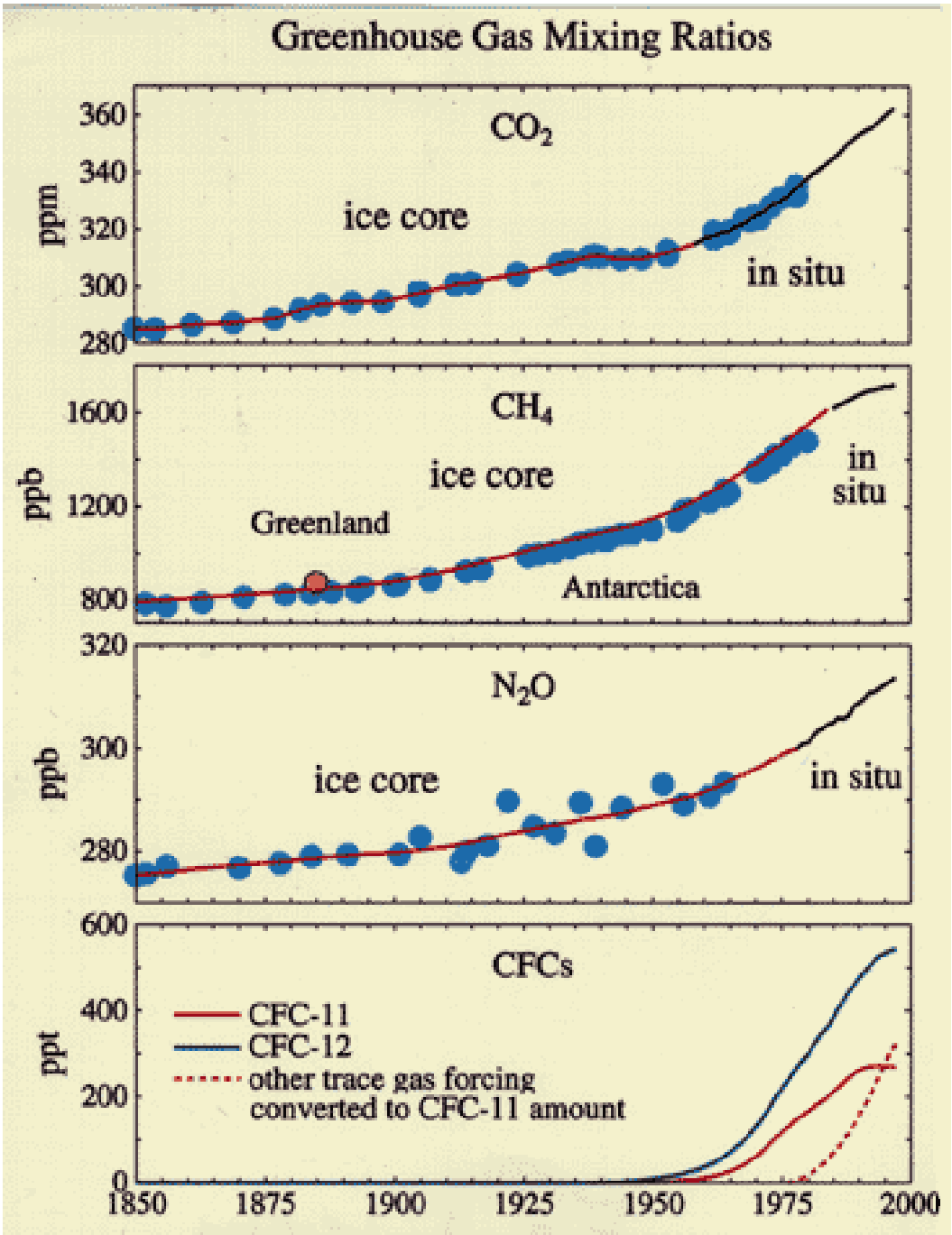

Fig. 3: Since the industrial revolution the content of the earth atmosphere of CO_2 and other greenhouse gases as CH_4. N_2O and CFCs has drastically increased (7). Today, the earth atmosphere contains more than 380ppm of CO_2.

power plans are promising, but will need decades till they can be implemeneted on a global level. Nuclear energy production requires only very little CO_2 emissions from the plant manufacture and the mining and preparation of the nuclear fuel, but it is non-renewable, the easily accessible world uranium is quite limited. In addition, the potential dangers of accidental release of radioactivity and highly toxic materials such as Plutonium, including the dangers of acts of terrorism, and the unsolved issue of the final, safe storage of nuclear waste

for several 10 millenniums make a scenario of solving the world energy problem by rapid production of 100s of new nuclear power plants very unlikely.

Turning now to renewable energies (RE), biomass provides a very large source of RE. It can be directly converted to electric energy via biogas, or processed to methanol or other hydrocarbons to produce biodiesel for transportation. However, the basic process of photosynthesis is very ineffective, so that this approach requires large acreage that has to compete with food production. The global sustainable energy potential has been estimated to be 100 EJ/a. (8).

Wind energy is attractive as production costs already today are at or below grid parity. However, wind is a highly unpredictable source of energy, and the installation of a high density of modern wind mills faces public opposition. Off-shore wind parks in shallow ocean waters currently appear to be an attractive alternative to onshore solutions, but they still have to be tested in terms of productivity and reliability under the very harsh conditions of the ocean. For onshore wind, a global sustainable potential of 140 EJ/a has been estimated (8).

Geothermal energy production has to be distinguished between shallow drilling for e.g. individual heat pumps, and deep drilling for power plants. The first is worth to optimize as part of increasing energy efficiency, the second is limited to favorable geological sites. For this, a sustainable capacity estimate of 30 EJ/a has been proposed (8).

The final, and virtually unlimited source of energy is direct solar energy: the 120 000 TW reaching the earth (9) have to be compared with the 13 TW currently consumed by humans. The sun brings to earth 3 780 000 EJ/a, i.e. in only one hour the current human energy need of 410 EJ/a can be supplied.

Therefore it appears to be obvious that in the long run, direct utilization of solar energy will become the dominant energy source. The question is only, how fast the energy mix will be changed: if the change is too slow, it will not help much to reduce global emissions of climate gases in order to avoid the disastrous climate change discussed above.

Solar energy can be harvested in two forms, as solar thermal energy that is very useful in low-temperature systems without concentration for the production of hot water and heat as well as cooling, e.g. (10), and high-temperature concentrator systems for the generation of electricity by means of a thermal power plant. The widespread introduction of low-T solar thermal systems in sun-rich countries is well under way, and it is spreading even to temperate regions such as Germany. First high-T solar thermal plants have been constructed, the cost of electric energy produced this way is not far from grid parity, however, it remains to be seen how quickly further cost reductions in this industry will be realized in the future.

Finally, direct photovoltaic (PV) energy conversion should be considered. This technology has experienced rapid growth in the last 5 years, with sustained global growth rates exceeding 30%. The result is a global PV market exceeding 2 GW_p of newly produced PV modules in 2006 (11). The main driving force behind this development was the passage of favorable support laws for this technology in key countries, especially Japan and Germany. Especially the German feed-in law, obliging utility companies to offer a simple, very favorable purchase price for all PV-generated energyy without a cap on the total supported PV power, has proven

to be highly effective in the rapid introduction and expansion of PV into the energy market. Other support systems, based e.g. on mandatory quotas for the amount of PV energy in the energy mix, have not shown a comparable impact on the PV market. Several countries in regions of higher sunshine than Germany are working on introducing similar laws based on a feed-in tariff, whereas the introduction of PV in the USA, where such a feed-in tariff is not yet available, has been comparatively slow.

About 90% of the current PV market is based on solar cells made out of crystalline silicon, see Fig. 4 (12), single crystal and multicrystalline Si. Single crystal Si cells from wafers like they are used in the general semiconductor industry generally yield a slightly higher energy conversion efficiency than cells made from multi-crystalline Si that can be crstallized unidirectional in big boules of 250kg and more. The increase in the total volume produced resulted in a reduction of costs that can be traced on a logarithmic learning curve (Fig. 5). The slope of this curve means that for each doubling of the accumulated total production volume the cost comes down by about 20%. Therefore it is essential to promote further global expansion of PV production levels in order to reach true grid parity with conventional power sources. At this point, the availability of PV power will limit the price increase of electricity from the limited and rapidly diminishing fossil sources.

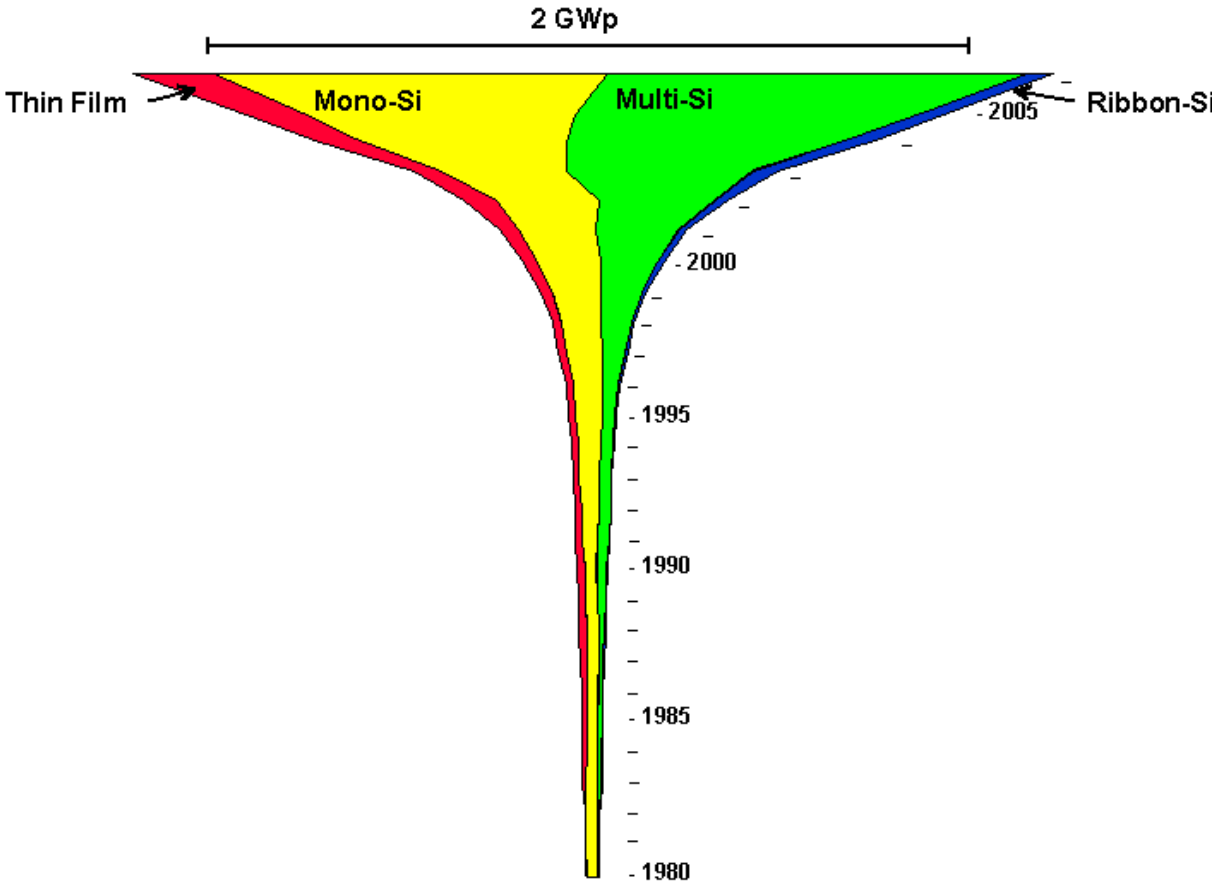

Fig. 4: World's current photovoltaics market is dominated by solar cells made out of crystalline silicone. Over 90% of the solar cells are made from mono- or multi-crystalline silicon (12).

In the last three years, this cost reduction based on higher production volumes was not reflected in the sales price of PV modules. The rapid expansion of the need for high-purity silicon, that is as well used in the semiconductor industry for the production of integrated circuits for memory and processor chips, resulted in a shortage of high-purity silicon feedstock material. This started in the last three years to reduce the production volume of newly built PV plants based on crystalline Si to less than their technical capacity.

This shortage of Si feedstock material is expected to be overcome in the coming years through the introduction of additional ressources of high-purity silicon using the traditional Siemens process, e.g. (13), or modifications of this process still using trichlorosilane to produce so-called solar-grade silicon, or by the introduction of purified metallurgical silicon (pmg-Si). This pmg-Si contains either significantly higher amounts of metal than high-purity Si, or higher amounts of dopants, or both, and is therefore sometimes refered to as 'dirty Si'. In parallel, efforts are being conducted to further decrease the amount of Si used per Watt of PV peak power by further cutting down on the kerff loss obtained when sawing the wafers, and by transitioning to thinner wafers.

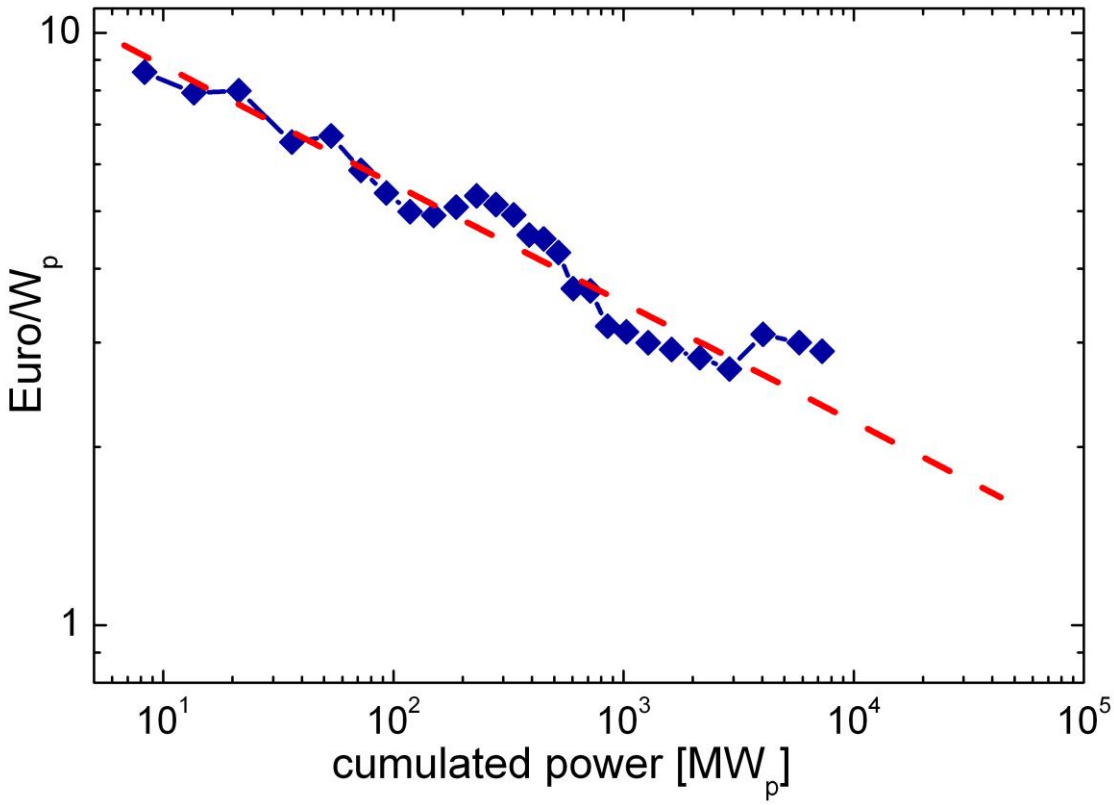

Fig. 5: The price experience curve exhibits an impressive decrease in PV module costs. The increase in the total volume produced resulted in a reduction of costs that for each doubling of the accumulated total production volume the module costs come down by 20% (12).

The shortage of high-purity Si has as well renewed efforts in thin film PV technologies, using thin films of amorphous Si, or avoiding Si completely by using polycrystalline thin films of alternative semiconductors such as CdTe, CuInS (CIS) or CuInGaS (CIGS). All of these technologies have the advantage of inexpensive, rapid processing of large sheets of material

deposited on rather inexpensive substrates. The key disadvantage, however, is based on the low efficiencies: a-Si modules cannot be produced on an industrial scale with long-term efficiencies above 8%, the other thin film techniques seem to have great difficulties exceeding a stable module efficiency above 10%. In addition, the thin film modules containing In, Cd and Te might never be able to be produced in the required GW_p - quantities, due to the scarcity of these elements. In the current situation of a shortage of high-purity Si the PV modules based on thin film technologies are an attractive alternative PV technology, but it remains to be seen whether this can be sustained once the Si feedstock limitation is overcome.

A technological challenge of great potential relevance is the utilization of upgraded metallurgical Si for low-cost solar cells of good efficiency in the 14-16% range, as is typical for multi-crystalline Si. It is expected that this material can become available soon in large quantities at very favorable cost compared to the common high-purity feedstock material, so that this technology has indeed the potential to take a sizable share of the PV market in the future.

Recent investigations of Buonassisi et al (14) have demonstrated that nano-defect engineering of metal clusters in Si can drastically improve the minority carrier diffusion length in Si with a high level of metal contaminants. The key result is that it is not just the metal concentration that determines the electrical properties, but the way the metal atoms are arranged: isolated metal atoms are effective recombination centers even in low concentration, but by converting them into large clusters separated by large distances the minority carrier diffusion length can improve considerably. This approach might make it possible to indeed process good solar cells out of purified metallurgical, comparatively ‘dirty’ Si.

In conclusion, the challenge of the impeding climate catastrophe caused by anthropogenic emissions of climate gases such as CO_2, that might even end the geological period known as the Holocene, makes rapid introduction of energy saving and emission avoiding technologies unavoidable. Among all renewable energies available direct utilization of solar energy appears to be most promising. Among those technologies especially photovoltaics based on crystalline Si will most likely be the dominant technology for the near future as it can deliver unlimited amounts of energy without being dependent on the use of any scarce materials.

ACKNOWLEDGEMENT

Ther author would like to thank G. Willeke for the use of graphic material and T. Schlegl for help with the preparation of this manuscript.

REFERENCES

(1) *Climate Change 2007, Fourth Assessment Report of the Intergovernmental Panel on Climate Change* [Eds. S. Solomon,D. Qin, M. Manning, Z. Chen, M. Marquis, K.B. Averyt, M. Tignor and H.L. Miller]. Cambridge University Press, Cambridge, United Kingdom and New York, NY, USA, 2007.

(2) G. Braunberger, J. Roebke, and T. Spreckelsen, *Wohl denen, die morgen im Norden leben*, Frankfurter Allgemeine Sonntagszeitung, June 17, 2007, p. K2.

(3) J.R. Petit, J. Jouzel, D. Raynaud, N.I. Barkov, J.M. Barnola, I. Basile, M. Bender, J. Chapellaz, J. Davis, G. Delaygue, M. Delmotte, V.M. Kotlyakov, M. Legrand, V. Lipenkov, C. Lorius, L. Pe.pin, C. Ritz, E. Saltzman, M. Stievenard, *420,000 years of climate and atmospheric history revealed by the Vostok Deep Antarctic ice core,* Nature **399**, 429 (1999).

(4) R.A. Muller, G.J MacDonald, *Glacial Cycles and Astronomical Forcing,* Science **277,** 215 (1997).

(5) A. Ganopolski, S. Rahmstorf, *Rapid changes of glacial climate simulated in a coupled climate model*, Nature **409**, 153 (2001).

(6) H.J. Schellnhuber (2002), private communication

(7) T.S. Ledley, E.T. Sundquist, S.E. Schwartz, D.K. Hall, J.D. Fellows, and T.L. Killeen, *Climate Change and Greenhouse Gases*, EOS **80**, 453 (1999).

(8) *German Advisory Council on Global Change* WBGU, 2003.

(9) G.W. Crabtree, N.S. Lewis, *Solar energy conversion*, Phys. Today**, 60**, 37 (2007).

(10) H.-M. Henning, *Solar assisted air conditioning of buildings - an overview*, Appl. Thermal Eng. **27**, 1734 (2007).

(11) *Die neue Masseinheit heisst GW*, Photon **4/07**, 52 (2007).

(12) G. Willeke, Fraunhofer ISE, 2007.

(13) *Handbook of Crystal Growth* [Ed. D.T.J. Hurle], NORTH-HOLLAND 1994.

(14) T. Buonassisi, A.A. Istratov, M.A. Marcus, B. Lai, Z. Cai, S.M. Heald, and E.R. Weber, *Nature Materials* **4**, 676 (2005).

Impressum:

Deutsche Physikalische Gesellschaft e.V.

Hauptstraße 5, D-53604 Bad Honnef
Tel. 02224-9232-0, Fax 02224-9232-50
dpg@dpg-physik.de
www.dpg-physik.de
www.weltderphysik.de

Berliner Geschäftsstelle:

Magnus-Haus
Am Kupfergraben 7, D-10117 Berlin
Tel. 030-201748-0, Fax 030-201748-50
magnus@dpg-physik.de

Pressekontakt:

presse@dpg-physik.de
http://presse.dpg-physik.de

Layout:

Prof. Dr. Hardo Bruhns
Meliesallee 5, 40597 Düsseldorf
E-Mail: ake@bruhns.info

Diese Publikation ist im Internet erhältlich unter
http://www.dpg-physik.de

AKE

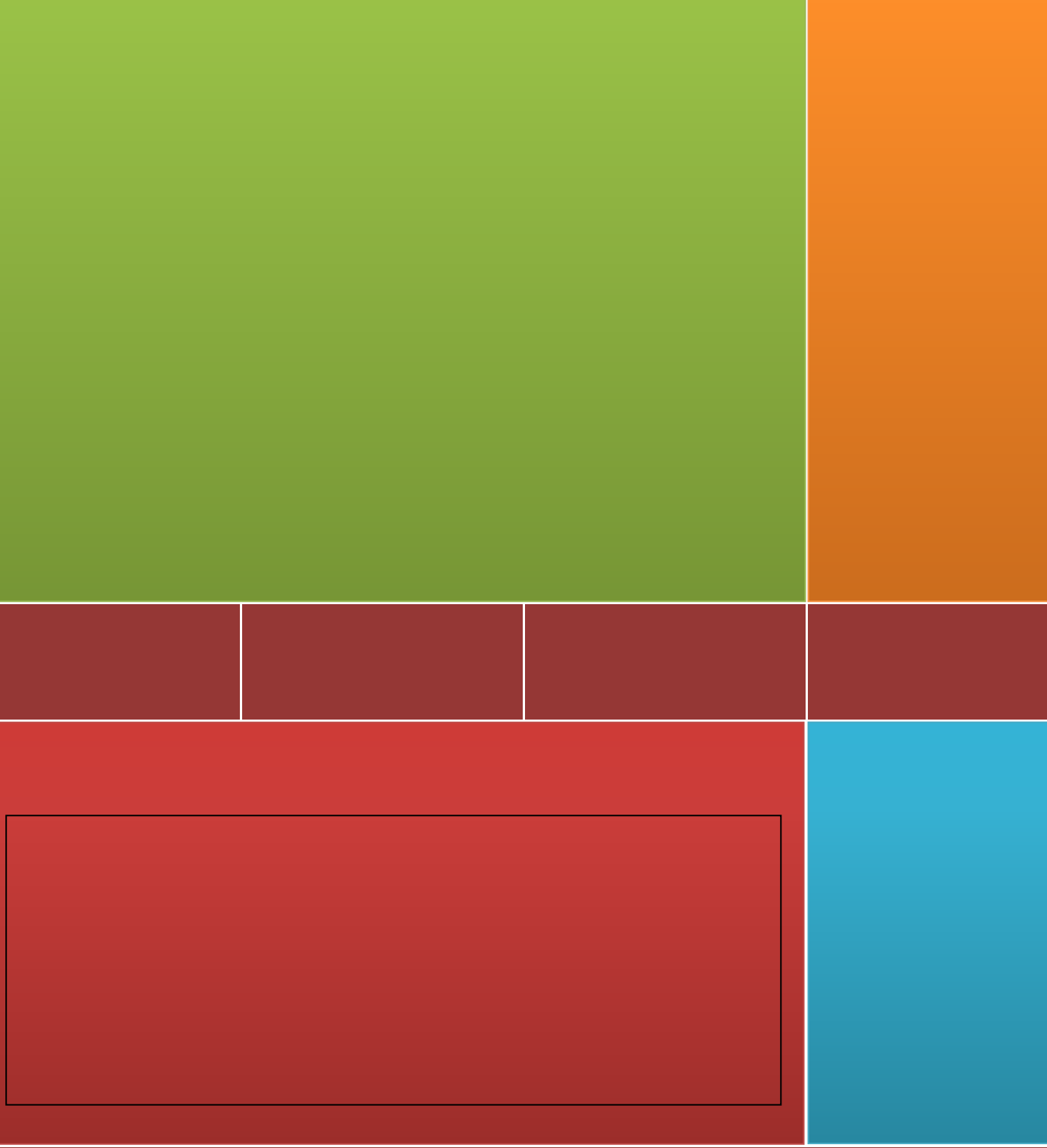

Arbeitskreis Energiein der DPG